Charles University in Prague

Faculty of Science

Department of Cell Biology

Master Thesis

Detailed Phenotype of the Transgenic Mice with Twinkle-PEO Mutations

Podrobná charakteristika transgenních myší s mutacemi Twinkle-PEO

Bc. Jana Buzková

Prague 2009

Supervised by:

Ing. Markéta Tesařová, PhD.

Laboratoř pro studium mitochondriálních poruch,
Klinika dětského a dorostového lékařství 1. LF UK a VFN,
Ke Karlovu 2, Praha 2

Special supervisior:

Professor Anu Suomalainen

Program of Molecular Neurology
Biomedicum Helsinki
University of Helsinki
Finland

Hereby, I declare this thesis was carried out by myself with guidance of my supervisors Ing. Markéta Tesařová PhD and Prof. Anu Wartiovaara and with the use of listed literature sources.

Prague 2009

Jana Buzková

This thesis was carried out at the Research Program of Molecular Neurology, Biomedicum Helsinki, University of Helsinki, Finland. This work was financially supported by Center of Excellence of Finnish Academy and the University of Helsinki, Finland.

For an excellent supervision, continuous encourage and trust during my university studies I would like to thank my supervisor Ing. Markéta Tesařová PhD. I want to thank to my special supervisior Prof. Anu Wartiovaara for her guidance, motivating discussion and for providing me the opportunity to work on this project with her Molecular Neurology team. My thanks go also to my other supervisior Henna Tyynismaa, PhD for her practical advices and patience with teaching me all the methods used in this project. I want to acknowledge all members in MitoLab and AW lab for their help and cooperative working. Finally, I would like to thank my family for their tireless support.

Abstract

Inherited mitochondrial disorders comprise a phenotypically and genetically heterogenous group of diseases that are caused by mutations in both mitochondrial and nuclear genomes. Only symptomatic cure is available for the patients, thus generating appropriate animal models is essential to understand the underlying pathological mechanisms and for development of therapeutic approaches.

The transgenic mice with Twinkle-PEO mutations function as a valuable tool for studying the adult-onset autosomal dominant progressive external ophthalmoplegia (adPEO). Mice, from the strain referred to as Deletor mice, express a moderately severe mutation in the mitochondrial DNA helicase Twinkle (Tyynismaa *et al.* 2005). The aim of the diploma thesis is to study autophagy and mitochondrial fragmentation in pathogenesis of mitochondrial myopathy in the mouse model for Twinkle-PEO. The chromosomal insertion site of Twinkle-PEO construct was localized in the non-coding region (chromosome 16, the C mouse line) and the construct expressing wild type Twinkle in the gene encoding transmembrane serine protease 11d (chromosome 5, the A mouse line). The presence of multiple deletions of mitochondrial DNA (mtDNA) was tested in several Deletor tissues, in particular the muscle, liver, kidney, testis and intestine and they were proved in the skeletal muscle and previously also in the brain (Tyynismaa *et al.* 2005). This result corresponds with the findings from PEO patients. Changes in the isoform pattern of Opa1, a crucial protein for a functional mitochondrial network in cells, were also reported in a case of patients and mouse models with mitochondrial dysfunction (Duvezin-Caubet *et al.* 2006). In the Deletor skeletal muscle, all Opa1 isofroms were found to be slightly elevated with significant increase in the level of L2-OPA1. In the brain tissue, a significant elevation of S-OPA1 isoforms was detected. In the Deletor skeletal muscle, where autophagy was previously seen by electron miscroscopy (Tyynismaa *et al.* 2005), the increased level of autophagy/mitophagy marker LC3-II was detected. Consistent to autophagy induction, acetylation of mitochondrial proteins on lysine residues was not increased in the Deletor muscle.

In conclusion, it has been proved that the transgenic disease model faithfully replicates the features of PEO patients and might help to study the pathogenicity of Twinkle-PEO mutations and the tissue specificity of mitochondrial disorders.

Abstrakt

Mitochondriální onemocnění představují fenotypově i geneticky velice heterogenní skupinu chorob, které mohou být způsobeny mutacemi v mitochondriálním i jaderném genomu. Jelikož je u pacientů dostupná pouze symptomatická léčba, vytvoření vhodných myší modelů je nezbytné pro pochopení patogenních mechanismů u těchto chorob a pro hledání vhodných terapeutických postupů.

Transgenní myši s Twinkle-PEO mutacemi jsou dnes vhodným nástrojem pro studium autosomálně dominantní progresivní externí oftalmoplegie (adPEO) s nástupem v dospělosti. Myši z linie označované jako „Deletor" exprimují mírně závažnou mutaci v mitochondriální DNA helikáze Twinkle (Tyynismaa *et al.* 2005). Hlavním cílem diplomové práce bylo studium autofagie a mitochondriální fragmentace v patologii mitochondriální myopatie u myšího modelu pro Twinkle-PEO. Konstrukt Twinkle-PEO byl lokalizován v nekódující oblasti chromozómu 16 (v myší linii C) a konstrukt umožňující nadprodukci „wild type" formy Twinkle helikázy v genu kódujícím transmembránovou serin proteázu 11d na chromozómu 5 (v myší linii A). Řada tkání myší linie Deletor (sval, játra, ledviny, varlata a část střeva) byla testována na přítomnost násobných delecí mitochondriální DNA (mtDNA). Přítomnost těchto delecí ve svalové a i v již dříve potvrzené mozkové tkáni (Tyynismaa *et al.* 2005) odpovídá poznatkům u pacientů s PEO. Změny v profilu izoforem proteinu Opa1, který je nezbytný pro udržení funkční mitochondriální sítě v buňkách, byly popsány u pacientů a myších modelů s mitochondriální poruchou (Duvezin-Caubet *et al.* 2006). Ve svalové tkáni myší Deletor byla nalezena mírně zvýšená hladina všech Opa1 izoforem, přičemž nejvyšší nárůst byl zjištěn u L2-OPA1 izoformy. Mírný nárůst S-OPA1 izoforem byl detekován v mozkové tkáni. Ve svalu myší Deletor byla zjištěna i zvýšená hladina LC3-II, proteinového markeru autofagie/mitofagie, což potvrzuje dřívější nálezy z elektronového mikroskopu (Tyynismaa *et al.* 2005). V souladu se zvýšenou hladinou autofagie, nebyla v kosterním svalu myší Deletor nalezena zvýšená acetylace lyzinových zbytků u mitochondriálních proteinů.

Závěrem, bylo dokázáno, že myší linie Deletor věrně kopíruje fenotyp pacientů s PEO a je tedy vhodným modelem pro studium patogeneze Twinkle-PEO mutací a tkáňové specifity mitochondriálních onemocnění.

Contents

Abbreviations

$\Delta\psi_m$	reduced membrane potential
2D-NAGE	two-dimension neutral agarose gel electrophoresis
AA	amino acid
AceCS2	acetyl-CoA synthetase 2
ADOA	autosomal dominant optic atrophy
ADP	adenine nucleotide diphosphate
adPEO	autosomal dominant progressive external ophthalmoplegia
AIF	apoptosis inducing factor
Ant	adenine nucleotide translocator
AT	A360T transgenic mouse
Atad3	ATPase family AAA domain-containing protein 3
ATG	autophagy related gene
ATP	adenine nucleotide triphosphate
BPB	bromphenol blue
BSA	bovine serum albumin
cDNA	coding DNA
CoA	Coenzyme A
CoQ	Coenzyme Q or ubiquinone
CoQH	ubisemiquinone
$CoQH_2$	ubiquinol
COX	cytochrome c oxidase
COX^-	negative cytochrome c oxidase activity
CPEO	chronic progressive external ophthalmoplegia
dCK	deoxycytidine kinase
DEL	Deletor mouse
DF, NF	defective fiber, normal fiber
dGK	deoxyguanosine kinase
DGUOK	gene encoding deoxyguanosine kinase
D-loop	displacement loop
DNC	deoxynucleotide carrier
dNTP	deoxynucleotide triphosphate
dRP	deoxyribosephosphate
dsDNA	double stranded DNA
ECL	enzymatic chemiluminescence
EDTA	2-[2-mDamino)ethyl-(carboxymethyl) amino]acetic acid
EGTA	glycol-bis(2-aminoethylether)-N,N,N',N'-tetraacetic acid
ENT1	equilibrate nucleosite transporter
EtBr	ethidium bromide
EtOH	ethanol
$FADH_2$	reduced flavin adenine dinucleotide

GABAA	gamma aminobutyric-acid-type-A
GABARAP	gamma aminobutyric-acid-type-A-receptor-associated protein
GATE-16	Golgi-associated ATPase enhancer of 16 kDa
GDH	glutamate dehydrogenase
GED	GTPase effector domain
GFP	green fluorescent protein
HEPES	4-(2-hydroxyethyl)-1-piperazineethanesulfonic acid
HMG	high mobility group
HSP	heavy strand promoter
H-strand	heavy-strand
IBM	inner boundary membrane
IOSCA	infantile onset spinocerebellar ataxia
IT_{H1}, IT_{H2}	transcription initiation site for heavy strand, 1 and 2
IT_L	transcription initiation site for light strand
KSS	Kearns-Sayre Syndrome
LHON	Leber hereditary optic neuropathy
L-OPA	long OPA isoforms
LSP	light strand promoter
L-strand	light strand
Map-LC3	microtubule-associated protein light chain 3
MEFs	mouse embryonic fibroblasts
MELAS	mitochondrial encephalomyopathy, lactic acidosis and stroke-like episodes
MERRF	myoclonic epilepsy with ragged red fibers
MPP	mitochondrial processing peptidase
MPT	mitochondrial permeability transition
mRNA	messenger RNA
mtDNA	mitochondrial DNA
mTerm	mitochondrial transcription termination factor
MTS	matrix-targeting sequence
mtSSB proteins	mitochondrial single stranded binding proteins
NAD	nicotinamide adenine dinucleotide
NADH	reduced nicotinamide adenine dinucleotide
NARP	neurogenic muscle weakness, ataxia and retinitis pigmentosa
NCR	non-coding region
nDNA	nuclear DNA
O_H	origin of heavy strand replication
O_L	origin of light strand replication
OM	outer membrane
Opa1	dynamine-related guanosine triphosphatase
Ori-Z	broad origin zone

OXPHOS	oxidative phosphorylation
PARL	mitochondrial rhomboid protease
PCR	polymerase chain reaction
PE	phosphatidylethanolamine
PEO	progressive external ophthalmoplegia
Polγ	mitochondrial DNA polymerase gamma
Polrmt	mitochondrial RNA polymerase
PS	Pearson Marrow-Pancreas Syndrome
PT	permeability transition
PVDF	polyvinylidene fluoride
RIs	replication intermediates
RITOLS	RNA-incorporation throughout the lagging strand
ROS	reactive oxygen species
RRF	ragged-red fibers
rRNA	ribosomal RNA
SBG	Serva Blue G
SDH	succinate dehydrogenase
SDH^+	positive succinate dehydrogenase activity
SDS	sodium dodecyl sulfate
SDs	standard deviations
SDS-PAGE	SDS-polyacrylamide gel electrophoresis
Sir2	silent information regulator 2
Sirt family	silent information regulator two family
S-OPA	short OPA1 isoform
ssDNA	single stranded DNA
SUCLA2	succinyl coenzyme A-ligase
TBS-T	Tris-buffer saline - 0.1% Tween 20
TCA cycle	tricarboxylic acid cycle
Tfam	mitochondrial transcription factor A
Tfb1m	mitochondrial transcription factor B1
Tfb2m	mitochondrial transcription factor B2
TK1	thymidine kinase 1
TK2	thymidine kinase 2
TM domain	transmembrane domain
Top1mt	mitochondrial topoisomerase I
tRNA	transfer RNA
WT	wild type

1. Introduction

Mitochondria are key organelles that play a central role in several cellular processes, in particular energetic metabolism, homeostasis, cell division, growth and death. Their crucial function is a production of ATP by oxidative phosphorylation (OXPHOS) process that requires activity of five multimeric enzyme complexes embedded in the inner mitochondrial membrane. Disruption of this energy supply can have devastating consequences for the cell, organ or individual. Mitochondria possess their own multicopy genome, which is maternally inherited. Only 13 from approximately 80 subunits of OXPHOS complexes are encoded by the mitochondrial genome, whereas the rest of the subunits as well as all proteins and enzymes involved in mitochondrial metabolism and mtDNA maintenance are encoded by the nuclear genome. Mutations in both mitochondrial DNA (mtDNA) and nuclear DNA (nDNA) have been identified as causative in number of multisystematic disorders, cancer, obesity and diabetes (Wallace 2005).

Twinkle, the only known mitochondrial DNA helicase, plays an essential role in the mtDNA maintenance (Spelbrink *et al.* 2001). Adult-onset progressive external ophthalmoplegia (PEO) is a mitochondrial disease with Mendelian inheritance that is caused by mutations in nuclear genes encoding mtDNA maintenance proteins and characterized by the presence of multiple mtDNA deletions in patients´ tissues (Zeviani *et al.* 1989). PEO patients with mutations in the gene encoding Twinkle helicase explain about 35% of autosomal dominant PEO cases (Lamantea *et al.* 2002). The “Deletor” mouse, a transgenic animal model for late-onset PEO with autosomal dominant mutation in Twinkle (Tyynismaa *et al.* 2005), mimics closely the PEO patients´ phenotype and is a tool to study the disease at a presymptomatic phase or to test different drugs for therapy approach. The experimental trials lead to better understanding of the pathogenic role of either mtDNA or nDNA mutations in mitochondrial disorders.

2. Aims of the thesis

The mouse model for studying late-onset mitochondrial disease was generated in 2005 in the laboratory of Prof. Anu Suomalainen (Tyynismaa *et al.* 2005). The general characterization of the transgenic mouse clearly showed its potential as a tool to study late-onset mitochondrial disease. The histological and molecular findings, for example COX negative/ SDH positive cells and accumulation of multiple mtDNA deletions in particular tissues, closely mimicked the findings in PEO patients (Suomalainen *et al.* 1997). Moreover, several structural changes of mitochondria have been found in the affected muscle fibers that have pointed to putative induction of autophagy/ mitophagy (Tyynismaa *et al.* 2005). This study is based on previous findings obtained from this mouse model.

The aim of the study was to further characterize the phenotype of the transgenic mice in detail. My specific aims were:

- To determine the chromosomal insertion site of the Twinkle transgene in the genome of two different transgenic mouse lines
- To study the presence of mitochondrial DNA deletions in variety of Deletor tissues
- To examine the respiratory deficient phenotype in proliferative tissue of the Deletor mice
- To study the role of autophagy and mitochondrial fragmentation in mitochondrial myopathy pathogenesis using appropriate protein markers such as LC3 or Opa1

3. Review of literature

3.1 Mitochondria

Mitochondria are essential cytoplasmic organelles existing in almost of all eukaryotic cells. According to the original endosymbiotic theory, mitochondria are direct descendents of the α-proteobacteria that became endosymbiont in a nucleus-containing but amitochondrial host cell (Margulis 1976). Whether the host cell already contained a nucleus is not clear, however the host cell provided the nuclear genome for subsequent transfer of genes related to mitochondrial biogenesis and function to nucleus (Gray *et al.* 1999). In 1998, a new hypothesis about mitochondrial origin in eukaryotes has been proposed. The hydrogen hypothesis assumes that eukaryotes originated through symbiotic metabolic association called syntrophy where strictly anaerobic archaebacterium dependent on hydrogen became a host of ancestral mitochondria, a fermentative α-proteobacterium that was able to respire and generated hydrogen and carbon dioxide as waste products (Martin and Muller 1998).

3.1.1 Structure and function of mitochondria in cells

Mitochondria in cells form a complex interconnected reticulum that is highly dynamic and interacts with other cellular components, in particular the cytoskeleton and endoplasmic reticulum (Mannella 2000). The main characteristics of these organelles, such as size, shape, mass or distribution may vary markedly between different cells or tissues with different energetic needs. Moreover, it has been demonstrated that functional mitochondria can be transferred to the target cells to rescue the mitochondrial functions (Spees *et al.* 2006).

Mitochondria are cellular organelles bounded by two membranes: the outer and inner membrane. The smooth outer membrane (OM) includes diverse set of enzymes, proteins controlling morphology of the organelle, members of the pro- and anti-apoptotic family as well as pore-forming components (porins) which allow the free passage for molecules up to 5 kDa. Complicated inner membrane consists of the inner boundary membrane (IBM) apposed to the OM and the crista membrane protruding as tubules or lamellae into the matrix of the organelle (figure 3.1). All

cristae are connected to the inner boundary membrane and to each other by a tubular structure called crista junctions with variable length but relatively constant diameter of 28 nm within a variety of healthy cells types (figure 3.1; Frey and Mannella 2000). This subdivision defines topologically distinct compartments, the intermembrane space between the outer and inner membrane, where enzyme for further ATP utilization are localized, and the mitochondrial matrix that includes multiple copies of mitochondrial DNA and several hundreds of proteins that participate in mitochondrial functions, such as citric acid cycle, biogenesis of heme, fatty acid oxidation, electron transport with energy transduction and Ca^{2+} reservoir.

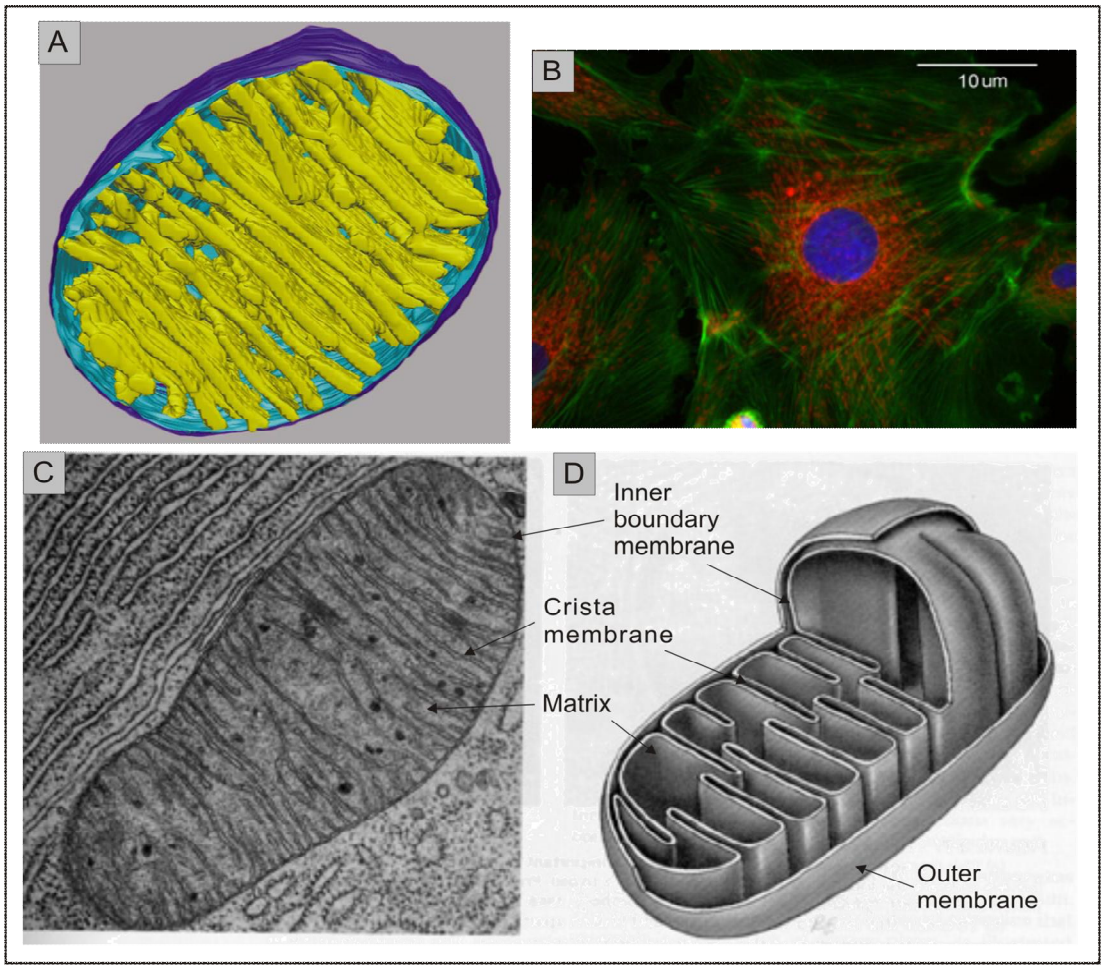

Figure 3.1: Mitochondria in cells. **A**, the entire computer model from segmented 3D tomograms showing cristae (in yellow), the inner boundary membrane (in light blue) and the outer membrane (in dark blue, Frey and Mannella 2000). **B**, fluoro-colored picture of bovine pulmonary cells, nucleus is visualized with DAPI (blue), mitochondria with FITC (red) and actin with TRITC (green, modified from www.rpgroup.caltech.edu/courses/PBL/size.htm), **C**, electron microscope image, **D**, drawing of the mitochondria, the structures are pointed (modified from homepages.cwi.nl/.. ./SiC/PICT/mitochondria.JPG).

3.1.1.1 The oxidative phosphorylation system

The main function of the inner boundary membrane is to enclose the matrix space and to transport ions, substrates and proteins through the specific carriers. The crista membrane, in form of tubules opened to the intermembrane space, is predominantly associated with oxidative phosphorylation (OXPHOS) and ATP production (Gilkerson *et al.* 2003). The OXPHOS system is organized into the four enzyme complexes (complex I-IV) that comprise electron-transport chain, also called mitochondrial respiratory chain, and the ATP synthase complex (complex V), which uses the free energy generated by electron transport along the respiratory chain to produce ATP. The subunits of the five enzyme complexes are encoded in both the nuclear and mitochondrial genome (figure 3.2, 3.3).

The electrons are generated from two coenzymes NADH and $FADH_2$ rising from degradation of pyruvate in citric acid cycle and fatty acid oxidation. NADH donate the electrons to complex I (NADH-ubiquinone oxidoreductase), the largest OXPHOS complex composed of 45 subunits, seven of which are encoded by mitochondrial DNA (Carroll *et al.* 2006). Complex II (Succinate: Coenzyme Q Oxidoreductase, SDH) that comprises of four subunits all of which are encoded by nuclear DNA, accepts the electrons donated from $FADH_2$. Complex I and Complex II pass the electrons to Coenzyme Q (CoQ or ubiquinone) and along the ubisemiquinone (CoQH) to Coenzyme QH_2 ($CoQH_2$ or ubiquinol). Coenzyme QH_2 transfers the electrons to Complex III (Coenzyme Q: Cytochrome c Oxidoreductase) consisting of 11 subunits, only one of which is encoded by mitochondrial genome. Complex III then reduces cytochome c, a mobile hydrophobic hemoprotein that transfers the electrons to Complex IV (Cytochome c Oxidase, COX) comprising of three mitochondrial and 10 nuclear encoded subunits. Complex IV catalyzes reduction of O_2, the terminal acceptor of the electrons, to produce H_2O (figure 3.2). The transfer of the electrons along the respiratory chain is utilized by Complex I, III and IV to transport protons from matrix to the intermembrane space and to generate an electrochemical gradient. Complex V (F_O/F_1 ATP synthase) that consists of 12-14 subunits of which two are encoded by mitochondrial genome, catalyzes the phosphorylation of ADP to ATP, using the energy of the protonic influx into the mitochondrial matrix through the channel in the structure of Complex V (figure 3.2). This process is also called energy transduction. ATP, a molecule capturing free energy for most of the energy-dependent cell processes, is released from

mitochondria through the adenine nucleotide translocator (Ant). The reactive oxygen species (ROS), dangerous by-products of OXPHOS, are results from the misdirection of the electrons directly to O_2 in early stages of respiratory chain. ROS are responsible for oxidative damage of proteins, lipids and amino acids within mitochondria, but also have important roles in cell signaling.

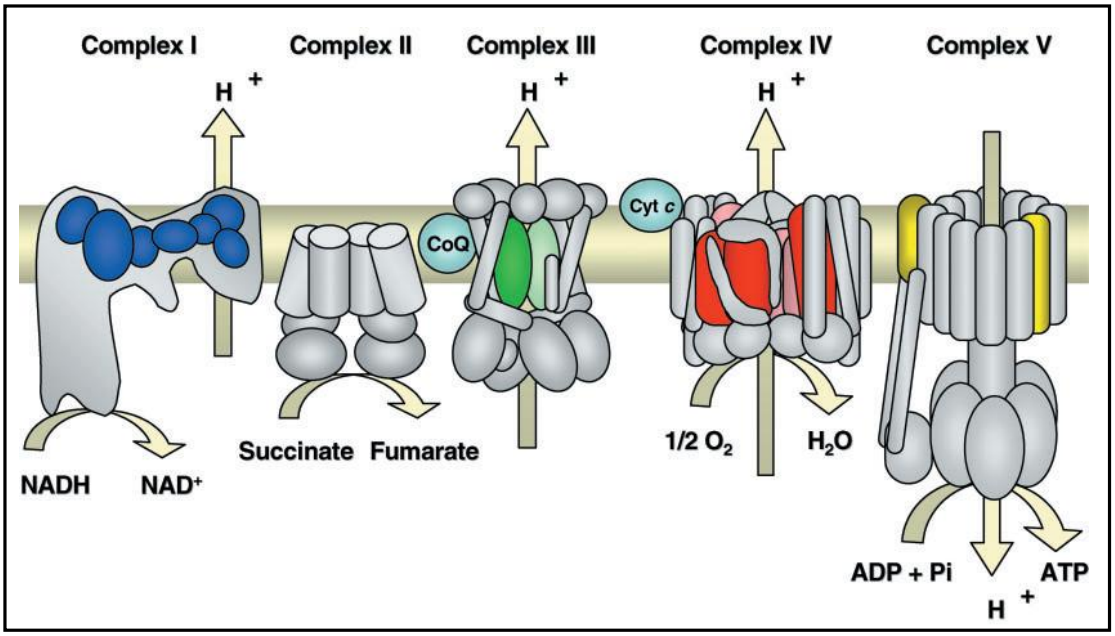

Figure 3.2: Creative drawing of the respiratory chain embedded in the cristae membrane. The mitochondrially encoded subunits of each complex are shown in different colors: complex I – blue, complex II – green, complex IV – red and complex V – yellow. The colors correspond to genes in mitochondrial DNA shown in figure 3.3, Cyc c – cytochorome c, CoQ - coenzyme Q (modified from Zeviani and Di Donato 2004).

3.1.1.2 Cycles of aerobic metabolism in mitochondria

The citric acid cycle, alternatively known as tricarboxylic acid (TCA) cycle or the Krebs cycle, is a common pathway for the aerobic oxidation of lipids, carbohydrates or proteins. Here, the final product acetyl-CoA is oxidized while the coenzymes (NADH and $FADH_2$), subsequently utilized in the respiratory chain and ATP production, are reduced. The enzymes of this main amphibolic cycle are localized in mitochondrial matrix, either free or associated with the inner membrane.

In humans, the oxidation of fats is quantitatively more important than glucose oxidation as a source of ATP. The fatty acid oxidation or β-oxidation is a process requiring oxygen for oxidation of fatty acyl-CoA to yield acetyl-CoA, NADH and $FADH_2$ in each cycle. That generates about six times more ATP than the oxidation

of the same amount of glycogen. Starvation causes increase of fatty acid oxidation that leads to production of ketone bodies by the liver (ketosis).

In addition to the production of energy supply, mitochondria play a key role in several biosynthetic pathways, such as synthesis of heme, nucleotides, amino acids or steroid hormones, regulation of calcium homeostasis or heat production.

3.1.2 Mitochondrial genome

Mitochondrial genome is polyploid and consists of hundreds to thousands copies of mitochondrial DNA (mtDNA) per cell. Several specific features distinguish mitochondrial genetics from the nuclear one. The sequence and the gene composition of human mtDNA is highly homologous to mouse mtDNA (Bibb *et al.* 1981).

Unlike the nuclear DNA (nDNA), mtDNA is a circular, double-stranded molecule comprising 16,569 bp that is organized in stable nucleoprotein complexes, called mitochondrial nucleoids that are devoid of histones (Spelbrink *et al.* 2001). These dynamic structures stabilize and protect mtDNA and are able to redistribute into the daughter cells as units of the mitochondrial inheritance (Garrido *et al.* 2003).

Mitochondrial genome is strictly maternally inherited. However, paternally derived mtDNA deletion in muscle has been identified in patient with mitochondrial myopathy (Schwartz and Vissing 2002), but the occurrence of paternal inheritance is rare event (Schwartz and Vissing 2004).

Fundamental aspect of mitochondrial genetics is homoplasmy and heteroplasmy. Normal individuals contain an identical genotype of mtDNA population, a state called homoplasmy. Heteroplasmy occurs when cells or tissues harbor a mixture of two or more mtDNA variants. Homoplasmic mutations affect whole population of mtDNA, whereas heteroplasmic mutations are present only in some copies of mtDNA. The proportion of mutant mtDNA may range from 0% to 100%. For expressing the clinical signs and biochemical defects of oxidative dysfunction, the mutant portion must reach a minimum critical level, called threshold that for tRNA mutations is over 90% and only 40 - 60% mutant mtDNA for deletion (Rossignol *et al.* 2003). The threshold effect for the disease onset is lower in tissues with high energy demands, such as heart, brain, skeletal muscle and retina.

In the presence of heteroplasmy, population of mitochondria is randomly distributed to the daughter cells during mitosis. The proportion of mutant mtDNA in daughter

cells may shift and the phenotype can change in time and vary between tissues. This phenomenon is known as mitotic segregation and may explain tissue-specific variety of symptoms common for mtDNA-related diseases (reviewed by Taylor and Turnbull 2005). Experiments with heteroplasmic mice have shown that mtDNA segregation is under nuclear control (Battersby *et al.* 2003).

3.1.2.1 Mitochondrial DNA

Mitochondrial DNA, first sequenced in 1981, has highly conserved structure and gene organization among mammals (Anderson *et al.* 1981). Using denaturing cesium chloride gradient, the strands of mtDNA duplex can be distinguish due to their different G + T base composition. The heavy strand (H-strand) comprises higher level of guanine compare to the higher level of cytosine involved in the light strand (L-strand, Kasamatsu and Vinograd 1974).

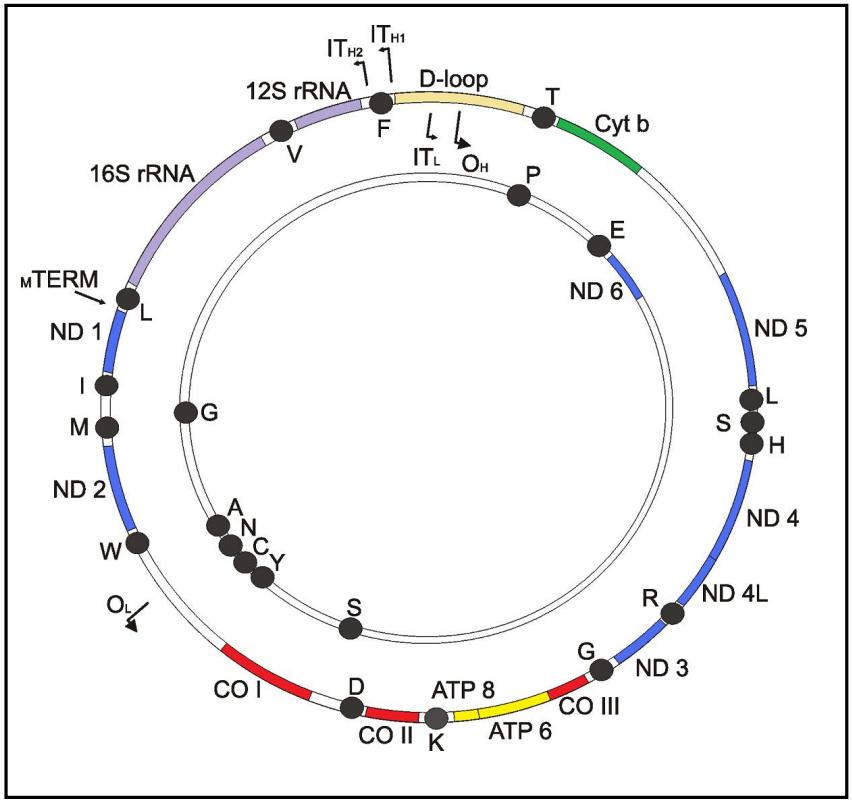

Figure 3.3: Map of human mitochondrial DNA. The outer circle represents the H-strand, containing the majority of genes. The certain colors of genes correspond to particular colors of the subunits in figure 3.2. The inner circle represents the L-strand. The rRNA genes and D-loop are also shown in color. The origins of H-stand (O_H) and L-strand (O_L) replication and direction of DNA synthesis are indicated by thick bent arrows; the transcription sites (IT_{H1}, IT_{H2}, IT_L) and direction of RNA synthesis are marked by thin bent arrows. The binding site for transcription terminator is denoted.

MtDNA contains 37 genes that encode 13 polypeptides, two ribosomal RNAs (12S rRNA and 16S rRNA) and 22 transfer RNAs (tRNAs). All the mtDNA-encoded proteins are essential components of multimeric OXPHOS complexes: seven of them (*MT-ND1, MT-ND2, MT-ND3, MT-ND4, MT-ND4L, MT-ND5* and *MT-ND6*) are subunits of complex I, one (cytochrome b, *CYT B*) of complex III, three (*MT-CO1, MT-CO2* and *MT-CO3*) of complex IV and two (*MT-ATP6* and *MT-ATP8*) of complex V (figure 3.3). The remaining subunits of these complexes, all subunits of complex II as well as all proteins involved in mtDNA expression and its regulation are encoded by nDNA (reviewed by Taanman 1999).

The mtDNA genes lack introns and most of intergenetic sequences as well as some of the protein termination codons are missing. Both rRNAs and tRNAs molecules are atypically small, thus they usually separate the protein genes from each other (Ojala *et al.* 1981).

The major regulation site of mtDNA is called the displacement loop (D-loop) and spans approximately 1000 bp, situated between the genes for $tRNA^{Phe}$ and $tRNA^{Pro}$ (Shadel and Clayton 1997). The triple-stranded D-loop structure is assembled from mtDNA duplex and a short H-strand segment annealed to the L-strand (figure 3.3). The D-loop is a part of the main non-coding region (NCR) containing the key regulatory elements for mtDNA replication and translation (H-strand and L-strand transcription promoters, HSP and LSP, respectively, and origin of H-strand replication, O_H), conserved sequence blocks and termination-associated sequences (Shadel and Clayton 1997).

3.2 MtDNA maintenance

3.2.1 Proteins of mtDNA maintenance

Only some of mtDNA molecules organized into mitochondrial nucleoids are actively replicated/ transcribed at the same time (He *et al.* 2007). Proteins maintaining mtDNA stability and expression are included in nucleoids composition, encoded by the nuclear genome and imported into mitochondria. Spontaneous or inherited pathogenic mutations in most of these proteins result in mtDNA defects in form of deletions, depletions or point mutations, which cause heterogeneous mitochondrial disorders. The construed list includes mtDNA maintaining proteins that directly or indirectly associate and influence mtDNA.

3.2.1.1 Mitochondrial DNA polymerase gamma

The key component of mtDNA maintenance is mitochondrial DNA polymerase gamma (Polγ) that is responsible for DNA synthesis in all replication, repair and recombination processes in animal cell mitochondria (Ropp and Copeland 1996). The human Polγ functions as heterotrimer consisting of catalytic subunit PolγA of 139 kDa, encoded by *POLG1* gene on chromosome 15q24, and a homodimer of accessory subunit PolγB of 53 kDa, coded by *POLG2* gene on chromosome 17q (Yakubovskaya *et al.* 2006). The catalytic subunit possesses both DNA polymerase and proofreading (3´-5´ exonuclease) functions. The C-terminal polymerase domain (pol-domain) is separated from N-terminal exonuclease domain (exo-domain) by a spacer or linker region. In addition, PolγA shows 5´-deoxyribosephosphate (dRP) lyase activity that is necessary for mtDNA repair through base excision repair pathway (Graziewicz *et al.* 2006). A functional binding of accessory subunit Polγ to the linker region of catalytic polypeptide stimulates its polymerase and proofreadng activity, enhance DNA binding and holoenzyme processivity (Fan *et al.* 2006). Pathogenic mutations in both *POLG1* and *POLG2* genes have been identified to underlie several neurodegenerative disorders (http://tools.niehs.nih.gov/polg/).

3.2.1.2 Mitochondrial DNA helicase - Twinkle

Twinkle is the only known mtDNA helicase which plays a key role in the mtDNA replication and maintenance in mammalian cells. The human protein that displays

striking similarity to bacteriophage T7 gene 4 primase/helicase (gp4), is encoded by *PEO1* gene (*C10orf2*) on chromosome 10q24 and consists of 684 amino acids (AA) that are encoded by five exons. Human splice variant called Twinky lacks part of the C-terminal helicase domain, but terminates with four unique amino acids that do not permit to form multimers (Spelbrink *et al.* 2001). The C-terminal helicase domain of Twinkle protein contains highly conserved Walker A and Walker B motifs involved in ATP binding and hydrolysis (figure 3.4). In contrast, function of the N-terminal region, homologous to T7 primase domain has not been assessed yet. Recently, its role in efficient binding to ssDNA has been demonstrated, although its presence in DNA helicase activity is not absolutely required (Farge *et al.* 2008). The linker region, present between primase and helicase domains, is required for multimerization and helicase activity (figure 3.4). Human protein is ubiquitously expressed with the highest level in the skeletal muscle (Spelbrink *et al.* 2001). The Twinkle colocalizes with mtDNA in mitochondrial nucleoid structures in stable hexameric form that catalyzes ATP-dependent unwinding of dsDNA in 5´-to-3´ directionality. Together with Polγ and mitochondrial single-stranded binding (mtSSB) proteins can create minimal mammalian mtDNA replisome to generate 16 kb dsDNA corresponding to full-length human mtDNA molecule (Korhonen *et al.* 2004).

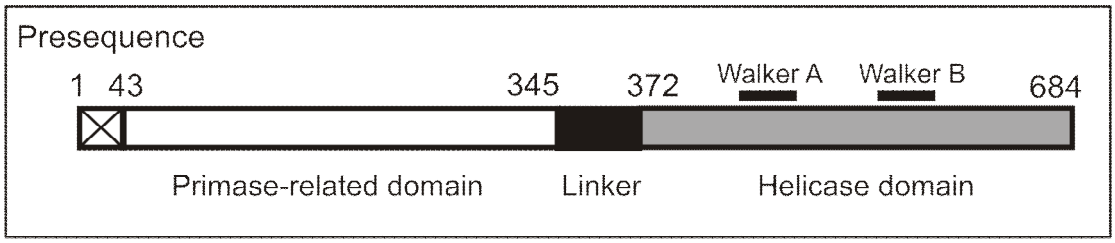

Figure 3.4: Schematic picture of the Twinkle protein. Predicted presequence and primase-related domain, which is similar to primase of bacteriophage T7, are possessed on the N-terminal part. The C-terminal helicase domain containing conserved Walker A and Walker B motifs is separated from the "primase" domain by the linker region.

Mutations in *PEO1* gene have been linked to several mitochondrial diseases associated with defects in mtDNA. Most of them cluster in the linker region and their implication on mtDNA maintenance have been recently studied using a three-dimensional Twinkle model (Korhonen *et al.* 2008). They have investigated that

some of the mutations absolutely abolish protein hexamerization and DNA helicase activity *in vitro* whereas others show only mild effects (Korhonen *et al.* 2008). However, experiments in cellular context have given slightly different results, consistent with late-onset phenotype suggesting mild functional defect (Goffart *et al.* 2009)

3.2.1.3 Mitochondrial single-stranded DNA binding protein

Human mitochondrial single-stranded DNA binding (mtSSB) protein of 132 AA, encoded on chromosome 7q34, forms a homotetramer that stabilizes the ssDNA during mtDNA replication (Tiranti *et al.* 1995). Stimulation of primer recognition and both DNA polymerase and proofreading activity of Polγ by mtSSB proteins enhance the mtDNA replication fidelity (Farr *et al.* 1999). Two new functions of mtSSB proteins in mitochondrial morphology maintenance have been proposed. MtSSB proteins have been suggested to regulate mitochondrial fusion and fission reaction and cellular response to apoptotic stimulation (Arakaki *et al.* 2006).

3.2.1.4 Adenine nucleotide translocator

The adenine nucleotide translocator (Ant), a channel embedded in the inner mitochondrial membrane, is responsible for exchange of intramitochondrial ATP for cytoplasmic ADP and consequently controls the ATP supply of the cell. The Ant functions as a dimer of 30 kDa polypeptides encoded by *SLC25A4* gene on chromosome 8 and has multiple isoforms with tissue-specific expression in mammals (Stepien *et al.* 1992). Human Ant1 is mainly expressed in heart and skeletal muscle, Ant4 in testis, Ant2 is either absent or expressed in proliferating tissues, while Ant3 is ubiquitously expressed. In contrast, three mouse Ant isoforms are homologous to the human Ant1, Ant2 and Ant4, but only expression pattern of Ant1 corresponds to Ant1 in humans (Levy *et al.* 2000; Dolce *et al.* 2005). Dominant mutations in *SLC25A4* gene affect its functions in mtDNA maintenance and cause mitochondrial diseases (Kaukonen *et al.* 2000).

3.2.1.5 Mitochondrial transcription factor A

Mitochondrial transcription factor A (Tfam) represents one of the main components of mitochondrial nucleoids and mtDNA maintenance. This 162-AA protein encoded by *TFAM* gene on chromosome 10q24, possesses two tandem HMG box domains

with DNA-binding properties that are necessary to enhance promoter-specific transcription of mtDNA together with mitochondrial transcription factor B1 and B2 (Dairaghi *et al.* 1995; Falkenberg *et al.* 2002). The amount of Tfam in mammalian cells closely correlates with amount of mtDNA but not with the transcription level due to the proposal model where mtDNA replication is coupled with mtDNA transcription (Kanki *et al.* 2004; Pohjoismaki *et al.* 2006). In mammals, Tfam can entirely cover and pack mtDNA to form nucleoid structures associated with mitochondrial inner membrane (Alam *et al.* 2003).

3.2.1.6 Mitochondrial DNA topoisomerase I

In mammalian cells, the mitochondrial topoisomerase I (Top1mt) is the only mitochondrial-specific enzyme responsible for maintaining mtDNA topology during replication and transcription. Top1mt that belongs to type IB topoisomerases is encoded on chromosome 8q24.3 and shows striking sequential and biochemical similarity to nuclear topoisomerase I except the mitochondrial targeting sequence in the N-terminal domain (Zhang *et al.* 2001). Human topoisomerase IIIα (hTop3α) has dual cellular localization due to its two potential start codons. The 1 001-AA isoform resides to mitochondria and 976-AA isoform to nucleus (Wang *et al.* 2002).

3.2.1.7 ATPase family AAA domain-containing protein 3

Recently, ATPase family AAA domain-containing protein 3 (Atad3) has been identified as DNA binding protein present in mitochondrial nucleoids that associate with mitochondrial inner membrane (He *et al.* 2007). This 72 kDa protein encoded on chromosome 1p36.33, preferentially binds to triple-stranded region of D-loop (7S DNA) but its variable amounts associated with mitochondrial nucleoids suggest only transient binding to subpopulation of mtDNA. The proposed role of Atad3 in mitochondria is in nucleoids formation and segregation (He *et al.* 2007).

3.2.2 Mitochondrial DNA replication and expression of mtDNA genes

3.2.2.1 MtDNA replication

Replication of mtDNA situated in the mitochondrial matrix proceeds throughout the cell cycle and also in post-mitotic cells. For more than 20 years, it had been believed to proceed by generally accepted strand-asynchronous, asymmetric mechanism (Clayton 1982). Recently, this orthodox model has been challenged by presenting new findings utilized by two-dimensional neutral agarose gel electrophoresis (2D-NAGE; Holt *et al.* 2000; Bowmaker *et al.* 2003).

In the strand-asynchronous model where the mtDNA molecules are replicated unidirectionally from two independent and temporally distinct origins, the DNA synthesis starts at O_H which is located downstream of the LSP in the D-loop region. It proceeds along the parental L-strand to produce full daughter H-strand. At two-thirds of the way from O_H, the replication fork reaches a 30-nucleotide long non-coding region which contains the origin of L-strand (O_L, figure 3.3). When parental H-strand is displayed, the L-strand origin is exposed and synthesis of daughter L-strand is initiated in the opposite direction (reviewed by Taanman 1999). The evidences that support asymmetrical model have been reported using atomic force microscopy and 2D-NAGE (Brown *et al.* 2005). Moreover, Brown et al have suggested that some of the mtRNAs, in form of R-loops, stably associate with mitochondrial dsDNA throughout the circular genome (Brown *et al.* 2008).

Replication in the strand-coupled model begins exclusively at or near the O_H and proceeds unidirectionally around the entire mtDNA molecule. In this model, mtDNA replication intermediates (RIs), called RITOLS (an acronym for RNA-incorporation throughout the lagging strand), consist of RNA-DNA hybrids that might function as primers for maturation of L-strand DNA that iniciates from the previsously designated O_L (Holt *et al.* 2000; Yang *et al.* 2002; Yasukawa *et al.* 2006). This model can also explain the findings from 2D-NAGE (Brown *et al.* 2005). Further analysis of replication intermediates has demonstrated that strand-coupled replication of mtDNA initiates bidirectionally in the broad origin zone (ori-Z) spanning 4-6 kbp downstream of the major non-coding region (NCR). After the replication fork arrest at O_H, the replication intermediates of ongoing synthesis are

undistinguishable from RIs in the unidirectional mechanism (Bowmaker *et al.* 2003). It seems that replication modes might be tissue-specific and/or different modes operate in the same cells, however the exact consensual mechanism of mtDNA replication as well as the incorporation of ribonucleotides into the RIs remains undetermined.

3.2.2.2 Transcription of mtDNA and translation of mitochondrial genes

The expression mode of mitochondrial genes reflects the peculiar features of mitochondrial genome structure. Transcription of H-strand is initiated from distinct sites as two overlapping units: the initiation site H1 (IT_{H1}), located 19 nt upstream of the gene for $tRNA^{Phe}$, produces a short polycistron that covers two rRNA genes and terminates at the end of the gene for 16S rRNA (figure 3.3). This transcript is produced 25 times more frequently than a long H-strand polycistron that starts at the initiation site H2 (IT_{H2}), close the 5´-end of gene for 12S rRNA. The long polycistronic molecule corresponds to almost whole H-strand, covering two 12 tRNA genes and 12 polypeptides genes. The initiation site for L-strand (IT_L), localized 150 bp from $IT_{H1,}$ gives arise to single polycistronic molecule that derives eight tRNAs and the ND6 mRNA (figure 3.3; Montoya *et al.* 1983). The mitochondrial H-strand and L-strand promoters (HSP and LSP, respectively) where the H1 and L initiation sites are located, contain enhancer elements immediately upstream to the initiation points as well as binding sites for specific transcription factors. Mitochondrial transcription is catalyzed by monomeric mtRNA polymerase (Polrmt) that requires Tfam and one of mitochondrial transcription factor B paralogues, Tfb1m or Tfb2m (Falkenberg *et al.* 2002). Only the transcription of short H-strand polycistron is specifically terminated by mitochondrial transcription terminator (mTerm), a 39 kDa protein that binds to 3´-end of $tRNA^{Leu}$ and constitutes the physical barrier for RNA polymerase (figure 3.3; Kruse *et al.* 1989).

Translation of mtDNA genes takes place on mitochondrial ribosomes or mitoribosomes that are localized in the matrix of the organelle and consist of 12S and 16S rRNAs encoded by mtDNA, and several proteins encoded by nuclear DNA. Mitochondria use modified genetic code with simplified decoding mechanism. The mitochondrial tRNAs and rRNAs are very small and tRNA genes flank all protein and rRNA genes to produce mature RNAs by processing the long polycistronic transcripts. Mitochondrial mRNAs lack the specific features of other mRNAs such

as 5´ and 3´-untranslated regions (might have 1-3 nt at untranslated 5´-end), 3´ polyadenylation signal (polyadenylation tail of 55 A residues starts immediately after stop codon) or 7-methylguanosine cap structure at 5´-end (Montoya *et al.* 1981, reviewed by Fernandez-Silva *et al.* 2003).

3.2.3 Mitochondrial nucleotide metabolism

For both nuclear and mitochondrial DNA synthesis, the pool of the precursors, deoxyribonucleotide triphosphates (dNTPs), is fundamental. On the basis of the actual stage of a cell or tissue, two separate pathways can salvage the mitochondrial dNTP pool with dNTPs. In growing or proliferative cells where nuclear DNA is replicated during the S-phase, the synthesis of dNTPs occurs *de novo* in cytosol (Reichard 1988). Here, two deoxynucleoside kinases: thymidine kinase 1 (TK1) and deoxycytidine kinase (dCK) phosphorylate deoxynucleosides to produce deoxynucloside monophosphates that are either transported to nucleus for nDNA replication or in form of diphosphates by the deoxynucleotide carrier (DNC) into the mitochondria (Dolce *et al.* 2001; Elpeleg 2003). In terminally differentiated or non-dividing cells the replication of nDNA does not occur and dNTP synthesis in cytosol is inhibited, deoxynucleosides for mitochondrial pool can be salvaged from extracellular fluid and intracellular degradation. In this salvage pathway, deoxynucleosides are introduced to mitochondrial matrix by equilibrate nucleoside transporter 1 (ENT1) and phosphorylated by mitochondrial deoxynucleoside kinases: thymidine kinase 2 (TK2) and deoxyguanosine kinase (dGK, Ferraro *et al.* 2005). Hence, replication of mtDNA proceeds throughout the cell cycle, independently on the nuclear DNA replication, and because mitochondrial dNTP pool is separated from the cytosol by impermeable inner mitochondrial membrane (Bestwick and Mathews 1982), the second salvage pathway becomes extremely important in case of non-dividing cells, such as in post-mitotic tissues (Pontarin *et al.* 2003). A balance of the four dNTPs in mitochondrial pool is essential for fidelity of mtDNA replication machinery, since several human diseases arise from inherited enzymatic deficiencies of either cytosolic or mitochondrial dNTP metabolism.

3.3 Opa1 protein and mitochondrial fragmentation

The Opa1 protein has been recently described as dynamin-related GTPase encoded in humans by the optic atrophy 1 (*OPA1*) gene on chromosome 3q28 (Delettre *et al.* 2000). The gene which spans more than 90 kbp, is composed of 30 coding exons and due to alternative splicing of either exon 4, 4b or 5b generates at least eight mRNA Opa1 isoforms. Particular isoforms are ubiquitously expressed throughout the human tissues (in the heart, skeletal muscle, liver, testis, kidney), predominantly in the brain and retina (Delettre *et al.* 2001; Olichon *et al.* 2007). The first heterozygous mutations in *OPA1* gene have been linked to autosomal dominant optic atrophy (ADOA, OMIM 165500), the most common non-syndromic mitochondrial hereditary optic neuropathy. So far, over 117 different mutations in the *OPA1* gene have been described causing ADOA (http://lbbma.univ-angers.fr/eOPA1/). Recently, optic atrophy with neuromuscular involvement, chronic PEO and the accumulation of multiple mtDNA deletions in the skeletal muscle, referred to as OPA1 ´plus´ syndrome has been characterized (Amati-Bonneau *et al.* 2008; Hudson *et al.* 2008).

3.3.1 Structure of Opa1 protein

The Opa1 protein, a large GTPase related to dynamin family, is localized to the inter-membrane space and associated with the inner mitochondrial membrane (Olichon *et al.* 2002). The Opa1 orthologs, the Msp1p in *Schizosaccharomyces pombe* (Pelloquin et al. 1999) and the Mgm1p in *Saccharomyces cerevisiae* (Shepard and Yaffe 1999) that are anchored to the matrix side of the inner membrane or to the outer membrane, respectively, are involved in mitochondrial morphology and maintenance. The Opa1 protein displays a coiled-coil C-terminal domain corresponding to the dynamin GTPase effector domain (GED) that is involved in catalytic activation, and the GTPase domain with three GTP-binding motifs and a dynamin signature. The N-terminal transmembrane domain (TM) is required for targeting the protein to the mitochondrial inner membrane (figure 3.5; Olichon *et al.* 2007; Akepati *et al.* 2008).

The function of Opa1 protein and its role in mitochondrial fragmentation is regulated by mitochondrial membrane potential ($\Delta\psi_m$) and correlates with processing of several Opa1 isoforms with distinct molecular sizes. mRNAs splice forms are

synthesized as precursors with the matrix-targeting signal (MTS) followed by a transmembrane domain. The N-terminal MTS is cleaved by the mitochondrial processing peptidase (MPP) during the import to form the mature long Opa1 isoforms (L-OPA1). Each long isoform, encoded by one of the eight mRNA splice forms, undergoes further processing at S1 cleavage site and some also a more C-terminal S2 cleavage site (in alternative exon 5b) to produce one or more short Opa1 isoforms (S-OPA1). It has been suggested that mitochondrial fusion depends only on L-OPA1 isoforms (Ishihara *et al.* 2006). Conversely, Song et al. found that mixture of long and short isoforms is important for efficient mitochondrial fusion activity (Song *et al.* 2007). At least three types of mitochondrial proteases are known to regulate Opa1 processing. Paraplegin, a subunit of the ATP-dependent m-AAA protease; mitochondrial rhomboid protease (PARL), an orthologue of Pcp1 protease that processes Opa1 orthologues Mgm1 and Yme1; and i-AAA protease (Duvezin-Caubet *et al.* 2007; Song *et al.* 2007).

However, detailed characterization of Opa1 isoforms in other model organisms has been absent. Recently, regulation of Opa1 processing in mouse tissues has been published. Akepati et al. showed that in mouse *OPA1* (*mOPA1*) gene exon 4 is not involved in alternative splicing resulting in four different splice variants. Further processing of Opa1 variants leads to a tissue-specific abundance of six isoforms (figure 3.5; Akepati *et al.* 2008).

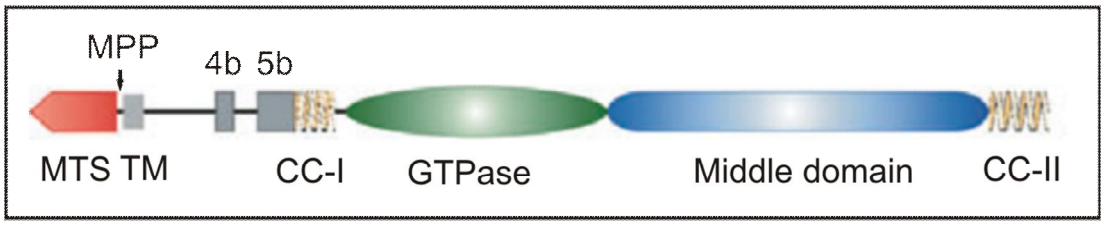

Figure 3.5: Structure of mouse Opa1 protein. Opa1 protein is imported into the mitochondria via MTS that is cleaved by MPP protease (denoted by the arrow) forming two long Opa1 isoforms. Domains 4b and 5b are encoded by exons 4b and 5b involved in alternative splicing. CC, coiled-coil domains; MPP, mitochondrial processing peptidase; MTS, matrix-targeting signal; TM, transmembrane domain; (modified from Akepati *et al.* 2008).

Loss of mitochondrial membrane potential ($\Delta\psi_m$) and ATP production due to mitochondrial dysfunction induces fast proteolytic processing of long to short Opa1 isoforms that leads to mitochondrial fragmentation and segregation of dysfunctional

mitochondria from the intact mitochondrial network. All Opa1 isoforms during the proteolytic conversion remain in mitochondria and are not release into the cytosol. The shift in the pattern of Opa1 isoforms was observed in patients and various model systems of human disorders associated with mitochondrial dysfunction (MERRF, MELAS, mtDNA depletion syndrome; Duvezin-Caubet *et al.* 2006).

3.3.2 Opa1 functions in cell

It has been already mentioned that Opa1 plays a key role in mitochondrial dynamics, but its precise function is not known and it is not clear how can mutated Opa1 impair mitochondrial function in cells. Olichon et al. showed that down-regulation of Opa1 in HeLa cells leads to fragmentation of the mitochondrial network due to fusion-fission imbalance, complete disorganization of the cristea, extreme sensitivity to endogenous apoptosis induction and dissipation of mitochondrial membrane potential (Olichon *et al.* 2003). Most of the mutations in *OPA1* gene cause premature truncation of the protein that leads to loss of the coiled-coil C-terminal domain and thus alteration of the GTPase activity which is necessary for the mitochondrial fusion (figure 3.5). Fibroblasts from patients with Opa1 mutation show fragmented mitochondrial network and decreased amount of Opa1 compared to the controls (Olichon *et al.* 2007; Zanna *et al.* 2008).

Recently, Zanna et al. have shown that Opa1 protein interacts with some respiratory complexes and apoptosis inducing factors (AIF) and thus reduced expression of Opa1 associates with significant impairment of oxidative phosphorylation, mostly at the level of complex I (Zanna *et al.* 2008).

3.3.3 Opa1 mouse models

In 2007, two groups have generated mouse models carrying mutations that are close to reported human mutations that cause ADOA.

Davies et al. have used nonsense mutation (1051C>T) in exon 8 of *OPA1* gene that results in truncation (Gln 285 to Stop: Q285X) of the protein immediately prior to the dynamin-related GTPase domain (Davies *et al.* 2007). Alavi et al. have reported a mouse model carrying a splice site mutation (c.1065+5G>A) that skips exon 10 and leads to an in-frame deletion in the GTPase domain of Opa1 protein (Alavi *et al.* 2007).

Both Opa1 mouse models display early embryonic lethality in the homozygous state. Heterozygous *OPA1* $^{WT/\ mut}$ mice show ~50% reduction in amount of Opa1 protein compared to controls that, in this state, is proposed to lead to haploinsufficiency. Moreover, they found increased fragmentation of the mitochondrial network in cells from *OPA1*$^{WT/mut}$ mice, optic nerve abnormalities (reduced number of axons, unusual shape of the remaining axons and mitochondria with disorganized cristea) and mild deficits in visual acuities that increased with age (Alavi *et al.* 2007; Davies *et al.* 2007). The Opa1 protein is essential in mammalian development and haploinsufficiency is the main disease mechanism. These conclusions are consistent with findings in human patients with ADOA (Davies *et al.* 2007).

3.4 Autophagy/mitophagy

The essential aspect of cell physiology is the maintenance of cellular homeostasis within the environmental stress conditions. Part of this maintenance involves regulation and modification of biosynthetic and degradation pathways. In eukaryotic cells are two main protein degradation routes where lysosomes present the end point of degradation. In the first route, extracellular material is delivered to lysosomes by pinocytosis, phagocytosis and receptor-mediated endocytosis. In the second one, intracellular components are achieved by macroautophagy, microautophagy or chaperon-mediated autophagy (Dunn 1994).

3.4.1 Macroautophagy

Macroautophagy, usually referred to as autophagy, is responsible for the bulk degradation, typically activated by fasting and nutrient deprivation, and is necessary for generating amino acids, fueling the Krebs cycle and maintaining the ATP production (Kim *et al.* 2007). Moreover, it is thought to be important for the turn-over of whole organelles and long-lived proteins at a steady state level of a cell (Edinger and Thompson 2003; Mizushima *et al.* 2004). In contrast, it has been suggested that autophagy is associated with neurodegenerative diseases, cancer and programmed cell death during embryogenesis (Edinger and Thompson 2003; Mizushima *et al.* 2004).

In general, the autophagy mechanism initiates from a single-membrane structure, also called isolation membrane or phagophore that encloses portion of cytoplasm and organelles, resulting in formation of a double-membrane spherical autophagosome. Then, the outer membrane of the autophagosome fuses with the lysosome and the sequestered content is degraded together with the autophagosomal inner membrane, also called autophagic body, by lysosomal hydrolases. This degrading structure is termed autolysosome/ autophagolysosome and its lifetime is short compared to other organelles (figure 3.6; Yoshimori 2004).

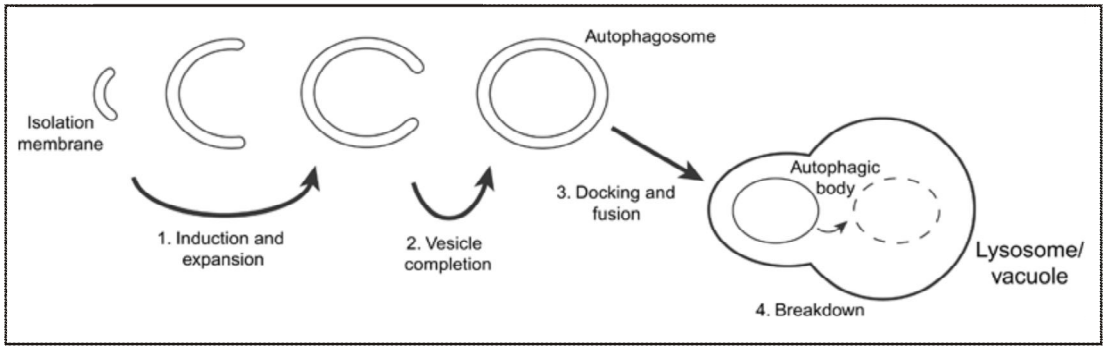

Figure 3.6: Model for autophagy. The basic mechanism is the sequestration of the cargo material by autophagosomes that lately fuse with lysosome/vacuole where autophagic body is consumed together with the cargo (van der Vaart *et al.* 2008).

So far, 31 gene products, encoded by autophagy-related (ATG) genes, have been identified to be required for the autophagic process in yeasts. However, the exact molecular function of most of them is unclear. Identification of their mammalian homologues suggests that molecular mechanisms of autophagy have been conserved in all eukaryotes (Klionsky *et al.* 2003). Most of these proteins (Atg3, Atg5, Atg7, Atg10, Atg12 and LC3) are involved in two ubiquitylation-like conjugation modifications of target proteins which function in formation of autophagosomes. (1) The Atg12-conjugation where Atg12 is attached to Atg5 is essential for the formation of pre-autophagosomes. Atg7, an E1-like enzyme, activates Atg12 which is transferred to Atg10, en E2-like enzyme, and conjugated to Atg5 to form an autophagosomal precursor. (2) LC3-modification where phosphatidylethanolamine (PE) is covalently linked to LC3, is essential for autophagosome formation (Mizushima *et al.* 2004; Tanida *et al.* 2004).

3.4.2 Microtubule-associated protein 1 light chain 3 (Map-LC3)

Microtubule-associate protein 1 (Map) light chain 3 beta (LC3) is essential for autophagy and widely use for its monitoring. In humans, three genes encode homologous LC3 proteins: *MAP1LC3A*, *MAP1LC3B* and *MAP1LC3C*, two of which (*LC3A* and *LC3B*) are conserved in mice (He *et al.* 2003). Like the LC3, a yeast orthologue Atg8 exists in two modified forms and plays a critical role in formation of autophagosomes in yeasts (Kabeya *et al.* 2000). After synthesis, Map1-LC3

(or ProLC3) is cleaved by cystein proteases generating a soluble LC3-I in cytosolic fraction and exposing its C-terminal glycine for further ubiquitylation-like reactions. Subpopulation of LC3-I is also activated by Atg7, transferred to Atg3, a second E2-like enzyme, and converted to LC3-II (Tanida *et al.* 2004). LC3-II is conjugated with PE and bound tightly to autophagosome and autolysosome membranes (figure 3.7). LC3 expression and following conversion are greatly enhanced under starvation conditions that induce autophagy. Thus, the number of autophagosomes correlates with the amount of LC3-II. When autophagosomes fuse with lysosomes, intra-autophagosomal LC3-II is degraded by lysosomal hydrolytic enzymes (figure 3.7; Kabeya *et al.* 2000; Kabeya *et al.* 2004).

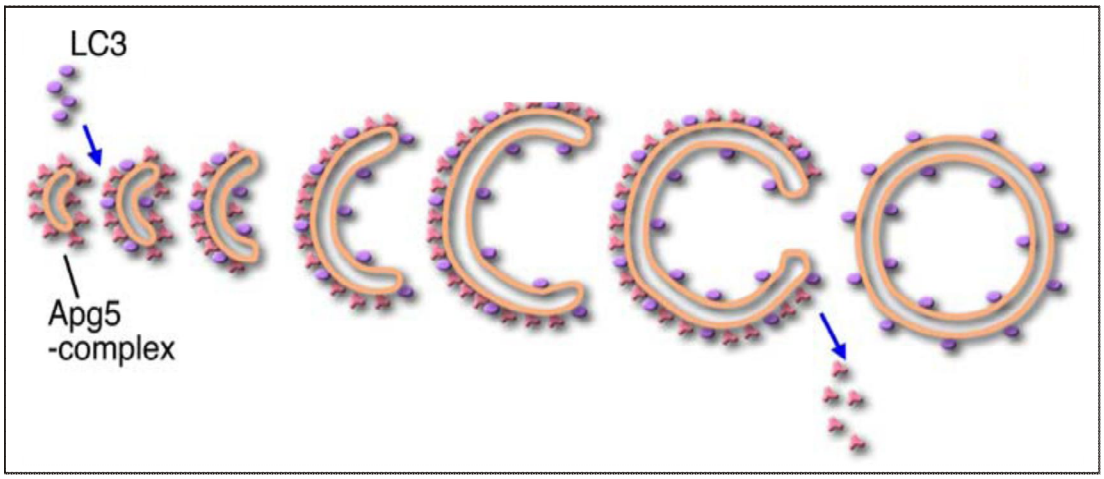

Figure 3.7: Schematic diagram of autophagosome formation in mammalian cells. A protein Apg5-complex in membrane of phagophore includes Apg5, Apg12 and Apg16L. It recruits LC3-II to the outer and inner membranes when the elongation of membranes is initiated. The Apg5-complex leaves the membrane just before or after membrane fusion, while LC3 remains (Yoshimori 2004).

Two more protein families have been identified as mammalian homologues of Atg8. γ-aminobutyric-acid-type-A (GABAA)-receptor-associated protein (GABARAP) and Golgi-associated ATPase enhancer of 16 kDa (GATE-16) also exist in form-II (PE-conjugated) and localize with LC3-positive autophagosomes induced by starvation. However, their precise role during autophagy is unknown (Kabeya *et al.* 2004).

3.4.2.1 LC3 mouse models

Transgenic mice systematically expressing LC3 fused with green fluorescent protein (GFP) and the method to monitor autophagy in mouse have been generated in 2004. Mizushima et al. have revealed five patterns of starvation that differ between organs. In the first group, autophagy is increasingly induced during the 48-starvation (e.g. heart, slow-twitching muscles); in the second group, the autophagy is significantly increased during the first 24-h starvation and then sustained (e.g. fast-twitching muscles, podocytes). In the third group, the autophagy is induced in the first 24-h starvation but reduced to basal level in the next 24-h (e.g. pancreas, liver). In the fourth group, the autophagy is constitutively active (e.g. thymic epithelial cells) in contrast to the fifth group where autophagy is not induced even after 48-h starvation (e.g. brain). The induction of autophagy is an organ specific process that does not always respond to nutrient starvation but might be more complex and involved in other regulations, for example in T-cell development (Mizushima *et al.* 2004).

Knockout mouse model of LC3β, a protein encoded by *MAP1LC3B* gene, has been generated by Cann et al. in 2008. Mice do not display compensatory increase in LC3α. Furthermore, their findings in starved LC3β -/- MEFs showed that LC3β is not required for the induction of autophagosomes under starvation conditions. Mouse can develop normally in the absence of LC3βI and II due to compensation by other ATG proteins (Cann *et al.* 2008).

3.4.3 Mitophagy

In general, autophagy is thought to be non-selective process. However, autophagosomes containing protein aggregates or specific organelles, such as endoplasmic reticulum, peroxisomes or mitochondria have been described. Thus, subgrouping the autophagy into selective and nonselective types has been defined; specific and exclusive elimination of structure as selective autophagy, whereas non-selective autophagy is when different components are eliminated randomly (van der Vaart *et al.* 2008).

Term mitophagy has been suggested to selective mitochondrial autophagy, though mechanisms targeting mitochondria for mitophagy are not well understood. Under normal conditions of living cells it has been demonstrated that autophagocytosed

mitochondria are characterized by three features. (1) Reduced membrane potential ($\Delta\psi_m$) of isolated non-fusing mitochondria that are produced by mitochondrial fission from intact mitochondrial network, (2) reduced Opa1 levels and (3) reduction of size. These mitochondria have reduced fusion capacity and are unlikely to be recovered by fusion into polarized network even before being targeted by autophagy (Twig *et al.* 2008). Mitochondrial dynamics where fusion triggers fission that is essential for autophagy, functions as a quality control mechanism that reins mitochondrial turnover (Twig *et al.* 2008).

In contrast, in hepatocytes during nutrient deprivation, mitochondrial fission occurs coordinately with autophagosomes formation. Moreover, phagophores or pre-autophagosomes go on to sequester completely the individual mitochondria which depolarize in about 10 min after ring closure. As mitochondria inside of autophagosomes or more specifically mitophagosomes depolarize, acidification occurs and sequestered content is degraded (Kim *et al.* 2007).

It has been previously proposed that mitochondrial permeability transition (MPT) represents a signal for targeting dysfunctional mitochondria to autophagic degradation during nutrient deprivation. In the MPT, opening of permeable transition (PT) pores in the mitochondrial inner membrane causes swelling that leads to depolarization and rupture of the outer membrane and release of cytochrome c into the cytosol (Elmore *et al.* 2001).

Recently, two new proteins involved in autophagic degradation have been found in yeasts. Uth1p, the protein initially identified in regulation of yeast lifespan, is mainly localized in mitochondrial outer membrane and is involved in the recognition of mitochondria by the autophagic machinery induced by rapamycin or nitrogen starvation (Kissova *et al.* 2004). Aup1p, encoded by YCR079w, is a yeast mitochondrial protein phosphatase homologue that localizes in the mitochondrial intermembrane space. This protein takes part in signal transduction mechanism that marks mitochondria for selective degradation through mitophagy in stationary phase yeast cells (Tal *et al.* 2007).

3.4.4 Mitochondrial protein acetylation on lysine residues

Dynamic post-translation modifications, such as a protein acetylation on lysine residues, play crucial role in regulation of many cellular processes including

DNA-protein interactions, subcellular localization, transcriptional activity and protein stability. Proteomic survey revealed 277 unique acetylation sites in 133 of mitochondrial proteins derived from both fed and fasted mouse liver mitochondria. This amount corresponds to ≈ 20% of all mitochondrial proteins (Kim *et al.* 2006).

Yeast silent information regulator 2 (Sir2) and its homologues belong to the Sirtuin family conserved from bacteria to humans (Onyango *et al.* 2002). This family of NAD+-dependent protein deacetylase/mono-ADP-ribosyl-transferase enzymes regulates gene silencing, aging, energy metabolism and mediates the effect of caloric restriction on lifespan extension in several organisms (Lin *et al.* 2002). In mammals, seven homologues (Sirt1-7) have been identified; three Sirtuins (Sirt1, Sirt6 and Sirt7) are localized to the nucleus; Sirt2 is the only one present in cytoplasm, and three Sirtuins (Sirt3, Sirt4 and Sirt5) reside in the mitochondria (Haigis and Guarente 2006).

3.4.4.1 Sirt3

Sirt3 is the first sirtuin identified in mitochondria (Onyango *et al.* 2002), however, its localization and function has been keenly discussed. Schwer et al. in 2002 have reported human Sirt3 (hSirt3) full-length protein of 43 kDa that is localized to mitochondrial matrix and is activated by cleavage of 142-AA from N-terminus (Schwer *et al.* 2002). In contrary, Scher et al. have proposed that full-length hSirt3 completely resides in nucleus and translocates to mitochondria under cellular stress, such as overexpression or apoptotic signals, where is localized in its processed form (Scher *et al.* 2007). Moreover, utilizing immunofluorescence microscopy, Cooper and Spelbrink have showed that hSirt3 is exclusive mitochondrial deacetylase (Cooper and Spelbrink 2008).

Discrepancies in localization of Sirt3 are not only the case of the human homologue. In 2005, Shi et al. have reported that murine Sirt3, preferentially expressed in brown adipose tissue, lacks N-terminal region corresponding to 142-AA residues of hSirt3 protein and is localized on the inner mitochondrial membrane (Shi *et al.* 2005). Recently, in agreement with their previous findings, Nakamura et al. have determined that murine Sirt3 resides in the inner mitochondrial membrane, but its localization is changed from mitochondria to nucleus when is co-expressed with Sirt5 (Nakamura *et al.* 2008). On the contrary, endogenous Sirt3 has been showed as soluble mitochondrial protein in mouse liver under both basal and stress conditions

(Lombard *et al.* 2007). In addition, they have generated *SIRT3* knockout mice that exhibit increase mitochondrial lysine acetylation compared to *SIRT4* and *SIRT5* knockout mice. Surprisingly, Sirt3-defficient mice are healthy and do not reveal morphological or metabolical alterations under starvation condition or cold exposure (Lombard *et al.* 2007).

Taken together, Sirt3 is thought to be a major mitochondrial deacetylase, but its exact function in cellular processes is not well known. Sirt3 shows regulation of mitochondrial functions. Its constitutive expression reduces membrane potential, decreases production of ROS and increases oxygen consumption (Shi *et al.* 2005). In 2006, two papers have demonstrated that reversible acetylation of acetyl-CoA synthetase 2 (AceCS2) modulated by Sirt3 in mitochondria, plays important role in acetate conversion for energy production under ketogenic conditions (Hallows *et al.* 2006; Schwer *et al.* 2006). Recently, two new enzymes have been identified to be deacetylated and thereby activated by human Sirt3: glutamate dehydrogenase (GDH), a central metabolic regulator in mitochondrial matrix, and isocitrate dehydrogenase 2, a key regulator in the tricarboxylic acid cycle (Schlicker *et al.* 2008).

3.4.4.2 Sirt4 and Sirt5

Sirt4 is also mitochondrial protein from Sirtuin family that resides in mitochondrial matrix, but lacks deacetylase activity. Sirt4 exhibits ADP-ribosyltransferase activity and is implicated in regulating amino acid-stimulation of insulin secretion in mice pancreatic β-cell by inhibition of GDH (Haigis *et al.* 2006).

Sirt5 is the least characterized protein from mitochondrial Sirtuins. Its substrates and functions in mammalian cells are largely unknown. Recently, Sirt5 has been localized to mitochondrial intermembrane space where deacetylates cytochrome c. However, it can translocate to mitochondrial matrix to play a role in communication between nucleus and mitochondria as Sirt3 translocates to nucleus when co-expressed with Sirt5 (Nakamura *et al.* 2008; Schlicker *et al.* 2008).

Sirt4- and Sirt5-deficient mice are healthy, fertile and do not exhibit increase mitochondrial protein hyperacetylation (Lombard *et al.* 2007).

3.5 Mitochondrial diseases

The mitochondrial diseases encompass a wide variety of multisystematic disorders with various combinations of clinical features that usually affect brain and muscle, probably because of their highest energetic requirements. Mitochondria are under the control of two genomes: mitochondrial, where 37 genes are directly or indirectly involved in OXPHOS, and nuclear that encodes all proteins operating in mitochondria. Genetic defects can occur in both genomes, thus mitochondrial disorders can be inherited by maternal or Mendelian trait or combination of the two.

3.5.1 Mutations in mtDNA causing mitochondrial disorders

The main features of mitochondrial diseases proceed from peculiar mitochondrial genetics that strikingly differ from nuclear. In general, mitochondria with all copies of mtDNA in cells are transmitted through the maternal line. Thus, homoplasmic mtDNA mutations are transmitted to all maternal offspring. In case of heteroplasmic mutations, the amount of mutant mtDNA differs between tissues and the threshold effect appears only with the high amount of mutant mtDNA molecules. Mutations of mtDNA can be divided in two groups: (1) inherited point mutations and (2) large-scale rearrangements (i.e. partial deletions and duplications).

3.5.1.1 Inherited point mutations in mtDNA

More than 200 point mutations may be homoplasmic or heteroplasmic and are usually maternally inherited (www.mitomap.org). Pathological mutations that arise in protein-enconding genes, affect specifically function of particular OXPHOS complex, while mutations in RNA genes impair the overall mitochondrial protein synthesis. Patients develop wide variety of clinical symptoms where abnormalities in central nervous system are frequently associated with mitochondrial myopathy. Most of the mutations in genes encoding complex I subunits have been associated with Leber hereditary optic neuropathy (LHON) characterized by acute or subacute loss of vision that usually affects males in early adulthood (Wallace *et al.* 1988). NARP, the neurogenic muscle weakness, ataxia and retinis pigmentosa is associated with mutations in *MT-ATP6* gene (Holt *et al.* 1990) and clinical features clearly correlate with the level of heteroplasmy. Furthermore, MELAS, a mitochondrial

encephalomyopathy with lactic acidosis and stroke-like episodes, is associated with the most frequent heteroplasmic point mutation in the $tRNA^{Leu}$ (3243A>G, Goto *et al.* 1990) and MERRF, a myoclonic epilepsy with ragged-red fibers (RRF) where transition 8344A>G in the $tRNA^{Lys}$ gene is the most common pathological mutation (Wallace *et al.* 1988, reviewed by McKenzie *et al.* 2004; Zeviani and Di Donato 2004).

3.5.1.2 MtDNA rearrangements

Over 100 large-scale mtDNA rearrangements including single large deletions or deletions conjugated with structurally related duplications, are always heteroplasmic (www.mitomap.org). A threshold level for rearranged molecules lacking a part of the mitochondrial genome, is 40 - 60% that is enough for OXPHOS failure. Three main diseases are associated with these mutations. CPEO, Chronic Progressive External Ophthalmoplegia is characterized with late-onset of ophthalmoplegia, proximal myopathy and exercise intolerance. Kearns-Sayre Syndrome (KSS) is usually sporadic disorder with the onset before age of 20 years, characterized by CPEO and pigmentary retinopathy, with additional features of cerebellar ataxia, cardiac conduction block and diabetes mellitus (Zeviani *et al.* 1988). Finally, Pearson Marrow-Pancreas Syndrome (PS) is a rare but usually fatal disorder involving hematopoetic system with severe exocrine pancreatic insufficiency (Rotig *et al.* 1990). Deletions can be found in muscle and blood in the comparable amount. However, multiple deletions of mtDNA are usually caused by defects in nDNA genes of mtDNA maintenance leading to subsequent intergenomic signaling impairment (reviewed by McKenzie *et al.* 2004; Zeviani and Di Donato 2004).

3.5.2 Instability of mtDNA caused by nDNA defects

3.5.2.1 Autosomal dominant progressive external ophthalmoplegia (adPEO)

Autosomal dominant PEO is a common mitochondrial disorder associated with multiple mtDNA deletions that belongs to the subgroup of human mitochondrial diseases caused by mutations in nuclear genes. The main clinical features of PEO patients include progressive weakness of extraocular muscles that limits the eye movements and general exercise intolerance. The disease onsets in the adulthood, the first signs arise in the range from 20 to 40 years of age. Muscle biopsies show the presence of RRF due to subsarcolemmal accumulation of abnormal mitochondria. The diagnosis depends on the detection of multiple mtDNA deletions in the skeletal muscle (Zeviani *et al.* 1989). Additional features are variable among families and may include sensory ataxia, motor peripheral neuropathy, cataracts, hearing loss, hypogonadism, parkinsonism, severe depression or avoidant personality (Suomalainen *et al.* 1997, reviewed by Spinazzola and Zeviani 2005). A secondary accumulation of large mtDNA deletions results from a primary defects in nDNA genes. Recently, the fifth gene that encodes Opa1 protein was attached to the group of four responsible genes: *POLG1, POLG2*, *PEO1* and *SLC25A4* (Amati-Bonneau *et al.* 2008; Hudson *et al.* 2008).

In 2000, the *SLC25A4* gene encoding Ant1 became the first gene linked to adPEO with multiple deletions, when Kaukonen et al. found one heterozygous missense mutation A114P and one sporadic mutation V289M, both in the transmembrane domain (Kaukonen *et al.* 2000). Phenotype of Ant1-PEO patients is relatively mild with slowly progressive myopathy and little extramuscular symptoms. Lately, new mutations, in particular T293C in Greek family and A90D mutation in German family have been found in adPEO families (Deschauer *et al.* 2005).

The mutations in *PEO1* gene that encodes Twinkle helicase protein are responsible for approximately 30% of the adPEO cases (Lamantea *et al.* 2002). The primarily identified missense mutations (i.e. A475P, A359T, W474C, W315L) and heterozygous 13 amino acids duplication (dup352-364) are localized in the linker region or in the helicase domain (figure 3.8). However, the impairment of hexamerization due to mutations in the linker region was not observed (Spelbrink *et al.* 2001). Lately, several new mutations in Twinkle in patients with adPEO, such as S369Y (Lewis *et al.* 2002), R303W (Agostino *et al.* 2003) or F370L (Jeppesen *et al.*

2008) have been described. Recently, using the molecular three-dimensional structure model of Twinkle has demonstrated that Twinkle with the pathogenic mutations (I367T and R374Q) in the linker region cannot form hexamers or unwind the duplex DNA due to lack of ATPase activity (Korhonen *et al.* 2008).

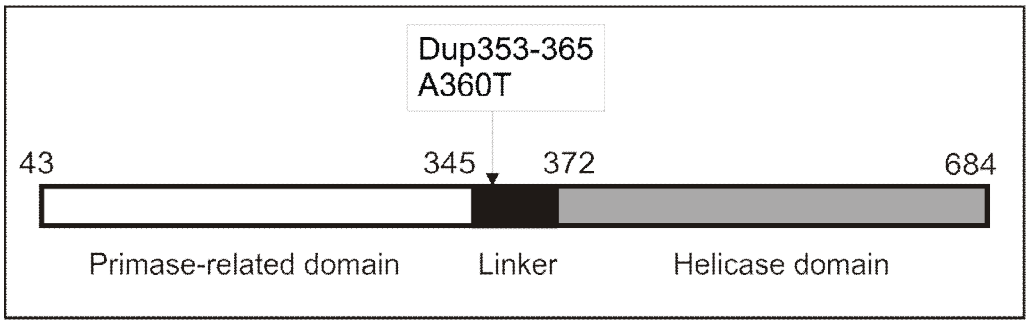

Figure 3.8: Schematic representation of mutations in Twinkle. The mutations in the linker were used to generate the transgenic Twinkle mice and the corresponding human mutations are linked to cause adPEO.

The dup352-364 mutation of PEO patient that affects the linker region of Twinkle protein has the most severe described phenotype of Twinkle-PEO patients (Spelbrink *et al.* 2001). They show multisystemic disorder with severe retarded depression. MtDNA deletions are detected in the skeletal muscle, brain and heart. The activities of respiratory chain enzymes show remarkable reduction in the skeletal muscle and brain. The various abnormalities in the mitochondria are observed in electron microscope in all tested tissues (Suomalainen *et al.* 1997).

The third gene, in which mutations are linked to adPEO, is *POLG1* encoding the catalytic subunit of mitochondrial Polγ. Dominant mutations are responsible for 45% of adPEO cases that have more complicated clinical phenotypes than those of Twinkle-PEO cases (Lamantea *et al.* 2002). The first heterozygous mutation (Y955C) was identified in the Belgium family diagnosed with symptoms of PEO, muscle weakness and multiple mtDNA deletions with RRF found in muscle biopsies (Van Goethem *et al.* 2001). To date, all autosomal dominant mutations in *POLG1* causing PEO (with one exception) are located in the polymerase domain of the enzyme, i.e. Y955C mutation leads to loss of polymerase activity and decrease in processivity of Polγ (Graziewicz *et al.* 2004). However, most of the mutations found in *POLG1* gene are associated with autosomal recessive PEO (arPEO) and patients are usually presented as compound heterozygotes with two arPEO alleles.

POLG2 gene encoding the accessory subunit of Polγ is the fourth gene where heterozygous dominant mutation causes adPEO with multiple mtDNA deletions (Longley *et al.* 2006). Mutated protein can not bind with the catalytic subunit and fails to stimulate progressive DNA synthesis. This leads to stalling of the Polγ in the replication fork and producing mtDNA deletions that cause COX deficiency in muscle fibers (Longley *et al.* 2006).

3.5.2.2 Other phenotypes caused by mutations in Twinkle

Infantile onset spinocerebellar ataxia (IOSCA, OMIM 271245), a typical example of the Finnish disease heritage, is caused by recessive mutations in the *PEO1* gene. This severe neurodegenerative disorder manifests at the age of 9-18 months as ataxia, muscle hypotonia and loss of deep tendon reflexes. Morphological characterization includes sensory axonal neuropathy and progressive neuropathy of the cerebellum, brain stem and spinal cord (Koskinen *et al.* 1994). Two pathological relevant mutations in *PEO1* gene have been linked to IOSCA patients. Finnish patients are either homozygotes for the founder missense substitution of an adenine to guanine leading to an Y508C change or compound heterozygote having the founder mutation and 1472C>T mutation affecting allelic expression level (Nikali *et al.* 2005). Interestingly, PEO patients with dominant Twinkle mutations are characterized by presence of multiple mtDNA deletions in the skeletal muscle, whereas IOSCA patients with recessive mutations do not show any signs of mtDNA defects but harbor mtDNA depletion in the brain and liver. Thus, IOSCA have become a member of mtDNA depletion syndromes (Hakonen *et al.* 2008).

MtDNA depletion syndrome (MDS) is a highly heterogeneous group of disorders associated with recessive mutations in nuclear genes of mtDNA maintenance proteins or dNTP metabolism enzymes. Clinically, they include hepatocerebral and myopathic forms of diseases, genetically characterized by a reduction in mtDNA copy number (Moraes *et al.* 1991). MDS associated genes include for example *TK2*, *DGUOK*, *POLG1*, *SUCLA2* or *TP* (reviewed by Sarzi *et al.* 2007). Recently, recessive pathological mutations in the Twinkle protein leading to MDS have been reported, two compound hetorozygotes for Y508C and A318T mutations (Hakonen *et al.* 2007) and two homozygous patients for T457I mutation (Sarzi *et al.* 2007).

3.5.2.3 Mutations in the *OPA1* gene causing ADOA

Autosomal dominant optic atrophy (ADOA, OMIM 165500) is non-syndromic mitochondrial hereditary optic neuropathy (http://lbbma.univ-angers.fr/eOPA1/). This disease usually begins before 10 years of age with moderate-to-severe loss of visual acuity, optic nerve pallor, abnormalities in color vision and centocoecal scotoma. Retinal ganglion cell degeneration has been suggested as a main cause that leads to atrophy of the optic nerve (Delettre *et al.* 2002).

Four gene loci have been linked to cause ADOA and other optic atrophies: *OPA1* (3q28-29), *OPA3* (19q13.2-13.3), *OPA4* (18q12.2-12.3) and *OPA5* (22q12.1-q13) (Olichon *et al.* 2007). Mutations, predominantly described in *OPA1* gene, include substitutions, deletions or insertions and are spread over the coding region of the gene, but their functional consequences in ADOA patients are not well understood. The R455H mutation of Opa1 that alters GTPase domain has been found to be involved in ADOA and moderate progressive deafness (ADOAD; Amati-Bonneau *et al.* 2005). Reduction of mtDNA copy number has been found in patients with ADOA associated with mutations in *OPA1* gene (Kim *et al.* 2005).

In 2008, two new cases of ADOA associated with multiple mtDNA deletions in skeletal muscle have been described. Hudson et al. have presented family with bilateral visual failure and optic atrophy of childhood onset, following by ophthalmoplegia, a combination of cerebellar and sensory ataxia in adulthood and hearing impairment. Affected respiratory chain complex I and mosaic defect of complex IV (COX) have been identified in a muscle homogenate or muscle fibers. Multiple mtDNA deletions have been detected in patient skeletal muscle. Sequencing of entire mitochondrial genome has revealed a previously unreported nucleotide transition in *MT-ATP6* gene (Hudson *et al.* 2008).

Amati-Bonneau et al. have reported new symptomatic form of optic atrophy with sensorineural deafness, cerebellar ataxia, axonal sensory-motor polyneuropathy and mitochondrial myopathy with RRF and COX negative fibers. The OPA1 ´plus´ symptoms, frequently complicated by CPEO and accumulation of multiple mtDNA deletions in the skeletal muscle, are caused by five dominant missense point mutations changing amino acids in Opa1 GTPase domain (Amati-Bonneau *et al.* 2008).

3.6 The transgenic Twinkle mice

3.6.1 Twinkle transgene and generating of mice

Transgenic Twinkle mice have been generated in the laboratory of Prof. Anu Suomalainen (Tyynismaa *et al.* 2005). The mutation corresponding to the in-frame 39-bp duplication at nucleotides 1053-1092 (c.1053_1092dup) of the human *PEO1* gen causing adPEO in patients, was used to create transgenic mouse with a duplication of amino acids 353-365 (dup353-365, figure 3.8) in mouse Twinkle protein and referred to as the Deletor mice ($Twinkle^{dup}$). The transition 1075G>A in the human *PEO1* gene, was designed to create transgenic mice with substitution of threonine for alanine at amino acid position 360 (A360T, figure 3.8) in mouse Twinkle protein and referred to as the AT mice ($Twinkle^{AT}$). Using pHBApr-1-neo with mouse Twinkle cDNA + intron 4 have allowed the expression of full-length Twinkle as well as its splice variant Twinky under β-actin promoter. The final DNA constructs were linearized with *Bgl*II and *Nde*I and after the purification they were injected to mouse fertilized oocytes by pro-nuclear microinjection. From pseudo-pregnant carrier females were obtained four founder mice (C, D, E, F mouse lines) expressing dup353-365 mutation that corresponds to dup352-364 mutation of PEO patients and three founder mice (G, H, I mouse lines) with A360T mutation that corresponds to A359T PEO patient mutation (Spelbrink *et al.* 2001). The transgenic mice developed normally, had a normal lifespan and could reproduce. Mice from F1 generation were bred to produce F2 homozygous mice that also had normal lifespan and development.

3.6.2 Characterization of the transgenic Twinkle mice

First signs of mitochondrial myopathy were noted at the age of 12 months in the Deletor skeletal muscle (figure 3.9). Histochemical analysis has shown COX negative (COX^-) muscle fibers without increased SDH staining (SDH^+), indicating dysfunction of respiratory chain without increased mitochondrial proliferation. Skeletal muscle of 18-month-old Deletor has shown COX^-/SDH^+ fibers (figure 3.9). All these findings correspond with the relative age of onset with human disease when related to the expected lifespan (Suomalainen *et al.* 1997). No changes in the

amount of COX^-/SDH^+ fibers in the Deletor heart muscle compared to wild type controls have been detected.

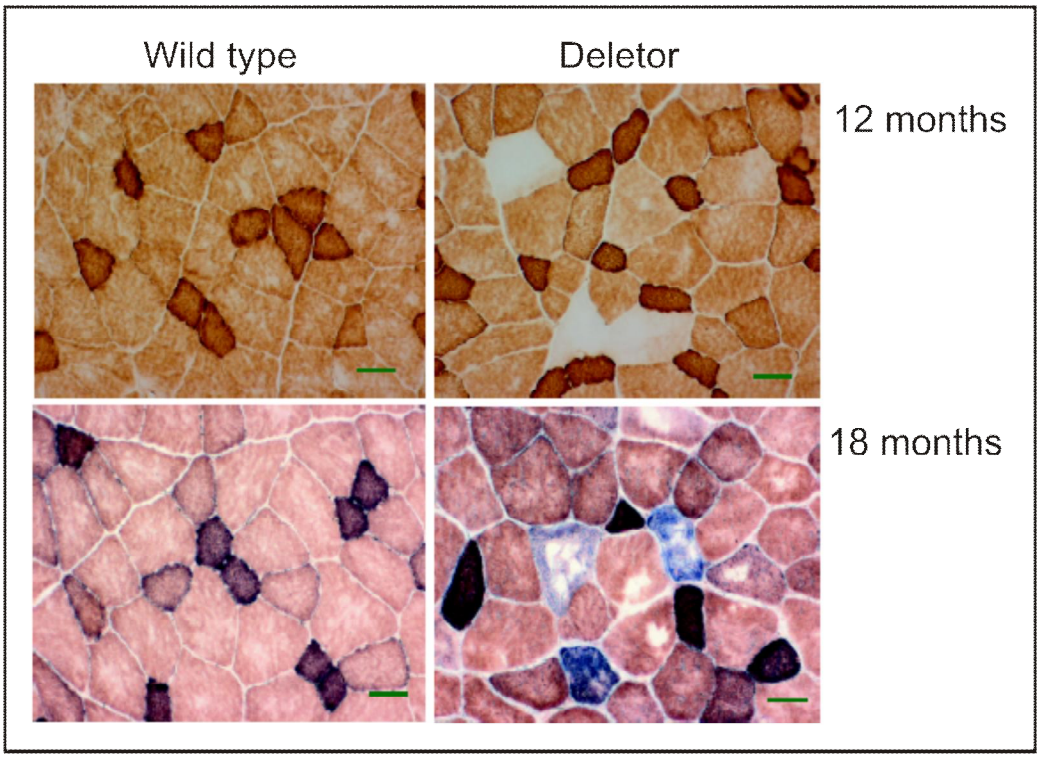

Figure 3.9: Histochemical double staining of the skeletal muscle. The muscle fibers with normal COX activity are stained light and dark brown (wild type 12 and 18 months). The COX deficient (COX^-) muscle fibres are not stained and remain white as shown in 12-month-old Deletor sample. The accumulation of mitochondria is shown by excessive SDH activity (SDH^+, blue) in affected muscle of the 18-month-old Deletor. Scale bars: 50 µm (modified from Tyynismaa *et al.* 2005).

Histochemical analysis of 18-month-old Deletor brain has shown COX^-/SDH^+ in ≈1% of Purkinje cells in the cerebellum; most of large pyramidal neurons and those of indusium griseum in the cerebrum. A few COX^-/SDH^+ neurons were identified from the olfactory bulbs, substantia nigra and the hypothalamus. MtDNA depletion or accumulation of mtDNA deletions could cause the COX deficiency in these neurons. Findings of COX deficiency in Purkinje cells of the transgenic mice or in humans have not been previously described but their loss has been noted in patients with mtDNA maintenance defects (Van Goethem *et al.* 2004).

The features of mild muscle phenotype with only few COX^- fibers present in AT mice were consistent with PEO patients carrying the same missense mutation. A359T human patient develop late-onset PEO at ≈ 50 years with moderate myopathy and no CNS involvement (Spelbrink *et al.* 2001).

Interestingly, only mildly decreased or low normal activities of respiratory chain complexes I, III and IV that contain mtDNA-encoded subunits were shown in affected muscles (Tyynismaa *et al.* 2005). In line with these findings, the transcript analysis has revealed impaired energy metabolism and signs of starvation in the Deletor muscle. Thus, a respiratory chain deficiency leads the cell to catabolism: activation of autophagy and utilization of structural proteins (Tyynismaa, personal comunication).

Furthermore, electron microscopy of the Deletor mildly affected muscle fibers has exhibited enlarged mitochondria and their increased number in subsarcolemmal region (figure 3.10). The cristea structures in these mitochondria have been recognizable compared to the severely affected fibers where large mitochondria had concentric cristae, resembling onion-like structures and electron-dense inclusions. Mitochondria found in autophagosomes point to autophagic degradation, called mitophagy (figure 3.10).

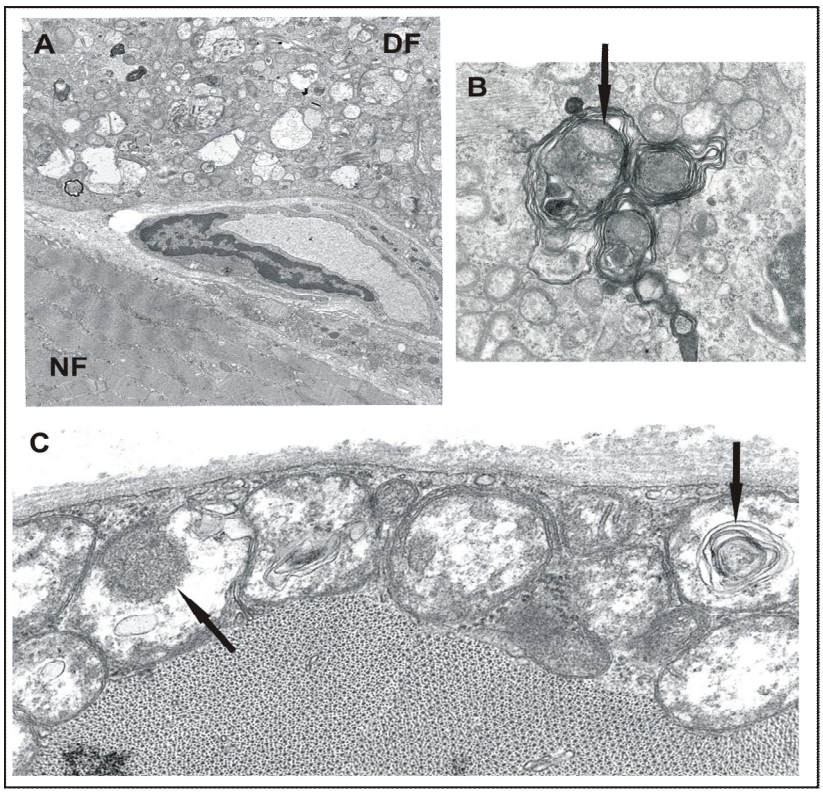

Figure 3.10: Electron microscopy pictures of the Deletor skeletal muscle. A, the muscle section shows a normal fiber (NF) with a highly organized structure and a defective fiber (DF) with an abnormal mitochondria. **B**, autophagosomes with sequestered mitochondria (indicated by arrow). **C**, the enlarged mitochondria in subsarcolemmal region of a muscle fiber. The left arrow points to an inclusion inside an enlarged mitochondria and the right arrow to onion-ring like cristae (modified from Tyynismaa *et al.* 2005).

Accumulation of multiple mtDNA deletions is main feature of patients with Twinkle-PEO mutations. The 3-kb "minimal mtDNA molecules" consisted of 12S rRNA, 16S rRNA and the D-loop region were amplified from muscle of the Deletor mice (figure 3.11). However, amplification of mtDNA from brain has revealed molecules from full-length to ≈3 kb in size (figure 3.11). DNA sequence analysis has revealed similar deletion hotspots in the muscle and brain suggesting that these sites form major deletions in transgenic Twinkle mice. The quantification of mtDNA copy number in the Deletor mouse tissues has revealed mtDNA depletion only in the brain. MtDNA level as well as somatic mtDNA point mutation load in the Deletor muscle samples was similar to those of the non-transgenic controls.

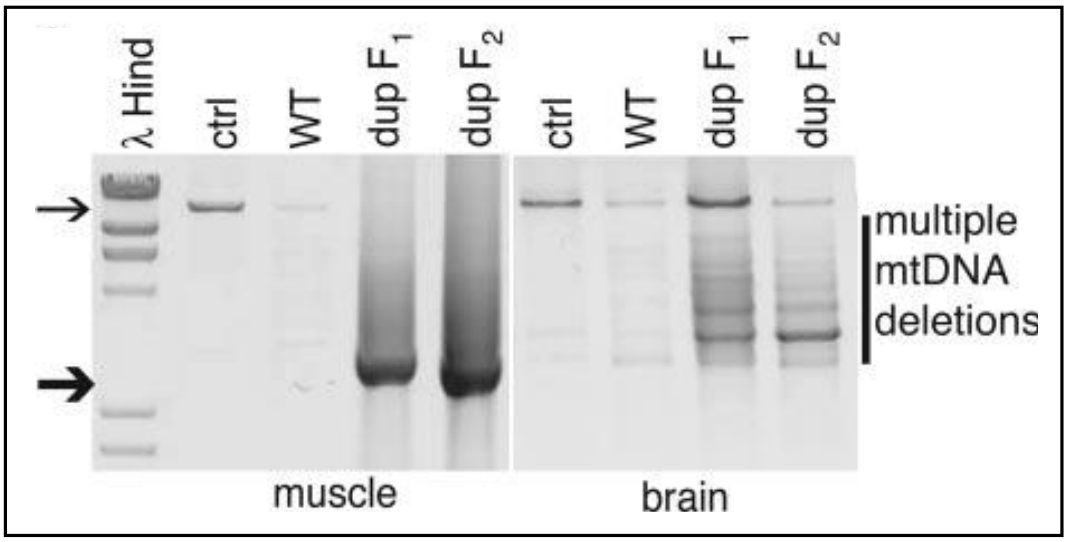

Figure 3.11: Multiple mtDNA deletions in the Deletor skeletal muscle and brain. The 3-kb "minimal mtDNA molecules" in the muscle are pointed by the thick arrow, whereas the full length mtDNA molecules by the thin arrow. The range of deleted mtDNA molecules in the brain is also indicated (modified from Tyynismaa *et al.* 2005).

4. Materials and Methods

4.1 Animals

This work was approved by the University of Helsinki, animal care committee (Helsinki, Finland), and all experiments were done in accordance with good practice of handling laboratory animals.

Transgenic animals of inbred strains FVB/N and BALB/c utilized in this work were generated in the laboratory of Prof. Anu Suomalainen (Tyynismaa *et al.* 2005) and referred to as the Deletor mice (C – F mouse lines). For the mtDNA deletions assays the liver, kidney, testis and intestine from the Deletor males and females mice aged 15 – 17 months were tested. The skeletal muscle, brain, liver and heart samples from mice aged 22 – 26 months were collected and used for tissue homogenates or mitochondrial enrichment isolation.

Transgenic animals referred to as the AT mice (G – I mouse lines) were also generated in the laboratory of Prof. Anu Suomalainen (Tyynismaa *et al.* 2005). The skeletal muscle and brain samples from males and females mice aged 15 – 17 months were tested for mtDNA deletions.

Wild type Twinkle overexpressor (A and B mouse lines), generated in the laboratory of Prof. Anu Suomalainen (Tyynismaa *et al.* 2004) were used to set up the method of DNA walking.

Deletor littermate mice with normal Twinkle genotype were used as wild type negative control. In each assay, animals at the same age as the Deletor or AT mouse littermates were tested.

4.2 Equipment

Centrifuges:

Centrifuge 5804R (Eppendorf, Germany)

Centrifuge Allegra 25R (Beckman Coulter, Inc., Germany)

PCR cycler:

PTC-200 (MJ Research, Biorad, USA)

Scanner:

Typhoon 9400 scanner (Amersham Biosciences, USA)

Freezer:

Thermo model 720 (-80 °C) (Thermo Electron Corporation, USA)

Electrolux Intuition (-20 °C)

Spectrophotometer:

UV-2401 PC (Shimadzu)

Nanodrop (ND-1000, NanoDrop Technologies, Inc,USA)

Western blotting equipment:

Glasses, tanks and plastic equipment (BioRad)

Semi-dry blotter:

Semiphor transphor unit (Amersham Biosciencies, USA)

Light Microscope:

Axioplan 2 Universal Microscope (Zeiss)

4.3 Buffers and solutions

Buffer used for DNA isolation

DNA isolation buffer – 200 ml:

5 ml 20 % SDS (MP biomedicals, LLC)

4 ml 5 M NaCl (Sigma)

10 ml 1 M Tris-HCl pH 8.1 (Sigma)

8 ml 0.5 M EDTA (Sigma)

Buffers for mitochondria isolation and sucrose gradient

HIM buffer – 500 ml:

200 mM mannitol (Sigma)

70 mM sucrose (Sigma)

10 mM HEPES (Sigma)

1 mM EGTA (Sigma)

pH 7.5 with KOH

1 M / 1.5 M sucrose – 2.2 ml each:

1 M / 1.5 M sucrose (Sigma)

10 mM HEPES pH 7.4 (Sigma)

10 mM EDTA (Sigma)

PBS – phosphate-buffered saline 1x

+ protease inhibitors (PBS+, Roche)

Buffer used for tissue homogenates

RIPA buffer:

0.75 M NaCl (Sigma)

5 % NP40 (Sigma)

2.5 % sodium deoxycholate (Sigma)

0.5 % SDS (MP biomedicals, LLC)

0.25 M Tris-HCl pH 8.0 (Sigma)

10 mM DTT (Sigma)

protease inhibitors

Loading buffer for SDS-PAGE -10 ml:

1.5 ml 1 M Tris-HCl pH 6.8

600 µl 20% SDS (MP biomedicals, LLC)

3 ml glycerol (Sigma)

1.5 ml β-merkaptoethanol (Sigma)

0.0018 g bromphenol blue

Buffers used for Blue-Native PAGE (BN-PAGE)

3x Gel Buffer (3xGB) – 100 ml:

(1.5 M aminocaproic acid, 150 mM Bis-tris , pH 7.0)

19.68 g aminocaproic acid (Sigma)

3.14 g Bis-Tris (Sigma)

MB2 buffer:

0.5 ml 3x GB

0.5 ml 2 M aminocaproic acid (13.12g /50 ml) (Sigma)

4 µl 500 mM EDTA (Sigma)

SBG – sample buffer – 10 ml:

(750 mM aminocaproic acid, 5 % Serva Blue G)

3.75 ml 2 M aminocaproic acid (13.12g /50 ml) (Sigma)

0.5 g Serva Blue G (Serva)

Solutions used for Coomassie Blue staining

Coomassie Fix solution:

50 % methanol (Fluka)

10 % acetic acid (Fluka)

Coomassie Blue solution – 1 l:

2 g Serva Blue (Serva)

75 ml glacial acetic acid (Fluka)

500 ml ethanol (Fluka)

Coomassie Blue distain solution:

450 ml methanol (Fluka)

100 ml acetic acid (Fluka)

400 ml H_2O

Solution used for Complex I activity assay

1 mM stock NADH (Roche)

Complex I activity solution – 20 ml:

4 ml 1mM NADH (Roche)

16 ml 0.1 mM Tris-HCl pH 7.4 (Sigma)

20 mg nitrotetrazolium blue chloride (Sigma)

Buffers used for COX/ SDH staining

0.05 M phosphate buffer:

Buffer A: 1.3799 g NaH_2PO_4 x H_2O (Sigma)

50 ml H_2O

Buffer B: 1.4196 g Na_2HPO_4 (Sigma)

50 ml H_2O

9.5 ml of buffer A, 40.5 ml of buffer B and H_2O were mixed to final volume 150 ml. pH 7.4 was determined and H_2O was added to get 200 ml of final volume.

COX-incubation buffer:

9 ml 0.05 M phosphate buffer

5 mg DAB (Sigma)

20 mg catalase (Sigma)

10 mg cytochrome c (Sigma)

750 mg sucrose (Sigma)

SDH-incubation buffer:

10 ml 0.05 M phosphate buffer

10 mg Nitro blue tetrazolium (Sigma)

50 mg sodium succinate (Fluka)

Table 4.1: Solutions for prepration SDS-PAGE

Solutions	Stacking gel	Separating gel		
	4 %	**10 %**	**12 %**	**15 %**
H_2O	6.1 ml	4.0 ml	3.4 ml	2.4 ml
0.5 M/1.5 M Tris-HCl	2.5 ml	2.5 ml	2.5 ml	2.5 ml
30 % acrylamid	1.3 ml	3.4 ml	4.0 ml	5.0 ml
20 % SDS	50 µl	50 µl	50 µl	50 µl
10 % APS	50 µl	50 µl	50 µl	50 µl
TEMED	5 µl	5 µl	5 µl	5 µl

5x running buffer – 1 l:

15 g Tris-HCl pH 8.3 (Sigma)

72 g Glycine (Sigma)

3 g SDS (MP biomedicals, LLC)

1x transfer buffer – 1 l:

2.213 g CAPS (Sigma)

100 ml methanol (Fluka)

pH 11 with NaOH

1x TBS-T – 1 l:

2.42 g Tris (Sigma)

8.0 g NaCl (Sigma)

1 ml Tween 20 (Amresco)

1x Towbin buffer – 1 l:

3.03 g Tris (Sigma)

14.41 g Glycine (Sigma)

0.5 g SDS (MP biomedicals, LLC)

200 ml methanol (Fluka)

4.4 Antibodies and enzymes

4.4.1 Antibodies

Table 4.2: The antibodies used for SDS-PAGE and BN-PAGE

Primary antibodies			
Name	**Animal source**	**Clonality**	**Company**
anti-LC3B	rabbit	polyclonal	Novus Biologicals
anti-OPA1	mouse	monoclonal	BD Transduction laboratories
anti-actin I-19	goat	polyclonal	Santa Cruz Biotechnology,Inc
anti-acetylated-lysine	rabbit	polyclonal	Cell Signaling Technology
anti-C-II-70 kDa	mouse	monoclonal	Mitosciences
anti-NDUFA9	mouse	monoclonal	Mitosciences
Secondary antibodies			
anti-rabbit	goat	monoclonal	Molecular Probes
anti-mouse	goat	monoclonal	Molecular Probes
anti-goat	goat	monoclonal	Calbiochem

4.4.2 Enzymes

DNA Polymerase:

High-Fidelity DNA polymerase Phusion (Finnzymes)

Dynazyme II DNA polymerase (Finnzymes)

Expand Long Template PCR system (Roche)

Ligase:

T4 DNA ligase (Clontech)

Restriction enzymes:

Dra I (Clontech)

EcoR V (Clontech)

Pvu II (Clontech)

Stu I (Clontech)

4.4.3 Molecular Markers

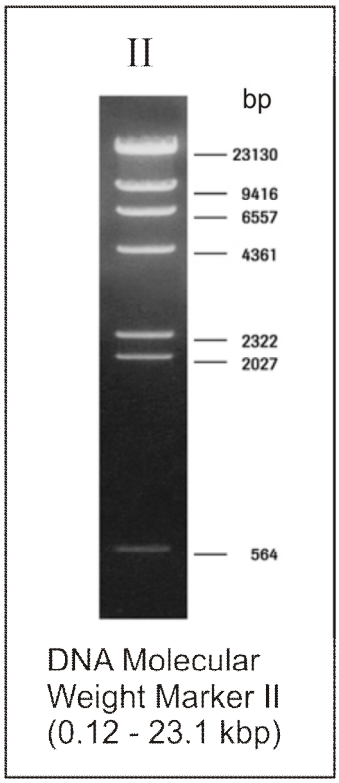

(Roche)

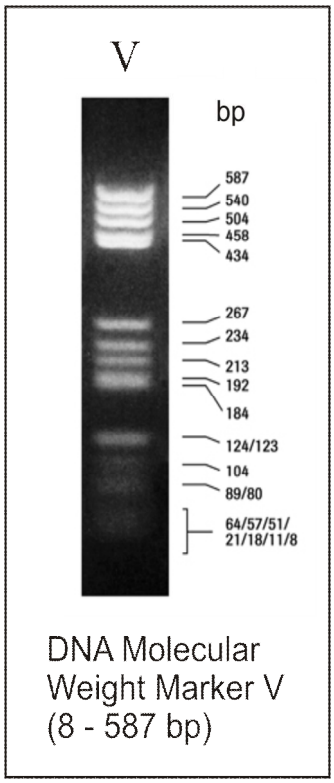

(Roche)

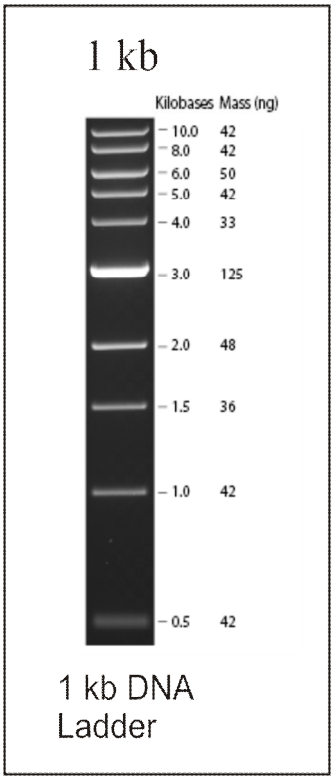

(New England Biolabs)

4.5 Methods:

4.5.1 Isolation of DNA from mouse tissues

DNA was extracted from snap frozen mouse tissue samples. Liver, testis, kidney and intestine from Deletor male and female mice and skeletal muscle and brain from AT male and female mice were allowed to melt on ice, homogenized with scalpel and then incubated with 0.4 mg Proteinase K (20 mg/ml, Sigma-Aldrich) and 700 µl of DNA isolation buffer in +55 ºC shaker over night. Then 700 µl of phenol (Amresco) was added to tubes and samples were centrifuged at 2 500 rpm for 5 min at +4 ºC. Aqueous upper-phases were collected and addition of phenol was repeated. Aqueous upper-phases were collected to new tubes where 700 µl of choloroform-isoamylalcohol (24:1, Fluka) was added and samples were centrifuged at 2 500 rpm for 5 min at +4 ºC. DNAs were purified with 1 300 µl of ice-cold 99 % EtOH (Fluka) and 130 µl of 7.5 M ammoniumacetate (Sigma) and stored in -20 ºC over night. Samples were then centrifuged at 13 000 rpm for 30 min at +4 ºC, supernatants were removed and pellets were purified in 500 µl ice-cold 70 % EtOH. After centrifugation at 13 000 rpm for 15 min at +4 ºC, supernatants were removed and DNA pellets were dissolved in 70 µl of TE-buffer (pH 7.5). DNA concentrations were measured by the NanoDrop spectrophotometer at 260 nm.

4.5.2 DNA Walking

4.5.2.1 Construction of DNA libraries

The Genome Walker Universal Kit (Clontech) was used to identify the exact position of the Twinkle transgene in genome of the wild-type Twinkle overexpresor (A) and the Deletor (C) mouse lines.

The Genome Walker libraries that contained un-cloned, adaptor-ligated genomic DNA fragments were prepared. To form Genome Walker libraries, 2.5 µg of genomic DNA from the A and C mouse lines were digested with 80 U of four different restriction enzymes (Dra I, EcoR V, Pvu II and Stu I, Clontech) with specific digestion buffers in 100 µl of reaction volume at +37 ºC over night (16-18h). To each library, 95 µl of phenol (Amresco) was added and span briefly at room temperature. Aqueous upper-phases were collected to new tubes and mixed with 95 µl of chloroform (Fluka). After separation of phases by brief spin at room

temperature, aqueous upper-phases were transferred and DNAs were purified by 190 µl of ice-cold 95 % EtOH (Fluka), 25 µl of NH_2Ac (7.5 M) and 2 µl of glycogen (10 µg/ µl, Sigma). Samples were centrifuged at 14 000 rpm for 15 min at +4 °C, supernatants were removed and pellets were washed in 100 µl of ice-cold 80 % EtOH (Fluka). After centrifugation at 14 000 rpm for 10 min at +4 °C, the final pellets were dissolved in 20 µl of TE-buffer (10/0.1, pH 7.5). To determine the approximate quantity of purified DNA, 1 µl from each reaction tube was removed, mixed with 5x BPB + glycerol and ran on a 0.6 % agarose + EtBr (20 µg/ 50ml) gel along the 1 kb DNA Ladder (New England Biolabs). From each reaction tube, 4 µl of digested, purified DNA was transferred to new tubes and incubated with 1.9 µl of Genome Walker adaptors (25 µM) and 3 U of T4 DNA ligase (6 U/µl, Clontech) with 10x Ligation Buffer in 8 µl of reaction volume at +16 °C over night. To hold the constant temperature, PCR cycler was used and the reaction was then stopped by increased temperature up to +70 °C for 5 min. Finally, 72 µl of TE-buffer (10/1, pH 7.5) were added to each tube.

4.5.2.2 PCR-based DNA walking

The genome libraries were used to polymerase chain reaction (PCR)-based DNA walking. The Genome Walker adaptor primers (AP) and nested primers designed to the 3´ end of the Twinkle transgene (Tw, figure 4.1 and table 4.3) were used to amplify the DNA fragments from each library.

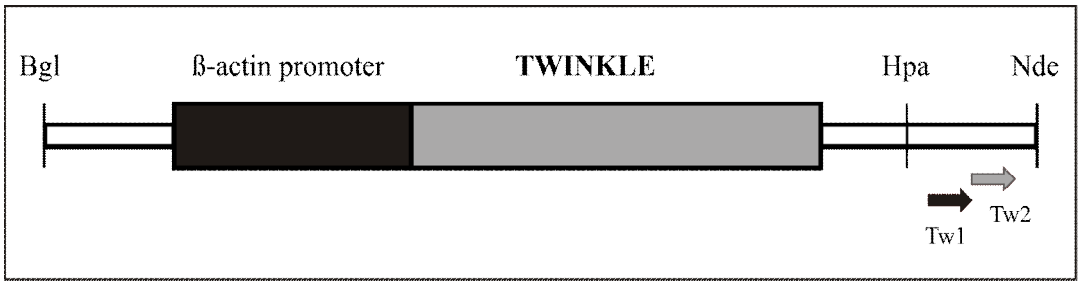

Figure 4.1: The Twinkle transgene and position of nested primers. In the construct, the Twinkle gene is expressed under the β-actin promoter and two primers with direction of DNA amplification are shown in color. Bgl, Hpa and Nde are restriction sites used for transgene construction. Tw, Twinkle.

Table 4.3: Primers for PCR-based DNA walking and sequencing reaction.

Name	Sequence
Tw1	5´- GTGAAAACCTCTGACACATGCAGCTC - 3´
Tw2	5´- GGAGACGGTCACAGCTTGTCTTGTAAG - 3´
AP1	5´- GTAATACGACTCACTATAGGGC - 3´
AP2	5´- ACTATAGGGCACGCGTGGT - 3´
T7 forward	5´- TAATACGACTCACTATAGGG - 3´
M13 reverse	5´- CAGGAAACAGCTATGAC - 3´

The primary PCR was performed in 50 µl of final volume containing 1 U of High-Fidelity DNA polymerase Phusion (2 U/ µl, Finnzymes) with HF Buffer, 1 µM of both primers AP1 and Tw1 (table 4.3), 0.2 mM of dNTPs and 1 µl of each DNA library. The initial step at 98 °C for 30 sec was followed by 7 cycles with 98 °C for 10 sec and 72 °C for 30 min. Subsequent 32 cycles consisted of 98 °C for 10 sec, 67 °C for 3 min with the final extension 67 °C for 7 min. The primary PCR products (5 µl) with 5x BPB + glycerol were analyzed on a 1.5 % agarose + EtBr (20 µg/ 50 ml) gel along 1 kb DNA Ladder (New England Biolabs).

In new tubes, 1 µl of each primary PCR was diluted into 49 µl of deionized water. The secondary PCR was performed in 50 µl of reaction volume containing 1 U of High-Fidelity DNA polymerase Phusion (2 U/ µl, Finnzymes) with HF Buffer, 1 µM of both primers AP2 and Tw2 (table 4.3), 0.2 mM of dNTPs and 1 µl of diluted primary PCR products. The initial step at 98 °C for 30 sec was followed by 5 cycles with 98 °C for 10 sec and 72 °C for 30 min. Subsequent 20 cycles consisted of 98 °C for 10 sec, 67 °C for 3 min with the final extension 67 °C for 7 min. The secondary PCR products (5 µl) with 5x BPB + glycerol were analyzed on a 1.5 % agarose + EtBr (20 µg/ 50 ml) gel along 1 kb DNA Ladder (New England Biolabs).

The strongest bands that presented the final products were purified from agarose gels using QIAquick Spin Gel Extraction Kit (Qiagen), cloned into pCR-Blunt II-TOPO (Invitrogen) according to manufacturer's instructions and sequenced with vector T7 forward and M13 reverse primers (table 4.3). Sequences were matched to the mouse genome through BLAST searches of NCBI Mouse Genome Resources (http://blast.ncbi.nlm.nih.gov/Blast.cgi).

4.5.2.3 Verification of the transgene integration site

The integration of the transgene to the identified genomic position was verified by PCR amplification using gw-primers (table 4.4). The PCR was performed in 25 µl of reaction volume containing 0.2 mM of dNTPs, 2 mM of $MgCl_2$, 1 µM of each primer, 1 U of Dynazyme II DNA polymerase (Finnzymes) with 10x Buffer and 25 ng of mouse genomic DNA. The initial step of the PCR program at 95 °C for 2 min was followed by 35 cycles of 95 °C for 1 min, 60 °C for 10 min and 72 °C for 30 min with the final extension at 72 °C for 10 min. The length of PCR product was 350 bp for A mouse line.

Table 4.4: Primers for verification and genotyping PCR.

Name	Sequence
gw-twinkle3F	5´- GCTTGTCTGTAAGCGGATGC - 3´
gw-chr5R	5´- GGCATCAGACATGTAGGCAGT - 3´
mTw1549F	5´- TGCAGTTCATGATGGGTCAC - 3´
mTw1719R	5´- TGCTGTCTGCAGTTCCTTGT - 3´

The results were then compared to results from genotyping PCR of five transgenic mice and five controls. The genotyping was based on amplification of the endogenous Twinkle and the transgene that was shorter due to lacking of intron 3. The PCR products of transgene and endogenous Twinkle were 161 bp and 339 bp long, respectively. The amplification of 50 ng of genomic DNA was done using 0.5 µM of both mTw1549F and mTw1719R primers (table 4.4) and performed in 25 µl of reaction volume containing 0.6 U of Dynazyme II DNA polymerase (Finnzymes) with 10x buffer, 0.2 mM of dNTPs and 2 mM of $MgCl_2$. The initial step at 95 °C for 4 min was followed by 35 cycles of 95 °C for 1 min, 56 °C for 1 min and 72 °C for 1 min with the final extension at 72 °C for 10 min. On 1 % agarose + EtBr (20 µg/ 50ml) gel, 10 µl of both Genome Walker and genotyping PCR products were run along the Marker V (DNA Molecular Weight Marker V, 8-587 bp, Roche). The gels were scanned on Typhoon 9400 scanner (Amersham Biosciences).

4.5.3 Long PCR of mtDNA

Long PCR was used for the detection of mtDNA deletions. The specific primers were designed to amplify different sizes of mtDNA molecules (table 4.5).

Table 4.5: MtDNA primers for long PCR.

Name	Sequence
mmtDNA-longF	5´- GAGGTGATGTTTTTGGTAAACAGGCGGCGGGGT - 3´
mmtDNA-longR	5´- GGTTCGTTTGTTCAACGATTAAAGTCCTACGTG - 3´

The PCR was performed in buffer 2 with 3.8 U of the Expand Long Template PCR system (Roche), 0.2 mM of dNTPs and 1 µM of both mmtDNA-longF and mmtDNA-longR primers in 50 µl of final reaction volume. The same PCR program was used for all tissue samples. The initial step at 92 ºC for 2 min was followed by 30 cycles at 92 ºC for 10 sec and annealing temperature 68 ºC for 12 min with the final extension at 68 ºC for 7 min. On 1% agarose + EtBr (20 µg/ 50 ml) gel, 5 µl of each PCR products with 5x BPB + glycerol were separated along the Marker II (DNA Molecular Weight Marker II, 0.12 – 23.1 kbp, Roche). Full-length mtDNA ran as upper band around 16 kbp and mtDNA deletions were presented as lower 3 – 10 kbp bands.

4.5.4 Mouse tissue sections and COX / SDH staining

Mouse intestine samples were collected and frozen by isopentane freezing method. Cryostat sections of 12 µm were separately or simultaneously stained with cytochrome c oxidase (COX) and succinate dehydrogenase (SDH). Frozen sections on glass plates were incubated in COX-incubation solution for 30 min at room temperature in moist chamber. After three washes in water, plates were incubated in SDH-incubation solution for 30 min at +37 °C in moist chamber. After three washes in water, plates were dehydrated in ascending alcohols (70 %, 94 % and three times in 100 %), cleared three times in xylene and mounted with xylene based DePeX mounting medium (Gurr, BDH). Stained sections were analyzed by light microscope (Axioplan 2 Universal Microscope, Zeiss).

4.5.5 Tissue homogenates

Fresh mouse tissue samples were homogenized in RIPA buffer. The samples were incubated on ice for 20 min and centrifuged at 13 000 x g for 5 min at +4 °C. Supernatants were collected and stored in -80 °C.

4.5.6 Enrichment of mitochondria

Fresh mouse tissue samples were homogenized with a teflon pestle in 5 ml of ice-cold HIM buffer and centrifuged at 600 x g for 20 min at +4 °C. Supernatants were collected and centrifuged at 10 000 x g for 10 min at +4 °C. Supernatants were then removed and pellets were resuspended in 2 ml of ice-cold HIM buffer. After the centrifugation at 10 000 x g for 10 min at +4 °C the final pellets were resuspended in 1x PBS+. Protein concentration was measured by the Bradford method (Bradford 1976) according to manufacturer's instructions (Bio-rad Laboratories, Inc.) using spectrophotometer.

4.5.7 Pure mitochondrial isolation using sucrose gradient

Fresh mouse tissue samples were collected and mitochondrial pellets were prepared by using the enrichment protocol. Pellets were resuspended in 400 µl of ice-cold HIM. Pure mitochondria were isolated by using sucrose gradient prepared by filling the centrifuge tubes with 2.2 ml of upper 1 M sucrose and 2.2 ml of lower 1.5 M sucrose solutions. Samples were centrifuged at 18 800 rpm for 1 h at +4 °C, the mitochondrial layers were collected, resolved in 1 ml of ice-cold HIM buffer and centrifuged at 12 000 rpm for 5 min at +4°C. The final pellets were resuspended in 200 µl of PBS+.

4.5.8 SDS-PAGE and Western Blotting

Proteins samples (10-40 µg) were mixed with loading buffer 1:1, denaturated at 95 °C for 5 min and loaded into the gel. Discontinuous gels consisting of 4 % upper stacking gel (pH 6.8, table 4.1) and lower resolving or separating gel (pH 8.8, table 4.1) of particular concentration were prepared according to the specific protein properties (table 4.6). Electroblotting method was used to transfer proteins onto

PVDF membranes (Immobilon-FL, Millipore). Membranes were blocked at room temperature on a shaker and probed with specific primary antibody at +4 ºC over night and then with secondary antibody at room temperature for 1h (table 4.2). After incubation with the primary and secondary antibody, membranes were washed three times for 5 min in Tris-buffered saline containing 0.1% Tween 20 (TBS-T) and signals were detected by ECL Plus Western Blotting Detection System (GE Healthcare) using Typhoon 9400 scanner (Amersham Biosciences) or by LumiGLO (LumiGLO Reagent and Peroxide, Cell Signaling Technology) on X-OMAT LS (Kodak) film. BenchMark Prestained Marker (Invitrogen) was used to estimate the protein sizes.

Table 4.6: Characteristics of conditions for specific proteins.

Tissue homogenates			
Protein	**Separat-ing gel**	**Blocking**	**Primary antibody**
LC3	15%	5% milk (TBS-T)	anti-LC3B (1:3000 dilution in 5% BSA (TBS-T))
OPA1	10%	5% milk (TBS-T)	anti-OPA1 (1:1000 dilution in 5% milk (TBS-T))
β-actin		1% BSA (TBS-T)	anti-actin I-19 (1:2000 dilution in 5% milk (TBS-T))
Mitochondria enrichment			
Acetylation on Lysine	12%	5% milk (TBS-T)	anti-acetylated-lysine (1:1000 dilution in 5% BSA (TBS-T))
Complex II		5% milk (TBS-T)	anti-C-II-70 kDa (1:10 000 dilution in 5% milk (TBS-T))

4.5.9 Mitochondrial samples for Blue native electrophoresis (BN-PAGE)

Fresh mouse tissue samples were used to prepare mitochondrial enrichment pellets for blue native electrophoresis. Concentrations of mitochondrial proteins that were resuspended in PBS+ were measured by the Bradford method (Bradford 1976) according to manufacturer's instructions (Bio-rad Laboratories, Inc.) using spectrophotometer and the samples were diluted to final concentration of 5 µg/µl with PBS+. Equal volumes of freshly prepared digitonin solution (4 mg/ml) to permeabilize cell membranes were added into the samples and incubated on ice for 5 min. Tubes were then filled up with PBS+ and centrifuged at 10 000 x g for 10 min at +4 °C, supernatants were removed and pellets were resuspended in MB2 buffer. 1/10 volume of 10 % lauryl maltoside (0.1 g/ml) was added to the samples, incubated on ice for 15 min and centrifuged at 20 000 x g for 20 min at +4 °C. Supernatants were collected and stored at -80 °C. Protein concentration was measured by the Bradford method (Bradford 1976) according to manufacturer's instructions (Bio-rad Laboratories, Inc.) using spectrophotometer.

4.5.10 Preparation of Blue native gel and electrophoresis

Blue native gels consisting of 4 % upper stacking gel and lower gradient gel prepared from 6 % and 15 % separating gel mixture were set up for separation of mitochondrial proteins from the skeletal muscle and brain. The protein samples were mixed with SBG - sample buffer and loaded on gel at 20 µg of total proteins. The Peptide Marker Kit (Amersham Biosciences) was used to evaluate the protein sizes. Proteins were transferred to PVDF membranes (Immobilon-FL, Millipore) by using semi-dry western blotting method (6 mA, 1.5 h). Membranes were blocked in 5 % milk (TBS-T) for 1h at room temperature and then probed with primary antibody for Complex I subunit NDUFA9 (1:500 dilution in 5 % BSA (TBS-T), table 4.2) at +4 °C over night. Then probed with secondary goat anti-mouse antibody (1:1000 dilution in 5 % milk (TBS-T), table 4.2). After incubation with secondary antibody, membranes were washed three times for 5 min in TBS-T and signals were detected by ECL Plus Western Blotting Detection System (GE Healthcare) using Typhoon

9400 scanner (Amersham Biosciences) or by LumiGLO (LumiGLO Reagent and Peroxide, Cell Signaling Technology) on X-OMAT LS (Kodak) film.

Immediately after electrophoretic separation of mito proteins, the Blue Native gels were incubated in Coomassie Fix solution for 20 min at room temperature and then stained with Coomassie Blue solution over night at room temperature. After the staining, gels were washed tree times in Coomassie Blue destaining solution for 20 min and dried.

Immediately after electrophoresis, the Blue Native gels of separated mito proteins were used for in-gel Complex I activity assay. Gels were incubated in 10 ml of 1 mM NADH solution for 10 min at room temperature and then with Complex I activity solution for 10 min at room temperature. Gels were washed in water over night and dried.

4.5.11 Statistical analysis

Signals were quantified by ImageQuant TL software (Amersham Biosciences) and statistical analysis was calculated with Student t-test using Microsoft Excel software that gave two-tailed P-values.

5. Results

5.1 Identification of the transgene integration site

5.1.1 Result of the BLAST search

Since the integration of transgene construct to nDNA is a random process, the knowledge of exact position in the mouse genome is required for the subtle Deletor characterization. The PCR-based Genome Walker kit was used to amplify PCR products that contained genomic sequence flanking the transgene integration site. The products were purified from the agarose gels, cloned into the sequencing vectors and sequenced. The sequences were matched to the mouse genome through BLAST searches of NCBI Mouse Genome Resources. The Twinkle transgene in the A mouse line was identified in band E1 on chromosome 5 in the intron 3 of *TMPRSS11d* gene (Transmembrane protease serine 11D; OTTMUSG00000028240). In the C mouse line the transgene was found in non-coding band A1 on chromosome 16.

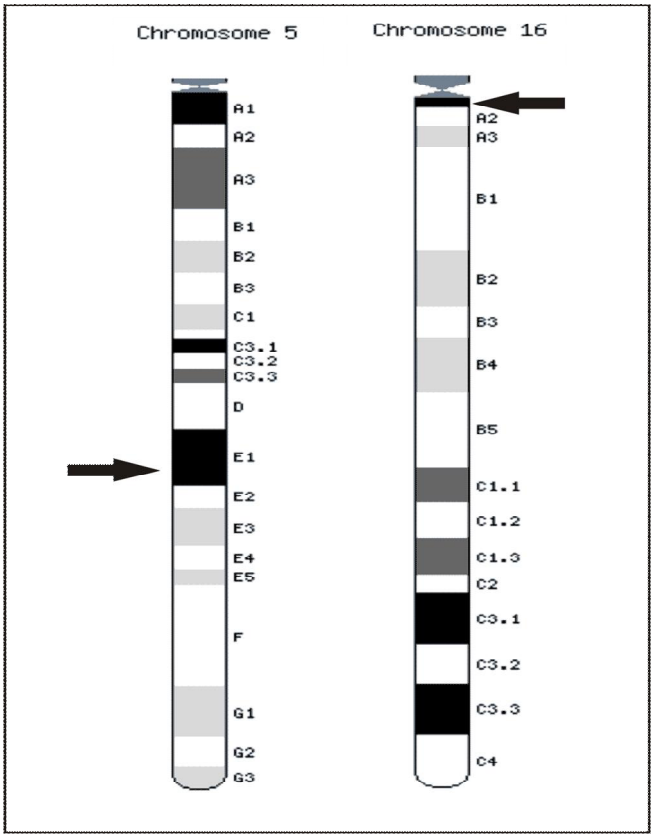

Figure 5.1: Integration sites of Twinkle transgene in A and C mouse lines. Particular integration sites on mouse chromosome 5 (band E1) and 16 (band A1) are indicated by arrows (modified from www.ensembl.com).

5.1.2 Verification of the transgene integration site

The genomic position of the Twinkle transgene in the A mouse line was verified by specific PCR by comparison to the mouse genotyping PCR. PCR products of five transgenic and five control mouse samples were separated on 1 % agarose gel + EtBr along the Marker V (figure 5.2). Specific PCR product validating the correct genomic position of the Twinkle transgene on chromosome 5 in the A mouse line was 350 bp (indicated by the arrow, figure 5.2). Transgene and endogenous Twinkle PCR products were 161 bp and 339 bp long, respectively (indicated by the arrows). In wild type samples PCR products of chromosome 5 as well as transgene Twinkle were missing. The genomic position of the Twinkle transgene in the C mouse line was verified using the same PCR method (data not shown).

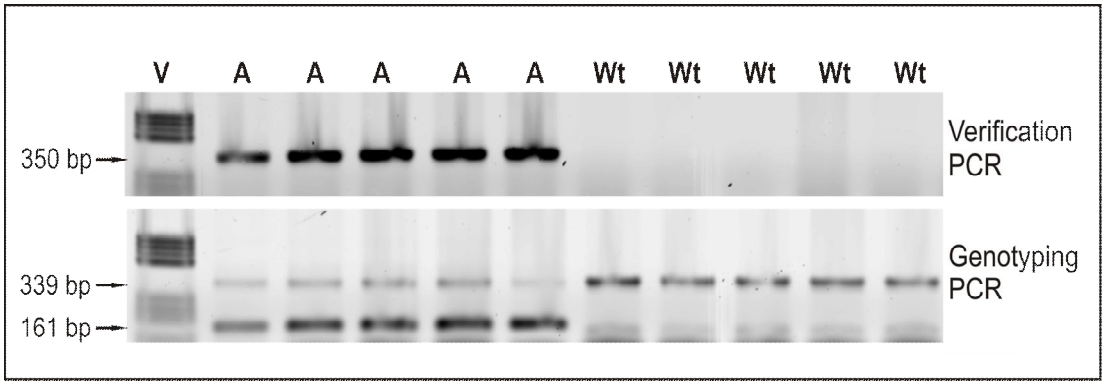

Figure 5.2: **Twinkle transgene integrated on chromosome 5 in the A mouse line**. PCR products from verification of the transgene integration site separated on agarose gel. A, A mouse line samples; Wt, wild type; V, Marker V.

5.2 MtDNA deletions in different tissues

5.2.1 Analysis of the Deletor mouse tissues

In the previous studies, the expression level of Twinkle transgene in particular tissues was examined and mtDNA deletions were found in the Deletor skeletal muscle and brain (Tyynismaa *et al.* 2005). Thus, additional tissues such as kidney, liver, testis and intestine of the Deletor male and female mice were tested. MtDNA was amplified by long PCR and the PCR products were analyzed on 1% agarose gels with EtBr (figure 5.3). The DNAs isolated from the skeletal muscle of wild type and the Deletor mice were used as negative and positive controls, respectively. The full-length mtDNA was successfully amplified in all tested samples, but prominent mtDNA deletions were found only in the skeletal muscle. Furthermore, no differences between males and females were observed. The shorter bands of mtDNA, detected in some tissue samples (i.e. in the kidney of the Deletor female sample), represented the mtDNA deletions whose amount does not reach the minimal critical level to manifest as disease phenotype in the particular tissue.

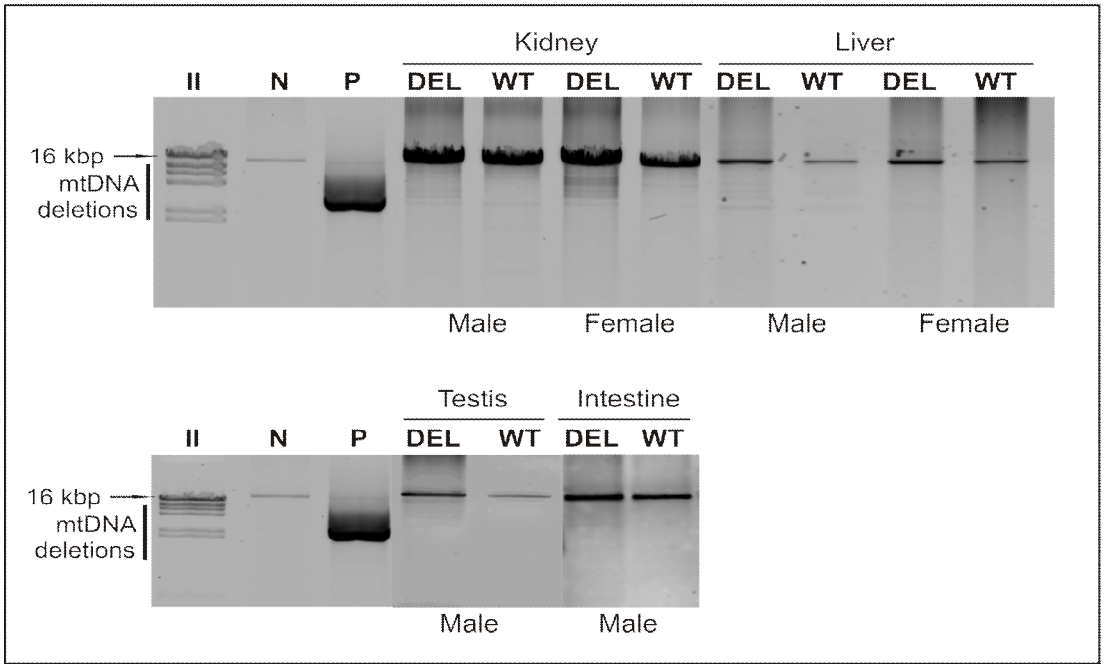

Figure 5.3: No mtDNA deletions in the Deletor mouse tissues other than the skeletal muscle. The full-length mtDNA (indicated by the arrow) was amplified in all tested tissue samples. MtDNA deletions of multiple sizes are indicated by the vertical line. DEL, Deletor; WT, wild type; II, DNA marker II; N, negative control; P, positive control.

5.2.2 Analysis of the AT mouse tissues

To further characterize the AT mice, mtDNA deletions detection assay in the skeletal muscle and brain of male and female mice was performed. MtDNA was amplified by long PCR and the PCR products were analyzed on 1% agarose gels with EtBr (figure 5.4). The DNAs isolated from the skeletal muscle of wild type and the Deletor mice were used as negative and positive controls, respectively. No prominent mtDNA deletions were found in the AT mouse tissue samples.

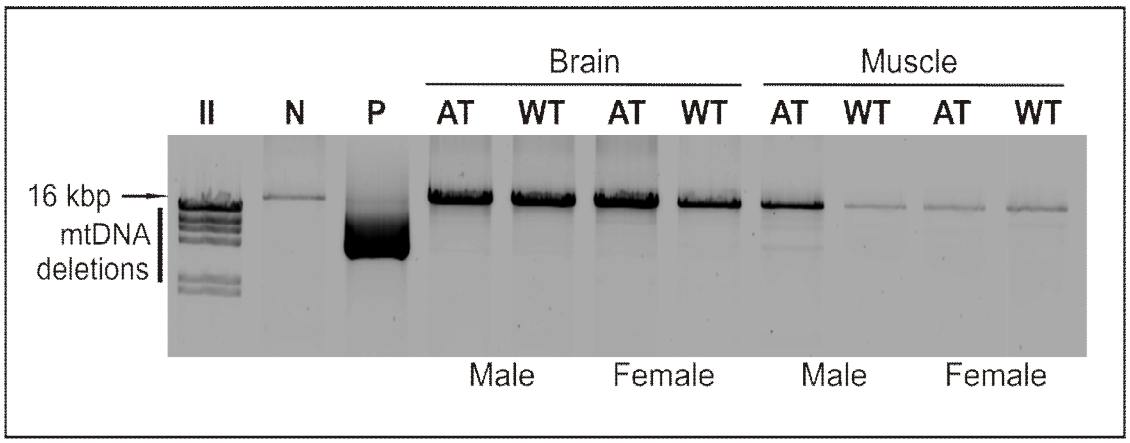

Figure 5.4: No mtDNA deletions in AT mouse tissues samples. The full-length mtDNA (indicated by the arrow) was amplified in all tested tissue samples. MtDNA deletions of multiple sizes are indicated by the vertical line. AT, A360T; WT, wild type; II, DNA marker II; N, negative control – DNA from the wild type skeletal muscle; P, positive control – DNA from the Deletor skeletal muscle.

5.3 COX/ SDH histochemistry of the Deletor mouse tissue

The secondary defects in mtDNA caused by mutations in nuclear genes of mtDNA maintenance proteins are usually manifested in post-mitotic tissues with the highest energetic needs. Whether these defects can be observed also in proliferative tissue, the mouse intestine tissue was analyzed for COX and SDH activity. The frozen intestine sections of the Deletor and wild type mice were separately or simultaneously stained for COX and/or SDH and analyzed by light microscope (figure 5.5). Histochemistry of intestine mucosa showed normal COX activity (COX^+, dark brown) and SDH activity (SDH^+, dark blue) in colonic crypts (figure 5.5). Either the white crypts indicating absence of COX activity (COX^-) or the bright blue crypts strongly stained with SDH indicating mitochondrial accumulation were not observed.

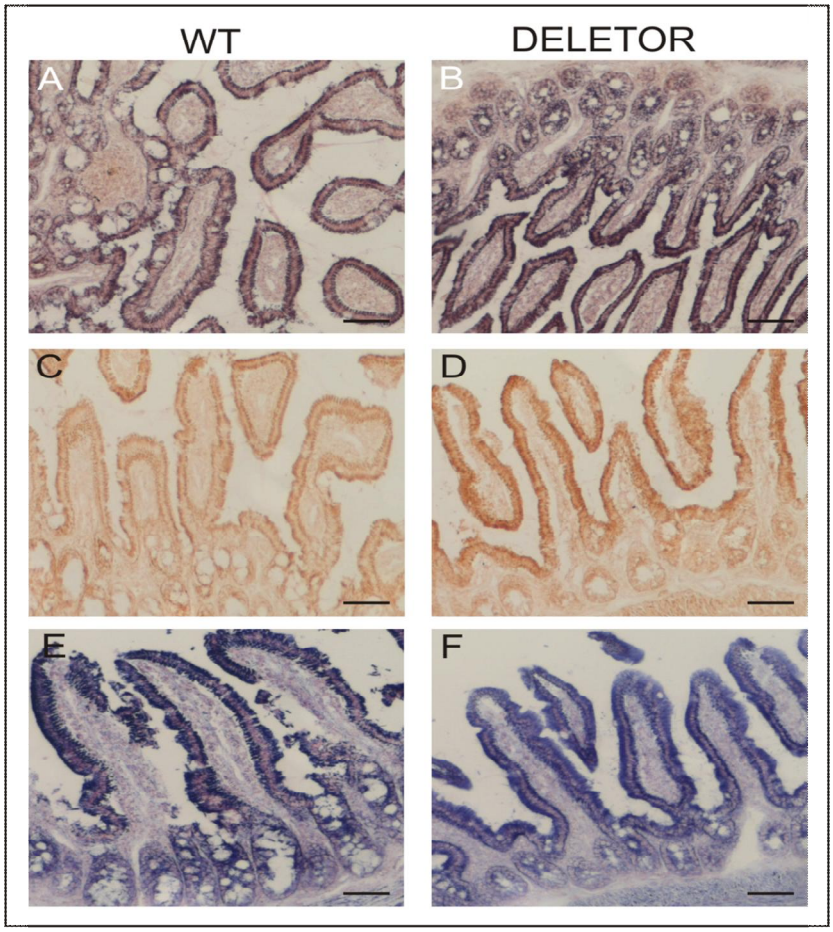

Figure 5.5: No COX^-/SDH^+ colonic crypts in the Deletor intestine. COX/ SDH histochemistry of the skeletal muscle. Double staining for COX/ SDH activities of the wild type (A) and Deletor (B) mouse tissue samples. Single staining for COX activity and for SDH activity of the wild type (C, E) and Deletor (D, F) mouse tissue samples, respectively. Scale bars: 50 µm.

5.4 Opa1 detection and mitochondrial fragmentation

5.4.1 Opa1 in different Deletor tissues

The shift in the pattern of Opa1 isoforms has been observed in several mouse models of human disorders characterized by mitochondrial dysfunction. To study Opa1 in the 24-month-old Deletor, the mouse brain, heart and liver homogenates with the wild type mouse counterparts were separated on 10 % resolving gel and the proteins were probed with monoclonal mouse anti-OPA1 antibody. β-actin was used as a loading control. Opa1 isoforms migrated as a mixture of at least five bands within the range of 80-100 kDa (figure 5.6). The particular bands that represented either the long isoforms (L1-, L2-OPA1) or the short isoforms (S3-, S4-, S5-OPA1) could not be distinguished for individual quantification, thus all long isoforms (L-OPA1) as well as S4 and S5-OPA1 from short isoforms (S-OPA1) were quantified as a single upper and lower band using Student t-test, respectively, and normalized against β-actin signal. Only S3-OPA1 could be quantified as a single band in all tested samples (figure 5.6). Significant increase was found in the level of S-OPA1 isoforms in the Deletor brain compared to the wild type tissue samples, $p = 0.003$ (figure 5.7 A). No clear shift to a specific isoform was seen in these tissues.

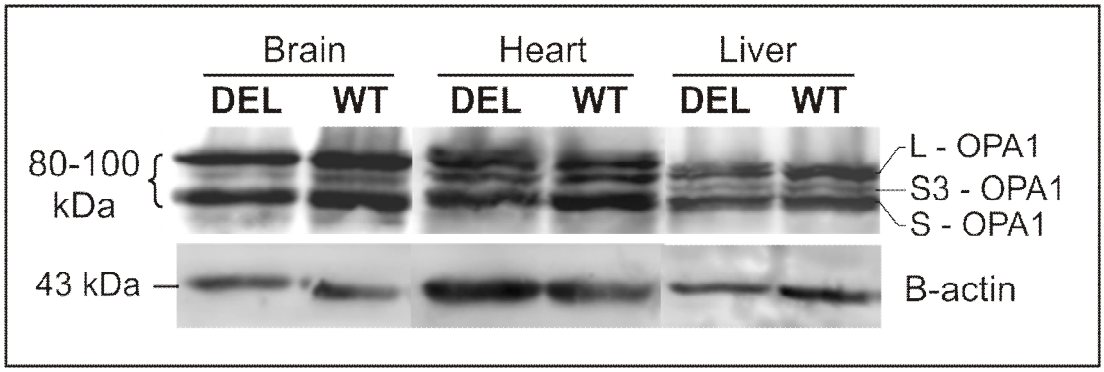

Figure 5.6: **Significant increase of S-OPA1 in the 24-month-old Deletor brain.** The immunodetection of Opa1 isoforms in the brain, heart and liver homogenates separated by SDS-PAGE. DEL, Deletor; WT, wild type.

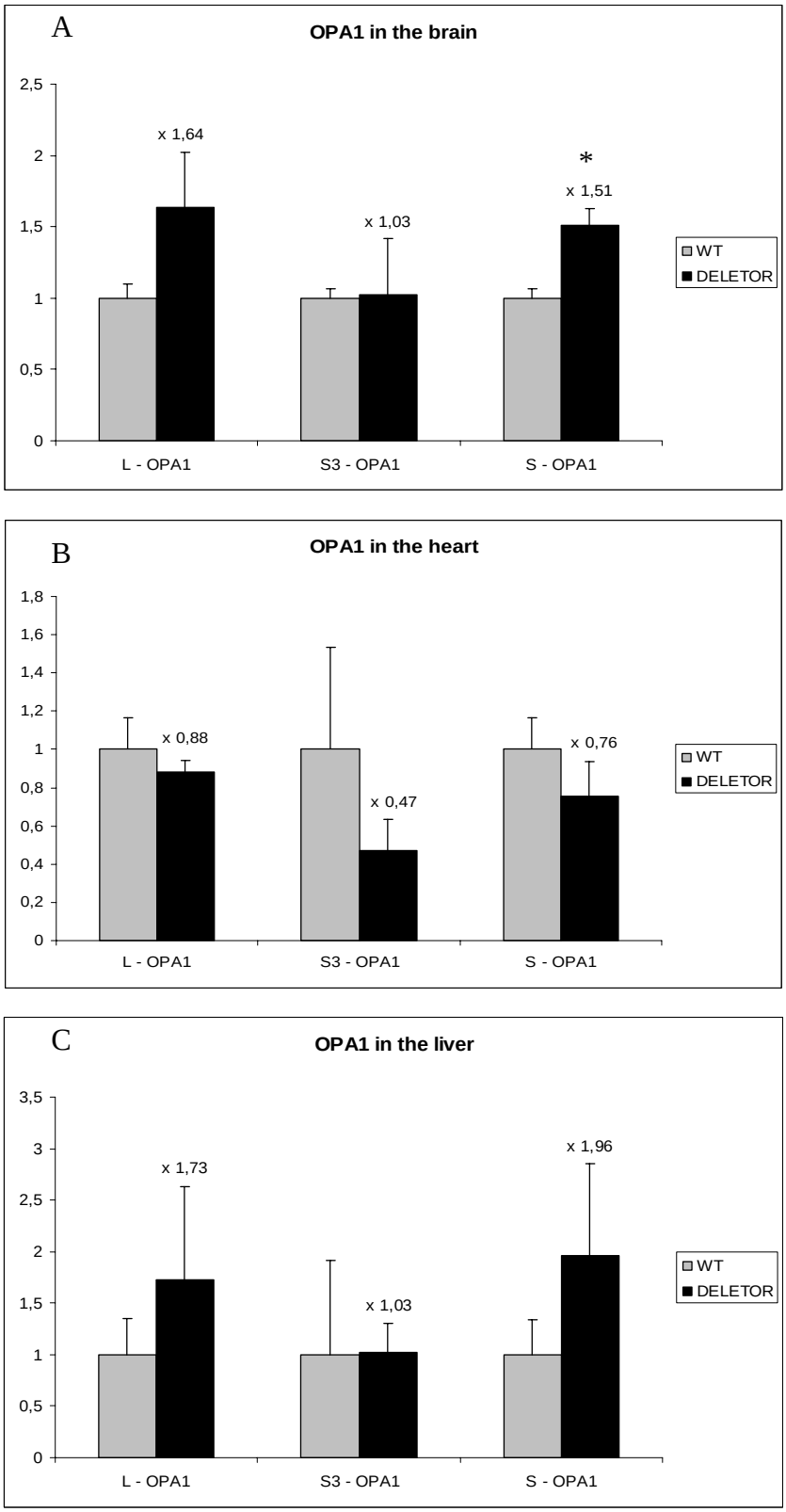

Figure 5.7: **Significant increase of S-OPA1 in the 24-month-old Deletor brain.** **A**, the quantification of Opa1 isoforms in the brain tissue (n = 3). Significant difference is indicated by the asterisk (p = 0,003). **B**, the quantification of Opa1 isoforms in the heart tissues (n = 3). **C**, the quantification of Opa1 isoforms in the liver tissue (n = 3). The standard deviations (SDs) are indicated. WT, wild type.

5.4.2 Opa1 in the Deletor skeletal muscle

In patients with mitochondrial diseases, the defects of mitochondrial functionality (such as mitochondrial respiratory chain) and morphology are mainly presented in the skeletal muscle. Thus, the tissue homogenates of the Deletor skeletal muscle, as a mouse model of adPEO, and the control mouse samples were separated on 10 % resolving gel and the proteins were probed with monoclonal mouse anti-OPA1 antibody. β-actin was used as a loading control (figure 5.8 A). Five bands within the range of 80-100 kDa were detected in all skeletal muscle samples, quantified separately and normalized against β-actin signal (figure 5.8 B). All Opa1 isoforms were slightly elevated and statistically significant increase was identified in the level of L2-OPA1 isoform in the Deletor compared to wild type samples (n = 4, figure 5.8 B).

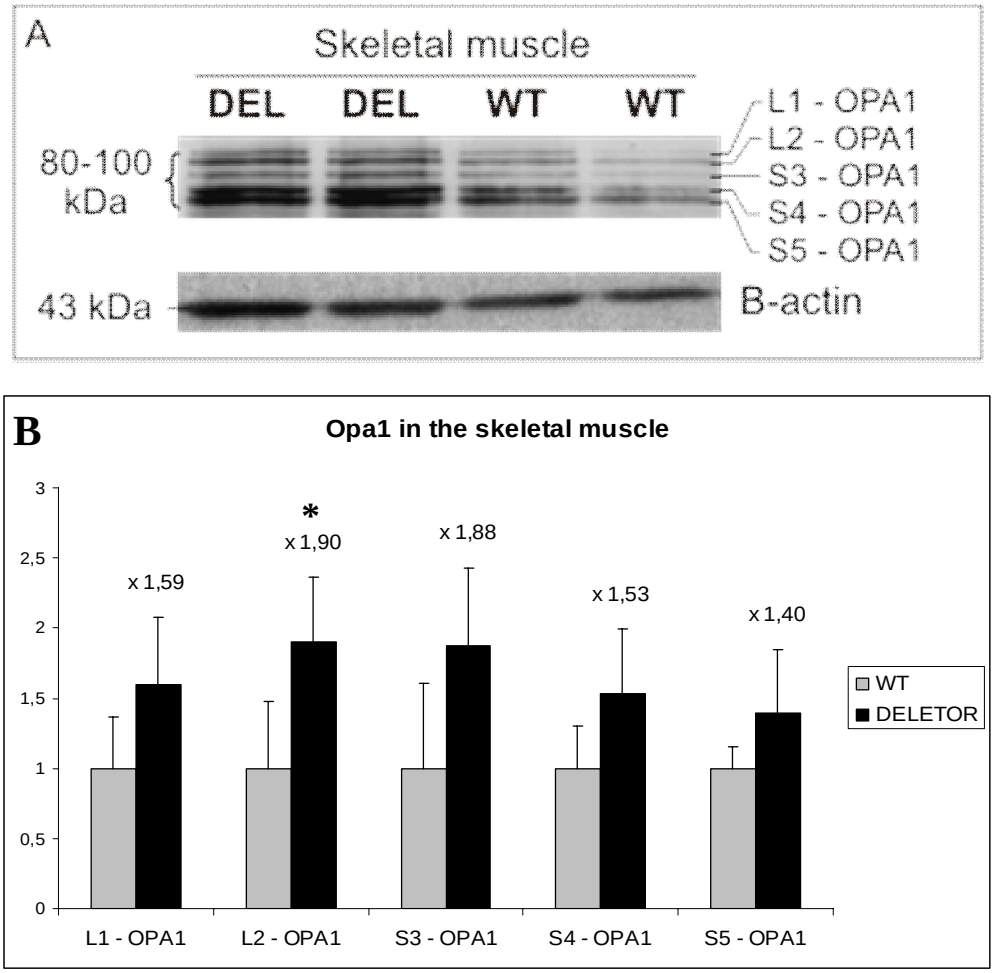

Figure 5.8: **Significant increase of L2-OPA1 isoform in the 24-month-old Deletor skeletal muscle (n = 4). A,** the immunodetection of Opa1 isoforms in the skeletal muscle samples separated by SDS-PAGE. **B**, the quantification of long and short Opa1 isoforms. Significant difference is indicated by the asterick (p = 0.04). The SDs are indicated. DEL, Deletor; WT, wild type.

5.5 Coomassie Blue staining of OXPHOS complexes

The mitochondrial enrichments of the skeletal muscle and brain of the Deletor and wild type mice were separated on Blue native electrophoresis and stained with Coomassie Blue (figure 5.9). Complexes of oxidative phosphorylation system (OXPHOS) were detected in their native form. Complex I, II, III and V were detected in both the skeletal muscle and the brain samples whereas complex IV was detected only in the skeletal muscle, by this method. The Coomassie Blue analysis showed discrepancies in Complex I in both Deletor tissues (figure 5.9).

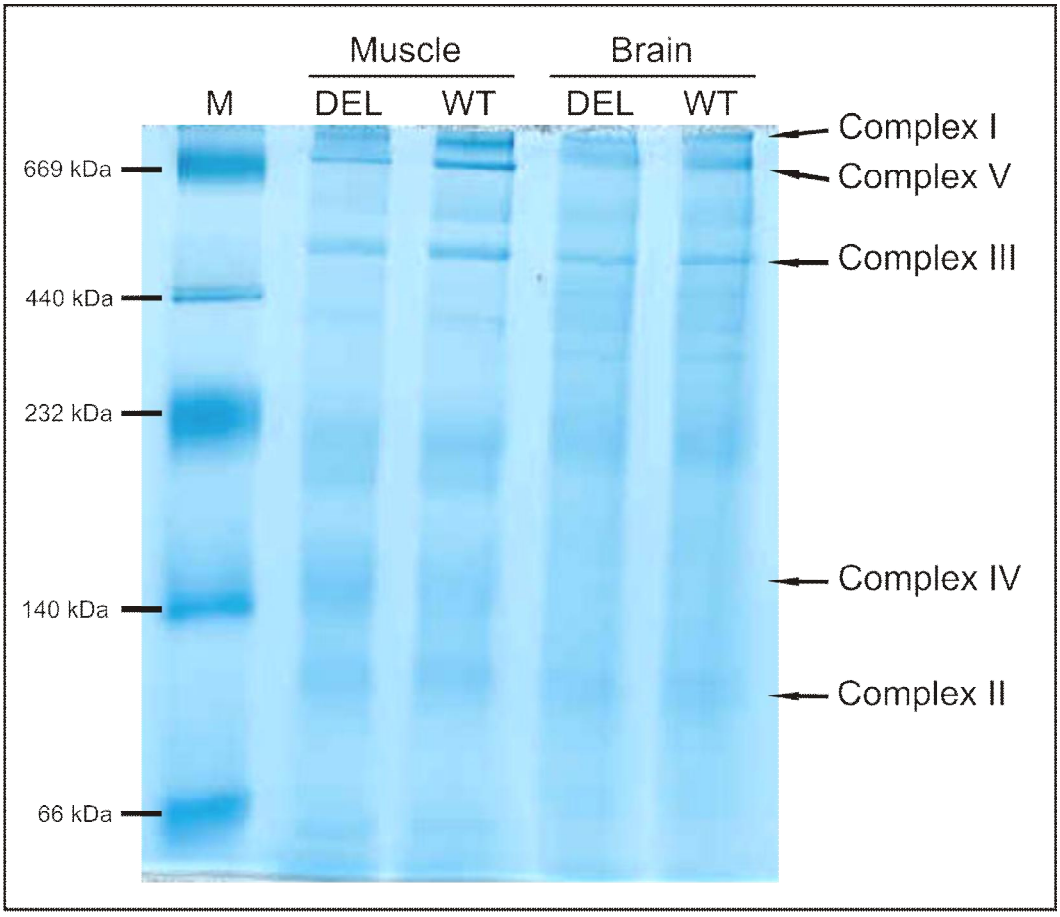

Figure 5.9: **Complexes of OXPHOS detected in the Deletor tissues.** The mitochondrial enrichments of the skeletal muscle and brain separated on Blue native gel stained with Coomassie Blue. Main protein sizes of molecular marker are indicated. DEL, Deletor; WT, wild type; M, Peptide marker.

5.6 Blue native electrophoresis and in-gel activity of Complex I in the Deletor skeletal muscle and brain

According to the findings from Coomassie blue staining in the skeletal muscle and brain samples, the amount and activity of Complex I were analyzed by Blue native electrophoresis of the Deletor compared to the non-transgenic mice. Proteins of mitochondrial enrichments were separated on gradient 6 - 15 % resolving gel. Complex I was detected by mouse monoclonal anti-NDUFA9 antibody, the activity was shown after incubation with NADH substrate. Complex I was detected in both tissues. Due to the isolation method, the Complex I in partly disrupted mitochondrial membranes was represented as upper band. Neither in the skeletal muscle nor in the brain was found a major difference in the amount or in the activity of Complex I (figure 5.10).

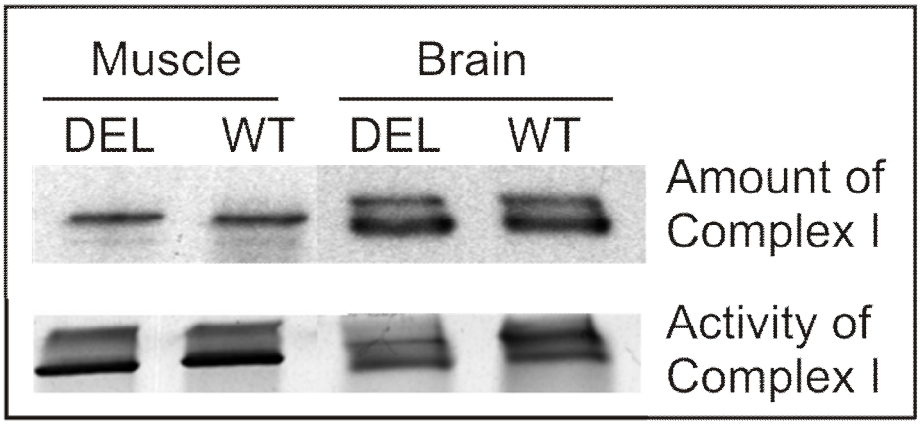

Figure 5.10: **No major difference in amount or activity of Complex I in the 24-month-old Deletor skeletal muscle and brain.** The immunodetection of Complex I and its in-gel activity in the skeletal muscle and brain samples separated by BN-PAGE. DEL, Deletor; WT, wild type.

5.7 Autophagy/mitophagy and detection of LC3

5.7.1 LC3 in the Deletor skeletal muscle

To confirm the findings of mitophagy observed by electron microscopy, the skeletal muscle samples of the Deletor and wild type mice were separated on 15 % resolving gel and the autophagy protein marker was detected by rabbit polyclonal anti-LC3B antibody. β-actin was used as a loading control. Both LC3-I and LC3-II bands were detected in all samples (figure 5.11 A). The bands were quantified and normalized against β-actin signal. LC3-II was significantly increased in the Deletor skeletal muscle compared to the wild type mouse samples (figure 5.11 B).

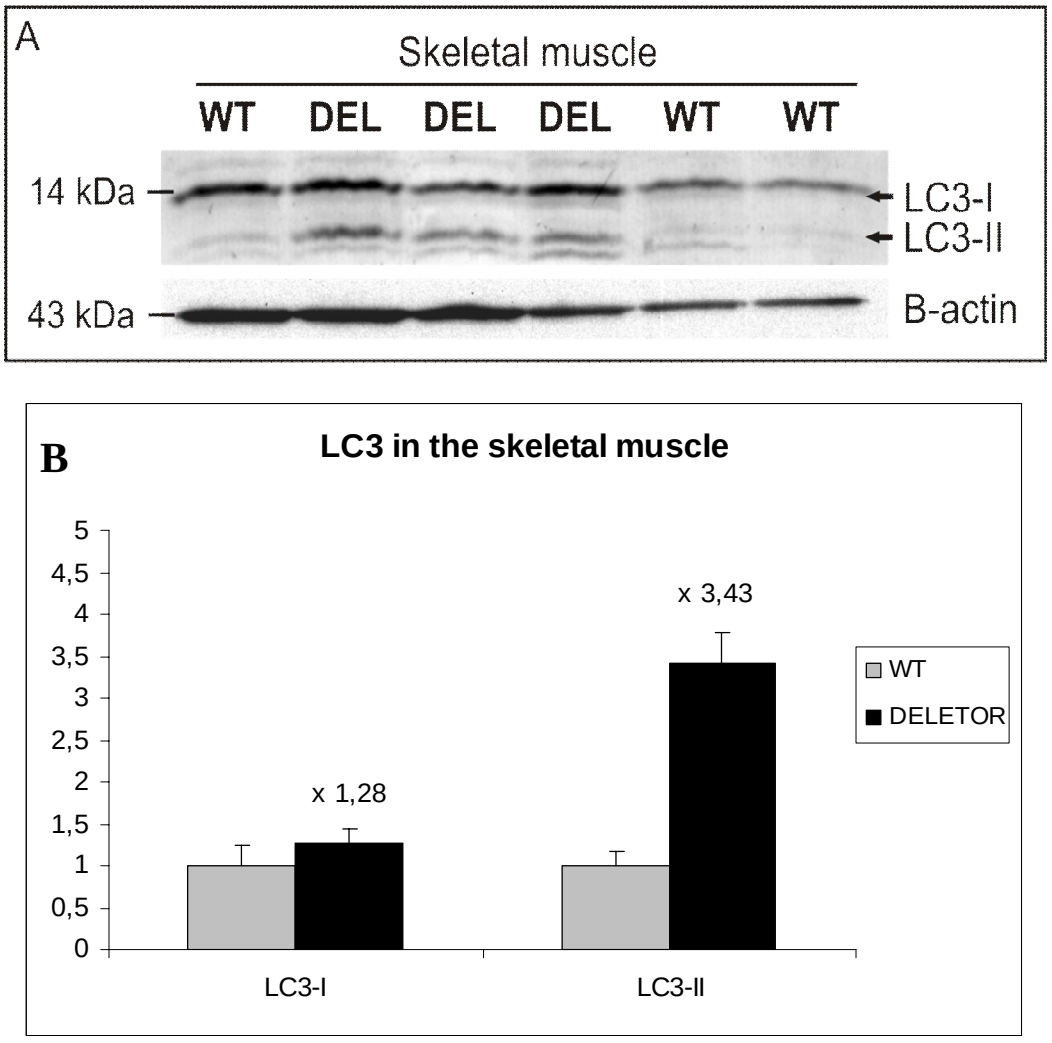

Figure 5.11: **The autophagy marker LC3-II is significantly increased in the 24-month-old Deletor skeletal muscle. A,** the immunodetection of LC3 in skeletal muscle homogenates separated by SDS-PAGE. LC3-I and LC3-II are indicated by arrows. **B**, the quantification of LC3 in the skeletal muscle samples, LC3-I: p= 0.18; LC3-II: p=0.0004 (n = 3). The SDs are indicated. DEL, Deletor; WT, wild type.

5.7.2 LC3 in different Deletor tissues

Analyzing the role of autophagy in different human pathologies, tissue homogenates from the brain, heart and liver of the Deletor and wild type mice were separated on 15 % resolving gel and probed with rabbit polyclonal anti-LC3B antibody. β-actin was used as a loading control. Both forms of LC3 were detected as two separate bands (figure 5.12 A). The bands were quantified separately and normalized against β-actin signal. Neither the amount of LC3-I nor of LC3-II was significantly changed in the tested samples (figure 5.13).

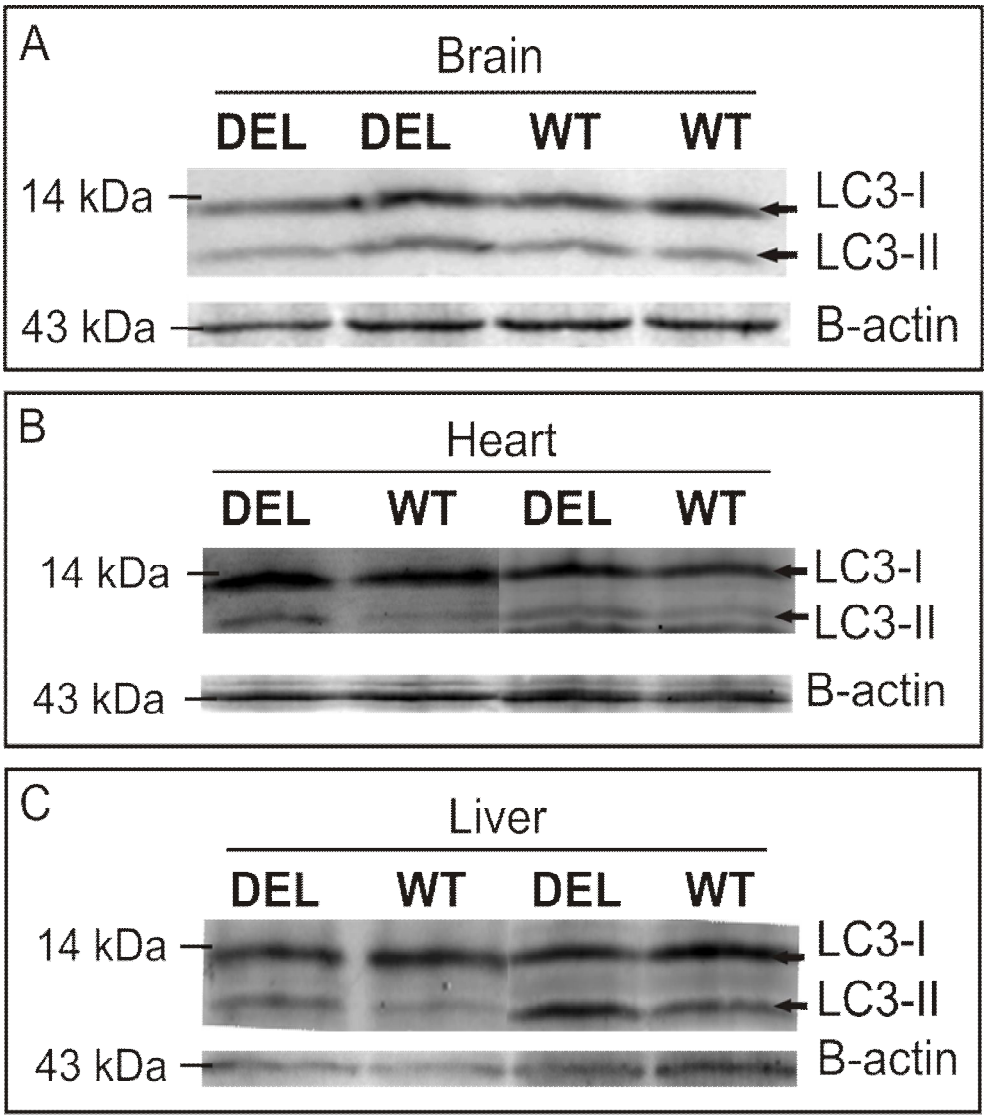

Figure 5.12: **The autophagy marker LC3-II is not significantly increased in the 24-month-old Deletor brain, heart and liver**. The immunodetection of LC3 in the brain (A), heart (B) and liver (C) homogenates separated by SDS-PAGE. LC3-I and LC3-II are indicated by the arrows. DEL, Deletor; WT, wild type.

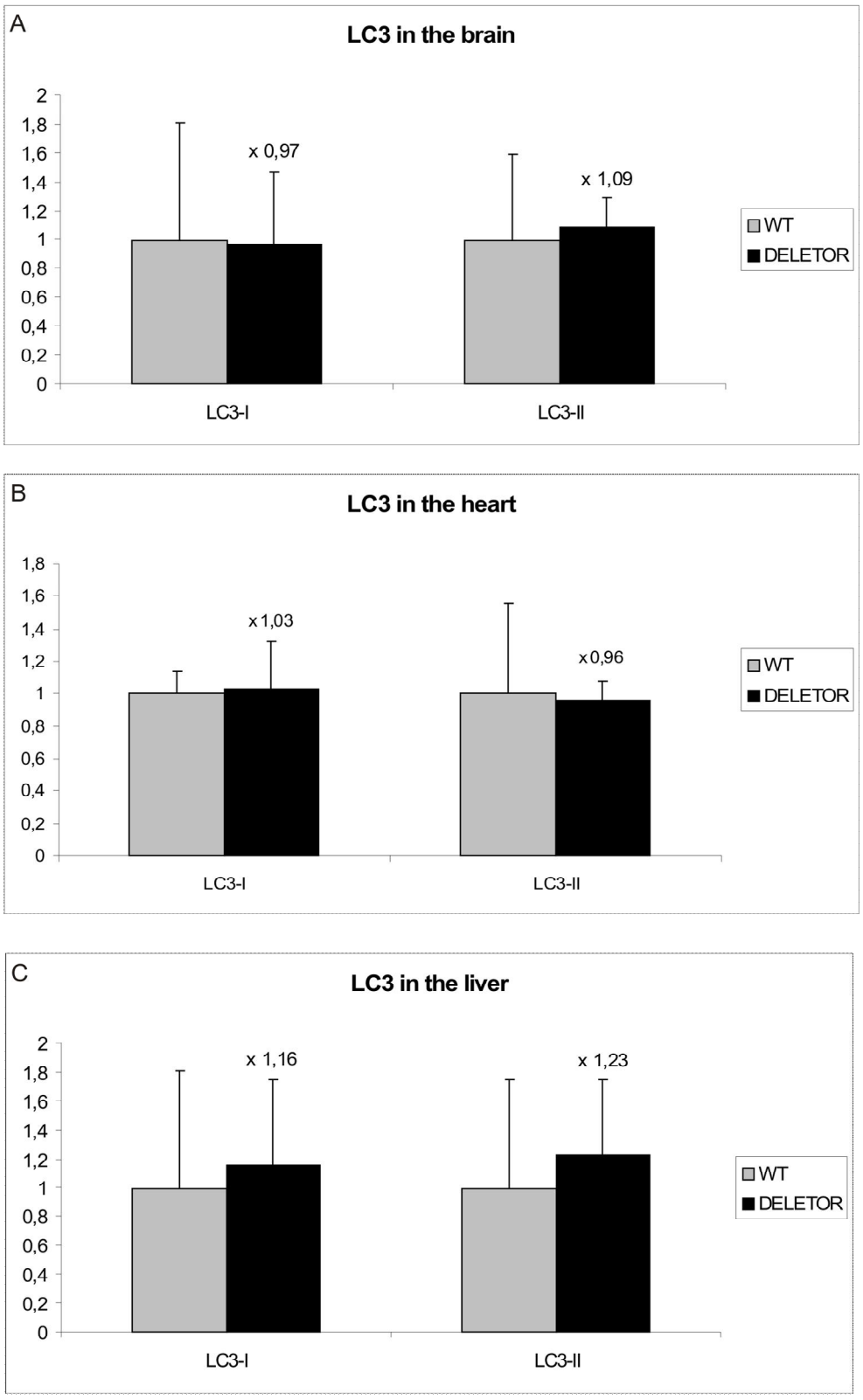

Figure 5.13: **The autophagy marker LC3-II is not significantly increased in the 24-month-old Deletor brain, heart and liver** (n = 3). The quantification of LC3 in the brain (A), heart (B) and liver (C). The SDs are indicated. WT, wild type.

5.8 *Protein acetylation on Lysine residues*

5.8.1 Pattern of acetylated proteins in different Deletor tissues

To test the theory that protein acetylation might be a specific signal for mitochondrial autophagy or degradation, the enriched fractions of mitochondria from the skeletal muscle, brain and liver of the Deletor and wild type mice were separated on 12 % resolving gel and acetylation was indicated by polyclonal rabbit acetylated-lysine antibody. Complex II subunit 70 kDa was used as a loading control (figure 5.14). Significant differences in the general pattern of mitochondrial protein acetylation between the Deletor and wild type mouse tissue counterparts (n = 3) were not found. However, a distinct difference was found in the pattern of mitochondrial protein acetylation among different tissues (figure 5.14).

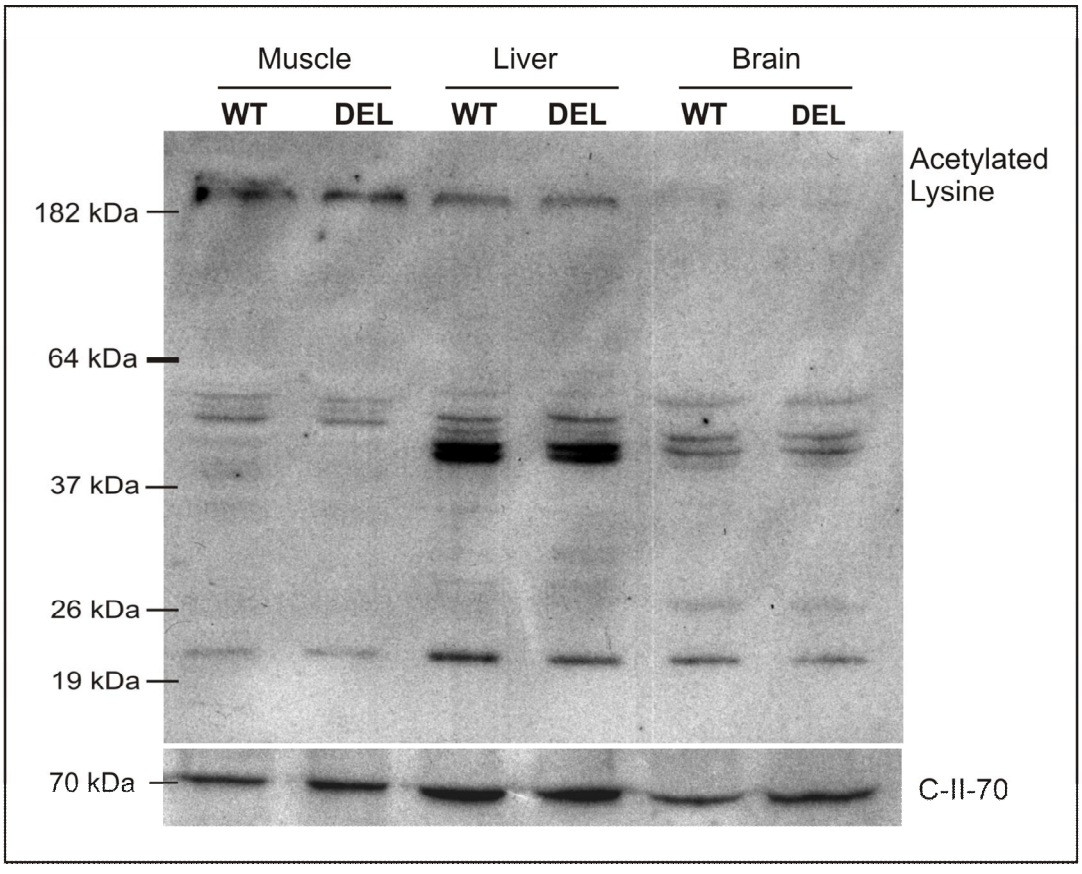

Figure 5.14: **Different general pattern of mitochondrial protein acetylation between the Deletor tissues.** The enriched mitochondrial fractions from the skeletal muscle, brain and liver samples separated by SDS-PAGE. Main protein sizes of the molecular marker are indicated. DEL, Deletor; WT, wild type; C-II-70, complex II subunit 70 kDa.

5.8.2 Pattern of acetylated proteins in the Deletor brain tissue

The minimal differences in the acetylation pattern could not be distinguish in mitochondrial enrichment, and therefore mitochondria were isolated from the brain tissue using sucrose gradient and separated on 12 % resolving gel. Acetylation was indicated by polyclonal rabbit acetylated-lysine antibody and complex II subunit 70 kDa was used as a loading control (figure 5.15). The Deletor and wild type brain tissue did not show difference in the general pattern of acetylation of mitochondrial proteins. However, changes in the abundance of individual bands of approximately 20 kDa and 35 kDa were revealed (indicated by arrows, figure 5.15).

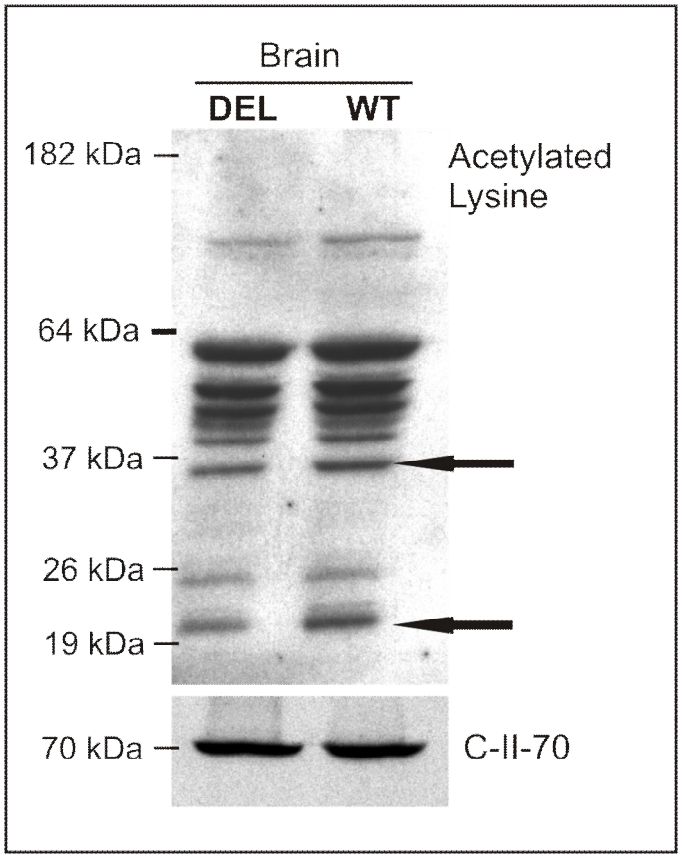

Figure 5.15: No difference in the general pattern of mitochondrial protein acetylation in the 24-month-old Deletor brain. Pure mitochondria from the Deletor and wild type brain samples separated by SDS-PAGE. Main protein sizes of the molecular marker are indicated. Differences in the individual bands are indicated by arrows. DEL, Deletor; WT, wild type; C-II-70, complex II subunit 70kDa.

6. Discussion

Mitochondrial diseases are a large group of disorders with extremely heterogeneous symptoms ranging from pure myopathy to multi-systemic involvement. They are characterized by defects in both mitochondrial and nuclear genome, leading to mitochondrial respiratory chain deficiency. Several mouse models for mitochondrial dysfunction have been generated and studied for presymptomatic disease progression or different therapeutic ideas. Since late-onset mitochondrial myopathy has been one of the most common manifestations of mitochondrial diseases in adulthood, the Deletor mouse with adPEO mutation in *PEO1* gene is a valuable tool for an understanding of mitochondrial pathogenesis.

6.1 Determination of Twinkle integration site in two transgenic mouse lines

The knowledge of exact integration site is an important feature of the transgenic mice, since the random insertion process to a coding sequence of any autosome can impair a function and/or expression of the particular gene product at the insertion site leading to false interpretation of the phenotype. Moreover, random incorporation into the sex chromosomes can lead to gender differences.

DNA walking is a method useful for finding an integration site of a transgene in the mouse genome, because it could be insert into any of 40 mouse chromosomes. In general, the transgene construct is integrated in the form of concatemer, a polymer of associated DNA fragments, which usually contains from one to ten copies of the original fragment. Thus, a semi-quantitative Southern blot method was utilized to determine the number of incorporated Twinkle constructs (Tyynismaa *et al.* 2004). Four copies of wild type Twinkle construct were identified in the A mouse line and three copies of dup352-364 Twinkle construct in the C mouse line. The integration site of wild type Twinkle construct was found on chromosome 5 in the intron 3 of *TMPRSS11d* gene (Transmembrane protease, serine 11D; OTTMUSG00000028240) of the A mouse line. The further study of the transmembrane serine protease impairment and its subsequent implications to mouse phenotype is required, but these were not the aim of this study. The non-coding band A1 on chromosome 16 was identified as the integration site in the Deletor C mouse

line. In this case, the construct does not seem to have any further implications on the Deletor phenotype.

6.2 MtDNA deletions are present in the Deletor skeletal muscle

Twinkle-PEO patients are characterized by muscle weakness and exercise intolerance with avoidant personality features frequently associated with multiple deletions of mtDNA. Deleted mtDNA molecules accumulate in patients´ brain, skeletal muscle and heart, but the highest expression of Twinkle in humans is in the skeletal muscle and pancreas (Spelbrink *et al.* 2001). Previously, multiple mtDNA deletions were showed in the Deletor skeletal muscle and brain, together with Twinkle transgene expression in the skeletal muscle, brain, liver, heart and kidney (Tyynismaa *et al.* 2005, personal comunication). In this study, the presence of mtDNA deletions was examined in several Deletor tissues, in particular the skeletal muscle, kidney, testis, liver and intestine. Apparent mtDNA deletions were detected only in the Deletor skeletal muscle. This result corresponds with the findings from PEO patients with dup352-364 mutation in the Twinkle protein and confirmed the Deletor mouse as an accurate model for late-onset adPEO. Moreover, the result might support the suggestion that different replication and/or reparing mechanisms can operate in different tissues and thus, mtDNA deletions can arise only in several ones (Goffart *et al.* 2009). No mtDNA deletions were observed in the skeletal muscle and brain of AT mice. Thus, these mice do not replicate the disease phenotype and may not be useful in Twinkle-PEO studies.

6.3 No respiratory deficient crypt cells present in Deletor intestine tissue

MtDNA mutations have been previously linked to limitation of mammalian lifespan. A homozygous transgenic mice expressing mitochondrial Polγ with defective proof-reading activity and referred to as “mutator mice”, have shown accumulation of somatic mtDNA point mutations that lead to respiratory chain dysfunction and phenotype of premature aging (Trifunovic *et al.* 2004). Recently, an accelerated accumulation of mtDNA deletions in the brain and heart has been described in these

mice resulting from dysfunction of Polγ during replication (Vermulst *et al.* 2008). Although, Twinkle together with Polγ are responsible for precise mtDNA replication, the Deletor that accumulates mtDNA deletions in the skeletal muscle and brain, did not show either the increase of mtDNA point mutation load or premature aging. These findings were obtained from post-mitotic mouse tissues using histochemical staining to detect loss of COX activity and respiration deficiency (Tyynismaa *et al.* 2005). To investigate whether dysfunctional Twinkle can result in the respiratory deficient phenotype also in replicative cells, such as colonic crypt stem cells, the histochemical analysis of the Deletor intestine was proceeded. The advantage of studying the colonic tissue is that colonic crypt stem cells are present at the crypt base and thus, majority of cells within an individual colonic crypt are the progeny of a single stem cell. If mtDNA rearrangements accumulated beyond a critical threshold in a stem cell, the whole crypt showed COX deficiency (Taylor *et al.* 2003). Neither the COX/SDH staining of frozen sections of the intestine from 24-month-old Deletor nor the long PCR analysis of mtDNA showed significant differences in this tissue compared to the nontransgenic littermate mice. The dup352-364 Twinkle mutation seems to affect the replication mechanism that leads to accumulation of mtDNA deletions and COX deficiency only in post-mitotic tissues but not in the proliferative cells. Hence, it might be possible that in the replicative cell the dNTP pool in mitochondria is supplied better by dNTPs from cytosol than in cell of post-mitotic tissues and thus, the stalling effect of mutant Twinkle can be exceeded. Recently, no mtDNA deletions have been observed in cultured cells from adPEO patients, even though the clear stalling/pausing of mutant Twinkle during mtDNA replication has been proved (Goffart *et al.* 2009).

6.4 Slight changes in the pattern of Opa1 isoform in the Deletor tissues

Mitochondria in cells form a dynamic reticulum that is maintained by a balance of fusion and fission events and dysfunction of these processes can play a key role in various diseases. Mitochondrial fusion is regulated through processing of protein Opa1 depending on mitochondrial inner membrane potential ($\Delta\psi_m$; Ishihara *et al.* 2006). This dynamin-related GTPase anchored in the inner membrane, exists in

L-OPA1 and S-OPA1 isoforms that both are likely important for Opa1 function in mitochondrial fusion (Song *et al.* 2007). Mutations in *OPA1* gene are known to cause autosomal dominant optic atrophy type 1 (ADOA) whose new form associated with multiple mtDNA deletions in the skeletal muscle and fragmentation of mitochondrial network has been recently reported (Amati-Bonneau *et al.* 2008; Hudson *et al.* 2008). Beside ADOA patients, the mitochondrial fragmentation and the shift in the pattern of Opa1 isoforms have been shown in various model systems of human disorders associated with mitochondrial dysfunction, such as in fibroblasts from "mutator mice" or in the heart tissue of Tfam knock-out mice (Duvezin-Caubet *et al.* 2006). Furthermore, the analysis of the skeletal muscle from patients diagnosed with respiratory chain defects, in particular with mtDNA depletion syndrome or MELAS, has shown this shift in Opa1 isoforms compared to healthy controls (Duvezin-Caubet *et al.* 2006).

Thus, one could expect that in the skeletal muscle of Deletor mice, a model for mitochondrial myopathy with mtDNA deletions, the shift in the pattern of Opa1 isoforms will be clearly observed. Surprisingly, all detected Opa1 isoforms were slightly elevated in the Deletor samples, compared to the wild type counterparts, suggesting an enhanced turnover of mitochondrial fusion/fission machinery. The significant increase was found in amount of L2-OPA1, the isoform that is processed to S4- and S5-OPA1 isoforms and is sufficient to restore the mitochondrial fusion and morphology and prevent the cells in culture from apoptosis (Frezza *et al.* 2006; Song *et al.* 2007). Therefore, the higher level of L2-OPA1 in the Deletor skeletal muscle may indicate the need of muscle fibres to protect against premature apoptosis due to respiratory deficient mitochondria, leading to upregulation of mitophagy.

Moreover, in the case of Deletor, a significant shift in the pattern of Opa1 isoforms to the short ones was detected in the brain samples, where in mouse tissue is present an extremely high level of L2-OPA1 isoform (Akepati *et al.* 2008). The slight increase of S-OPA1 isoform might reflect only a small amount of respiratory deficient cells in the Deletor brain. In the heart and liver tissues the particular bands of L-OPA1 and S-OPA1 isoforms were well resolved but not significantly increased compare to the wild type counterparts.

Nevertheless, in the Deletor skeletal muscle and brain all respiratory chain complexes were showed with no difference compared to the wild type tissues. Neither the amount of complex I nor its in-gel activity was changed in tested tissues

of the Deletor and wild type mice. These results can be related to findings from fibroblasts of ADOA patients, where BN-PAGE did not show significant difference either, but the amount of complex I was slightly increased and its activity was slightly reduced (Zanna *et al.* 2008).

6.5 Mitophagy proved in the Deletor skeletal muscle

Autophagy is an ongoing process that, at basal conditions, is responsible for degradation of structural proteins and damaged organelles. In cells, a functional and an intact mitochondrial network is maintained by interplay between mitochondrial fusion and fission leading to degradation of nonfunctional mitochondrial in process called mitophagy. Under the starvation conditions, the salvaging function of autophagy becomes important, especially in post-mitotic tissues.

In the case of Deletor skeletal muscle, the primary mutation in *PEO1* gene causes accumulation of mtDNA deletions and a respiratory chain deficiency with signs of starvation that lead to the dissipation of $\Delta\psi_m$ (Tyynismaa *et al.* 2005, personal comunication). Depolarized mitochondria are unable to fuse with the mitochondrial network and give arise to separated mitochondrial entities overloaded with mitochondrial proteins and altered cristae structure. This population of damaged mitochondria are sequestered and degraded via mitophagy. Damaged mitochondria that escape from the degradation process, increase in size and thus cannot be autophagocytosed. Subsequently, in function of time, the enlarge mitochondria accumulate in subsarcolemmal region of affected muscle fibers (figure 6.1; reviewed by Mijaljica *et al.* 2007). Suggestive structures that could represent all the described autophagy stages have been observed in sections of the Deletor skeletal muscle using the electron microscopic analysis (Tyynismaa *et al.* 2005)

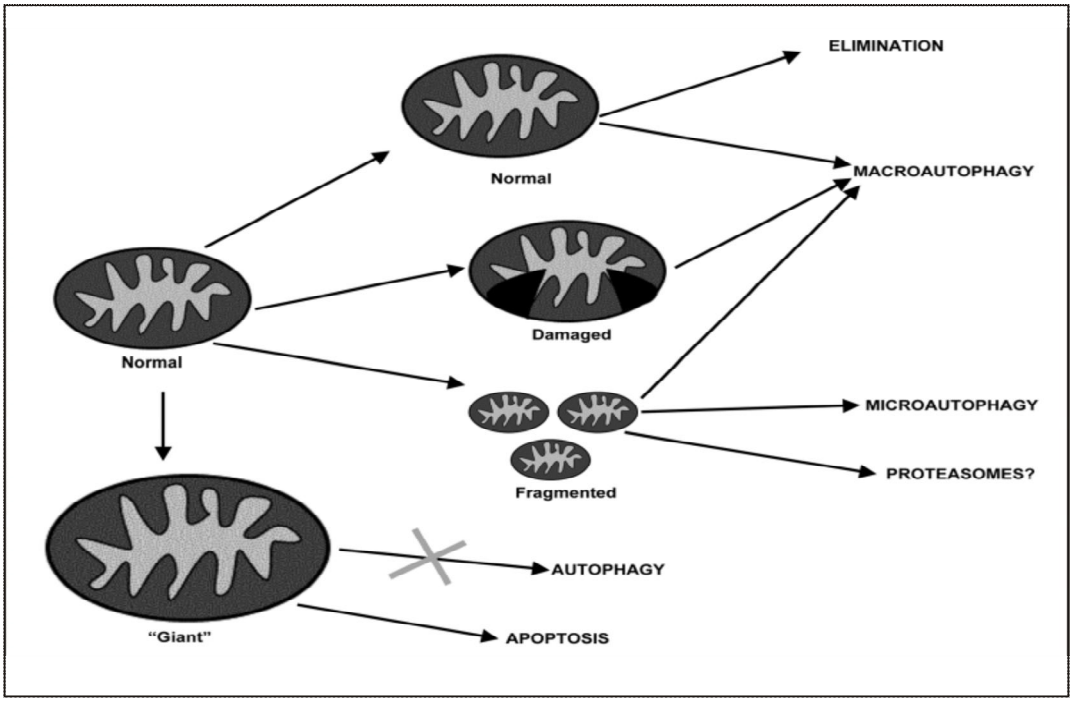

Figure 6.1: Different fates of mitochondria. The elimination mechanisms of damaged mitochondria from mammalian cells under the starvation condition (Mijaljica *et al.* 2007).

Regarding to the previous findings, the autophagy marker LC3 was examined in the skeletal muscle and the significant increase in amount of LC3-II was detected in the Deletor compared to the wild type counterparts. Since the amount of LC3-II is closely correlated with the number of autophagosomes, this result underlies the upregulation of mitophagy in the Deletor skeletal muscle and supports the suggestion of Goffart et al. They have assumed that replication stalling may induce the increased rate of mitochondrial turnover via mitophagy combined with an increased rate of replication in order to maintain normal mtDNA steady-state levels (Goffart *et al.* 2009). Thus far, the increased level of Opa1 isoforms detected also in the Deletor skeletal muscle might be consistent with this idea.

Finally, induced autophagy is linked to devastating neurodegenerative diseases and different forms of cancer, thus the LC3 immunoblotting analysis of the Deletor brain, heart and liver tissue samples was performed. Neverthless, significant increase in the amount of LC3-II was not observed in the Deletor tissues compared to the nontransgenic samples.

6.6 Tissue-specific pattern of protein acetylation in the Deletor tissues

The unanswered question remains what is the initiation signal that triggers the mitochondrial autophagy? Are mitochondria that need to be recycled, marked for autophagy? It has been observed that fission of mitochondrial network can produce uneven daughter mitochondria where one daughter mitochondrion with reduced $\Delta\psi_m$ is unable to re-fuse with the mitochondrial network and is likely to be autophagocytosed whereas the other daughter mitochondrion with hyperpolarized $\Delta\psi_m$ would fuse again with the network (Twig *et al.* 2008).

The possible signal might be a posttranslational modification of long-lived proteins, such as acetylation on lysine residues, since acetylation of ≈ 20% of all mitochondrial proteins and three mitochondrial protein deacetylases have been already described (Haigis and Guarente 2006; Kim *et al.* 2006). The hyperacetylated proteins would be separated into the depolarized daughter mitochondrion and non-acetylated to hyperpolarized one. A similar phenomenon has been observed in budding yeast *Saccharomyces cerevisiae* and other unicellular systems (Aguilaniu *et al.* 2003; Nystrom 2007). A general pattern of mitochondrial protein acetylation in the skeletal muscle, brain and liver tissue samples was performed, but revealed no differences between the Deletor and control mice. However, a clear difference in the general acetylation pattern was found between different tissues. To detect the subtle changes in the protein acetylation, the pure mitochondria from brain tissue were isolated using sucrose gradient. No difference in the general pattern was observed either. However, slight changes in particular bands were detected. Their identification was not the aim of this study, but their further clarification would be of great interest to establish. These results showed that marked changes in the overall number of acetylated proteins do not exist in the Deletor tissues.

Overall, results in this study have proved the Deletor mice as transgenic disease model that faitfully replicates the features of PEO patients in tissues accumulating mtDNA deletions without possible differences between gender of transgenic mice, and that Twinkle-PEO is truly a disease of post-mitotic cells. The results from Opa1 and LC3 analysis in the skeletal muscle may suggest to the fundamental role of mitophagy as protection against defective mitochondria in late-onset myopathy of Twinkle-PEO.

7. Conclusions

The results of this thesis respond to the specific aims:

- The position of the wild type Twinkle contruct in the A mouse line is in the intron 3 of the *TMPRSS11d* gene (Transmembrane protease, serine 11D; OTTMUSG00000028240) on chromosome 5; the dup353-365 Twinkle contruct in the C mouse line is integrated into the non-coding band A1 on chromosome 16. The expression and function study of transmembrane serine protease 11D in the wild type Twinkle overexpressor (A line) is required. This assay excluded the possible gender differences.

- The presence of mtDNA deletions only in the skeletal muscle and brain tissues, but not in other tested samples, proved the Twinkle transgenic mice referred to as Deletor as valuable disease mouse model. Histochemical analysis of the Deletor intestine supported the Twinkle-PEO as a disease of post-mitotic tissues.

- Slightly elevated levels of Opa1 isoforms in the Deletor skeletal muscle might suggest a defect in mitochondrial morphology resulting in upregulation of mitophagy. In the Deletor brain tissue, a mild increase in the level of S-OPA1 isoforms was observed, but no clear shift in the pattern of Opa1 isoforms was detected either in the brain or in the liver and heart.

- The amount of LC3-II, consistent with enhanced level of mitophagy, was significantly increased in the Deletor skeletal muscle. No changes in the level of either LC3-I or LC3-II in other tissues were detected. These results might indicate an essential role of mitophagy in late-onset mitochondrial myopathy.

- The tissue specific pattern of lysine-acetylated mitochondrial proteins was observed among different tissues (the heart, brain and skeletal muscle). Nevertheless, specific pattern of lysine-acetylated proteins, as a signal of damaged mitochondria in the Deletor tissues, was not detected.

8. References

Agostino, A., L. Valletta, P. F. Chinnery, G. Ferrari, F. Carrara, R. W. Taylor, A. M. Schaefer, D. M. Turnbull, V. Tiranti and M. Zeviani (2003). "Mutations of ANT1, Twinkle, and POLG1 in sporadic progressive external ophthalmoplegia (PEO)." Neurology **60**(8): 1354-6

Aguilaniu, H., L. Gustafsson, M. Rigoulet and T. Nystrom (2003). "Asymmetric inheritance of oxidatively damaged proteins during cytokinesis." Science **299**(5613): 1751-3

Akepati, V. R., E. C. Muller, A. Otto, H. M. Strauss, M. Portwich and C. Alexander (2008). "Characterization of OPA1 isoforms isolated from mouse tissues." J Neurochem **106**(1): 372-83

Alam, T. I., T. Kanki, T. Muta, K. Ukaji, Y. Abe, H. Nakayama, K. Takio, N. Hamasaki and D. Kang (2003). "Human mitochondrial DNA is packaged with TFAM." Nucleic Acids Res **31**(6): 1640-5

Alavi, M. V., S. Bette, S. Schimpf, F. Schuettauf, U. Schraermeyer, H. F. Wehrl, L. Ruttiger, S. C. Beck, F. Tonagel, B. J. Pichler, M. Knipper, T. Peters, J. Laufs and B. Wissinger (2007). "A splice site mutation in the murine Opa1 gene features pathology of autosomal dominant optic atrophy." Brain **130**(Pt 4): 1029-42

Amati-Bonneau, P., A. Guichet, A. Olichon, A. Chevrollier, F. Viala, S. Miot, C. Ayuso, S. Odent, C. Arrouet, C. Verny, M. N. Calmels, G. Simard, P. Belenguer, J. Wang, J. L. Puel, C. Hamel, Y. Malthiery, D. Bonneau, G. Lenaers and P. Reynier (2005). "OPA1 R445H mutation in optic atrophy associated with sensorineural deafness." Ann Neurol **58**(6): 958-63

Amati-Bonneau, P., M. L. Valentino, P. Reynier, M. E. Gallardo, B. Bornstein, A. Boissiere, Y. Campos, H. Rivera, J. G. de la Aleja, R. Carroccia, L. Iommarini, P. Labauge, D. Figarella-Branger, P. Marcorelles, A. Furby, K. Beauvais, F. Letournel, R. Liguori, C. La Morgia, P. Montagna, M. Liguori, C. Zanna, M. Rugolo, A. Cossarizza, B. Wissinger, C. Verny, R. Schwarzenbacher, M. A. Martin, J. Arenas, C. Ayuso, R. Garesse, G. Lenaers, D. Bonneau and V. Carelli (2008). "OPA1 mutations induce mitochondrial DNA instability and optic atrophy 'plus' phenotypes." Brain **131**(Pt 2): 338-51

Anderson, S., A. T. Bankier, B. G. Barrell, M. H. de Bruijn, A. R. Coulson, J. Drouin, I. C. Eperon, D. P. Nierlich, B. A. Roe, F. Sanger, P. H. Schreier, A. J. Smith, R. Staden and I. G. Young (1981). "Sequence and organization of the human mitochondrial genome." Nature **290**(5806): 457-65

Arakaki, N., T. Nishihama, A. Kohda, H. Owaki, Y. Kuramoto, R. Abe, T. Kita, M. Suenaga, T. Himeda, M. Kuwajima, H. Shibata and T. Higuti (2006). "Regulation of mitochondrial morphology and cell survival by Mitogenin I and mitochondrial single-stranded DNA binding protein." Biochim Biophys Acta **1760**(9): 1364-72

Battersby, B. J., J. C. Loredo-Osti and E. A. Shoubridge (2003). "Nuclear genetic control of mitochondrial DNA segregation." Nat Genet **33**(2): 183-6

Bestwick, R. K. and C. K. Mathews (1982). "Unusual compartmentation of precursors for nuclear and mitochondrial DNA in mouse L cells." J Biol Chem **257**(16): 9305-8

Bibb, M. J., R. A. Van Etten, C. T. Wright, M. W. Walberg and D. A. Clayton (1981). "Sequence and gene organization of mouse mitochondrial DNA." Cell **26**(2 Pt 2): 167-80

Bowmaker, M., M. Y. Yang, T. Yasukawa, A. Reyes, H. T. Jacobs, J. A. Huberman and I. J. Holt (2003). "Mammalian mitochondrial DNA replicates bidirectionally from an initiation zone." J Biol Chem **278**(51): 50961-9

Bradford, M. M. (1976). "A rapid and sensitive method for the quantitation of microgram quantities of protein utilizing the principle of protein-dye binding." Anal Biochem **72**: 248-54

Brown, T. A., C. Cecconi, A. N. Tkachuk, C. Bustamante and D. A. Clayton (2005). "Replication of mitochondrial DNA occurs by strand displacement with alternative light-strand origins, not via a strand-coupled mechanism." Genes Dev **19**(20): 2466-76

Brown, T. A., A. N. Tkachuk and D. A. Clayton (2008). "Native R-loops persist throughout the mouse mitochondrial DNA genome." J Biol Chem **283**(52): 36743-51

Cann, G. M., C. Guignabert, L. Ying, N. Deshpande, J. M. Bekker, L. Wang, B. Zhou and M. Rabinovitch (2008). "Developmental expression of LC3alpha and beta: absence of fibronectin or autophagy phenotype in LC3beta knockout mice." Dev Dyn **237**(1): 187-95

Carroll, J., I. M. Fearnley, J. M. Skehel, R. J. Shannon, J. Hirst and J. E. Walker (2006). "Bovine complex I is a complex of 45 different subunits." J Biol Chem **281**(43): 32724-7

Clayton, D. A. (1982). "Replication of animal mitochondrial DNA." Cell **28**(4): 693-705

Cooper, H. M. and J. N. Spelbrink (2008). "The human SIRT3 protein deacetylase is exclusively mitochondrial." Biochem J **411**(2): 279-85

Dairaghi, D. J., G. S. Shadel and D. A. Clayton (1995). "Addition of a 29 residue carboxyl-terminal tail converts a simple HMG box-containing protein into a transcriptional activator." J Mol Biol **249**(1): 11-28

Davies, V. J., A. J. Hollins, M. J. Piechota, W. Yip, J. R. Davies, K. E. White, P. P. Nicols, M. E. Boulton and M. Votruba (2007). "Opa1 deficiency in a mouse model of autosomal dominant optic atrophy impairs mitochondrial morphology, optic nerve structure and visual function." Hum Mol Genet **16**(11): 1307-18

Delettre, C., J. M. Griffoin, J. Kaplan, H. Dollfus, B. Lorenz, L. Faivre, G. Lenaers, P. Belenguer and C. P. Hamel (2001). "Mutation spectrum and splicing variants in the OPA1 gene." Hum Genet **109**(6): 584-91

Delettre, C., G. Lenaers, J. M. Griffoin, N. Gigarel, C. Lorenzo, P. Belenguer, L. Pelloquin, J. Grosgeorge, C. Turc-Carel, E. Perret, C. Astarie-Dequeker, L. Lasquellec, B. Arnaud, B. Ducommun, J. Kaplan and C. P. Hamel (2000). "Nuclear gene OPA1, encoding a mitochondrial dynamin-related protein, is mutated in dominant optic atrophy." Nat Genet **26**(2): 207-10

Delettre, C., G. Lenaers, L. Pelloquin, P. Belenguer and C. P. Hamel (2002). "OPA1 (Kjer type) dominant optic atrophy: a novel mitochondrial disease." Mol Genet Metab **75**(2): 97-107

Deschauer, M., G. Hudson, T. Muller, R. W. Taylor, P. F. Chinnery and S. Zierz (2005). "A novel ANT1 gene mutation with probable germline mosaicism in autosomal dominant progressive external ophthalmoplegia." Neuromuscul Disord **15**(4): 311-5

Dolce, V., G. Fiermonte, M. J. Runswick, F. Palmieri and J. E. Walker (2001). "The human mitochondrial deoxynucleotide carrier and its role in the toxicity of nucleoside antivirals." Proc Natl Acad Sci U S A **98**(5): 2284-8

Dolce, V., P. Scarcia, D. Iacopetta and F. Palmieri (2005). "A fourth ADP/ATP carrier isoform in man: identification, bacterial expression, functional characterization and tissue distribution." FEBS Lett **579**(3): 633-7

Dunn, W. A., Jr. (1994). "Autophagy and related mechanisms of lysosome-mediated protein degradation." Trends Cell Biol **4**(4): 139-43

Duvezin-Caubet, S., R. Jagasia, J. Wagener, S. Hofmann, A. Trifunovic, A. Hansson, A. Chomyn, M. F. Bauer, G. Attardi, N. G. Larsson, W. Neupert and A. S. Reichert (2006). "Proteolytic processing of OPA1 links mitochondrial dysfunction to alterations in mitochondrial morphology." J Biol Chem **281**(49): 37972-9

Duvezin-Caubet, S., M. Koppen, J. Wagener, M. Zick, L. Israel, A. Bernacchia, R. Jagasia, E. I. Rugarli, A. Imhof, W. Neupert, T. Langer and A. S. Reichert (2007). "OPA1 processing reconstituted in yeast depends on the subunit composition of the m-AAA protease in mitochondria." Mol Biol Cell **18**(9): 3582-90

Edinger, A. L. and C. B. Thompson (2003). "Defective autophagy leads to cancer." Cancer Cell **4**(6): 422-4

Elmore, S. P., T. Qian, S. F. Grissom and J. J. Lemasters (2001). "The mitochondrial permeability transition initiates autophagy in rat hepatocytes." Faseb J **15**(12): 2286-7

Elpeleg, O. (2003). "Inherited mitochondrial DNA depletion." Pediatr Res **54**(2): 153-9

Falkenberg, M., M. Gaspari, A. Rantanen, A. Trifunovic, N. G. Larsson and C. M. Gustafsson (2002). "Mitochondrial transcription factors B1 and B2 activate transcription of human mtDNA." Nat Genet **31**(3): 289-94

Fan, L., S. Kim, C. L. Farr, K. T. Schaefer, K. M. Randolph, J. A. Tainer and L. S. Kaguni (2006). "A novel processive mechanism for DNA synthesis revealed by structure, modeling and mutagenesis of the accessory subunit of human mitochondrial DNA polymerase." J Mol Biol **358**(5): 1229-43

Farge, G., T. Holmlund, J. Khvorostova, R. Rofougaran, A. Hofer and M. Falkenberg (2008). "The N-terminal domain of TWINKLE contributes to single-stranded DNA binding and DNA helicase activities." Nucleic Acids Res **36**(2): 393-403

Farr, C. L., Y. Wang and L. S. Kaguni (1999). "Functional interactions of mitochondrial DNA polymerase and single-stranded DNA-binding protein. Template-primer DNA binding and initiation and elongation of DNA strand synthesis." J Biol Chem **274**(21): 14779-85

Fernandez-Silva, P., J. A. Enriquez and J. Montoya (2003). "Replication and transcription of mammalian mitochondrial DNA." Exp Physiol **88**(1): 41-56

Ferraro, P., G. Pontarin, L. Crocco, S. Fabris, P. Reichard and V. Bianchi (2005). "Mitochondrial deoxynucleotide pools in quiescent fibroblasts: a possible model for mitochondrial neurogastrointestinal encephalomyopathy (MNGIE)." J Biol Chem **280**(26): 24472-80

Frey, T. G. and C. A. Mannella (2000). "The internal structure of mitochondria." Trends Biochem Sci **25**(7): 319-24

Frezza, C., S. Cipolat, O. Martins de Brito, M. Micaroni, G. V. Beznoussenko, T. Rudka, D. Bartoli, R. S. Polishuck, N. N. Danial, B. De Strooper and L. Scorrano (2006). "OPA1 controls apoptotic cristae remodeling independently from mitochondrial fusion." Cell **126**(1): 177-89

Garrido, N., L. Griparic, E. Jokitalo, J. Wartiovaara, A. M. van der Bliek and J. N. Spelbrink (2003). "Composition and dynamics of human mitochondrial nucleoids." Mol Biol Cell **14**(4): 1583-96

Gilkerson, R. W., J. M. Selker and R. A. Capaldi (2003). "The cristal membrane of mitochondria is the principal site of oxidative phosphorylation." FEBS Lett **546**(2-3): 355-8

Goffart, S., H. M. Cooper, H. Tyynismaa, S. Wanrooij, A. Suomalainen and J. N. Spelbrink (2009). "Twinkle mutations associated with autosomal dominant progressive external ophthalmoplegia lead to impaired helicase function and in vivo mtDNA replication stalling." Hum Mol Genet **18**(2): 328-40

Goto, Y., I. Nonaka and S. Horai (1990). "A mutation in the tRNA(Leu)(UUR) gene associated with the MELAS subgroup of mitochondrial encephalomyopathies." Nature **348**(6302): 651-3

Gray, M. W., G. Burger and B. F. Lang (1999). "Mitochondrial evolution." Science **283**(5407): 1476-81

Graziewicz, M. A., M. J. Longley, R. J. Bienstock, M. Zeviani and W. C. Copeland (2004). "Structure-function defects of human mitochondrial DNA polymerase in autosomal dominant progressive external ophthalmoplegia." Nat Struct Mol Biol **11**(8): 770-6

Graziewicz, M. A., M. J. Longley and W. C. Copeland (2006). "DNA polymerase gamma in mitochondrial DNA replication and repair." Chem Rev **106**(2): 383-405

Haigis, M. C. and L. P. Guarente (2006). "Mammalian sirtuins--emerging roles in physiology, aging, and calorie restriction." Genes Dev **20**(21): 2913-21

Haigis, M. C., R. Mostoslavsky, K. M. Haigis, K. Fahie, D. C. Christodoulou, A. J. Murphy, D. M. Valenzuela, G. D. Yancopoulos, M. Karow, G. Blander, C. Wolberger, T. A. Prolla, R. Weindruch, F. W. Alt and L. Guarente (2006). "SIRT4 inhibits glutamate dehydrogenase and opposes the effects of calorie restriction in pancreatic beta cells." Cell **126**(5): 941-54

Hakonen, A. H., S. Goffart, S. Marjavaara, A. Paetau, H. Cooper, K. Mattila, M. Lampinen, A. Sajantila, T. Lonnqvist, J. N. Spelbrink and A. Suomalainen (2008). "Infantile-onset spinocerebellar ataxia and mitochondrial recessive ataxia syndrome are associated with neuronal complex I defect and mtDNA depletion." Hum Mol Genet

Hakonen, A. H., P. Isohanni, A. Paetau, R. Herva, A. Suomalainen and T. Lonnqvist (2007). "Recessive Twinkle mutations in early onset encephalopathy with mtDNA depletion." Brain **130**(Pt 11): 3032-40

Hallows, W. C., S. Lee and J. M. Denu (2006). "Sirtuins deacetylate and activate mammalian acetyl-CoA synthetases." Proc Natl Acad Sci U S A **103**(27): 10230-5

He, H., Y. Dang, F. Dai, Z. Guo, J. Wu, X. She, Y. Pei, Y. Chen, W. Ling, C. Wu, S. Zhao, J. O. Liu and L. Yu (2003). "Post-translational modifications of three members of the human MAP1LC3 family and detection of a novel type of modification for MAP1LC3B." J Biol Chem **278**(31): 29278-87

He, J., C. C. Mao, A. Reyes, H. Sembongi, M. Di Re, C. Granycome, A. B. Clippingdale, I. M. Fearnley, M. Harbour, A. J. Robinson, S. Reichelt, J. N. Spelbrink, J. E. Walker and I. J. Holt (2007). "The AAA+ protein ATAD3 has displacement loop binding properties and is involved in mitochondrial nucleoid organization." J Cell Biol **176**(2): 141-6

Holt, I. J., A. E. Harding, R. K. Petty and J. A. Morgan-Hughes (1990). "A new mitochondrial disease associated with mitochondrial DNA heteroplasmy." Am J Hum Genet **46**(3): 428-33

Holt, I. J., H. E. Lorimer and H. T. Jacobs (2000). "Coupled leading- and lagging-strand synthesis of mammalian mitochondrial DNA." Cell **100**(5): 515-24

Hudson, G., P. Amati-Bonneau, E. L. Blakely, J. D. Stewart, L. He, A. M. Schaefer, P. G. Griffiths, K. Ahlqvist, A. Suomalainen, P. Reynier, R. McFarland, D. M. Turnbull, P. F. Chinnery and R. W. Taylor (2008). "Mutation of OPA1 causes dominant optic atrophy with external ophthalmoplegia, ataxia, deafness and multiple mitochondrial DNA deletions: a novel disorder of mtDNA maintenance." Brain **131**(Pt 2): 329-37

Ishihara, N., Y. Fujita, T. Oka and K. Mihara (2006). "Regulation of mitochondrial morphology through proteolytic cleavage of OPA1." EMBO J **25**(13): 2966-77

Jeppesen, T. D., M. Schwartz, E. Colding-Jorgensen, T. Krag, S. Hauerslev and J. Vissing (2008). "Phenotype and clinical course in a family with a new de novo Twinkle gene mutation." Neuromuscul Disord **18**(4): 306-9

Kabeya, Y., N. Mizushima, T. Ueno, A. Yamamoto, T. Kirisako, T. Noda, E. Kominami, Y. Ohsumi and T. Yoshimori (2000). "LC3, a mammalian homologue of yeast Apg8p, is localized in autophagosome membranes after processing." EMBO J **19**(21): 5720-8

Kabeya, Y., N. Mizushima, A. Yamamoto, S. Oshitani-Okamoto, Y. Ohsumi and T. Yoshimori (2004). "LC3, GABARAP and GATE16 localize to autophagosomal membrane depending on form-II formation." J Cell Sci **117**(Pt 13): 2805-12

Kanki, T., K. Ohgaki, M. Gaspari, C. M. Gustafsson, A. Fukuoh, N. Sasaki, N. Hamasaki and D. Kang (2004). "Architectural role of mitochondrial transcription factor A in maintenance of human mitochondrial DNA." Mol Cell Biol **24**(22): 9823-34

Kasamatsu, H. and J. Vinograd (1974). "Replication of circular DNA in eukaryotic cells." Annu Rev Biochem **43**(0): 695-719

Kaukonen, J., J. K. Juselius, V. Tiranti, A. Kyttala, M. Zeviani, G. P. Comi, S. Keranen, L. Peltonen and A. Suomalainen (2000). "Role of adenine nucleotide translocator 1 in mtDNA maintenance." Science **289**(5480): 782-5

Kim, I., S. Rodriguez-Enriquez and J. J. Lemasters (2007). "Selective degradation of mitochondria by mitophagy." Arch Biochem Biophys **462**(2): 245-53

Kim, J. Y., J. M. Hwang, H. S. Ko, M. W. Seong, B. J. Park and S. S. Park (2005). "Mitochondrial DNA content is decreased in autosomal dominant optic atrophy." Neurology **64**(6): 966-72

Kim, S. C., R. Sprung, Y. Chen, Y. Xu, H. Ball, J. Pei, T. Cheng, Y. Kho, H. Xiao, L. Xiao, N. V. Grishin, M. White, X. J. Yang and Y. Zhao (2006). "Substrate and functional diversity of lysine acetylation revealed by a proteomics survey." Mol Cell **23**(4): 607-18

Kissova, I., M. Deffieu, S. Manon and N. Camougrand (2004). "Uth1p is involved in the autophagic degradation of mitochondria." J Biol Chem **279**(37): 39068-74

Klionsky, D. J., J. M. Cregg, W. A. Dunn, Jr., S. D. Emr, Y. Sakai, I. V. Sandoval, A. Sibirny, S. Subramani, M. Thumm, M. Veenhuis and Y. Ohsumi (2003). "A unified nomenclature for yeast autophagy-related genes." Dev Cell **5**(4): 539-45

Korhonen, J. A., V. Pande, T. Holmlund, G. Farge, X. H. Pham, L. Nilsson and M. Falkenberg (2008). "Structure-function defects of the TWINKLE linker region in progressive external ophthalmoplegia." J Mol Biol **377**(3): 691-705

Korhonen, J. A., X. H. Pham, M. Pellegrini and M. Falkenberg (2004). "Reconstitution of a minimal mtDNA replisome in vitro." EMBO J **23**(12): 2423-9

Koskinen, T., P. Santavuori, K. Sainio, M. Lappi, A. K. Kallio and H. Pihko (1994). "Infantile onset spinocerebellar ataxia with sensory neuropathy: a new inherited disease." J Neurol Sci **121**(1): 50-6

Kruse, B., N. Narasimhan and G. Attardi (1989). "Termination of transcription in human mitochondria: identification and purification of a DNA binding protein factor that promotes termination." Cell **58**(2): 391-7

Lamantea, E., V. Tiranti, A. Bordoni, A. Toscano, F. Bono, S. Servidei, A. Papadimitriou, H. Spelbrink, L. Silvestri, G. Casari, G. P. Comi and M. Zeviani (2002). "Mutations of mitochondrial DNA polymerase gammaA are a frequent cause of autosomal dominant or recessive progressive external ophthalmoplegia." Ann Neurol **52**(2): 211-9

Levy, S. E., Y. S. Chen, B. H. Graham and D. C. Wallace (2000). "Expression and sequence analysis of the mouse adenine nucleotide translocase 1 and 2 genes." Gene **254**(1-2): 57-66

Lewis, S., W. Hutchison, D. Thyagarajan and H. H. Dahl (2002). "Clinical and molecular features of adPEO due to mutations in the Twinkle gene." J Neurol Sci **201**(1-2): 39-44

Lin, S. J., M. Kaeberlein, A. A. Andalis, L. A. Sturtz, P. A. Defossez, V. C. Culotta, G. R. Fink and L. Guarente (2002). "Calorie restriction extends Saccharomyces cerevisiae lifespan by increasing respiration." Nature **418**(6895): 344-8

Lombard, D. B., F. W. Alt, H. L. Cheng, J. Bunkenborg, R. S. Streeper, R. Mostoslavsky, J. Kim, G. Yancopoulos, D. Valenzuela, A. Murphy, Y. Yang, Y. Chen, M. D. Hirschey, R. T. Bronson, M. Haigis, L. P. Guarente, R. V. Farese, Jr., S. Weissman, E. Verdin and B. Schwer (2007). "Mammalian Sir2 homolog SIRT3 regulates global mitochondrial lysine acetylation." Mol Cell Biol **27**(24): 8807-14

Longley, M. J., S. Clark, C. Yu Wai Man, G. Hudson, S. E. Durham, R. W. Taylor, S. Nightingale, D. M. Turnbull, W. C. Copeland and P. F. Chinnery (2006). "Mutant POLG2 disrupts DNA polymerase gamma subunits and causes progressive external ophthalmoplegia." Am J Hum Genet **78**(6): 1026-34

Mannella, C. A. (2000). "Introduction: our changing views of mitochondria." J Bioenerg Biomembr **32**(1): 1-4

Margulis, L. (1976). "Genetic and evolutionary consequences of symbiosis." Exp Parasitol **39**(2): 277-349

Martin, W. and M. Muller (1998). "The hydrogen hypothesis for the first eukaryote." Nature **392**(6671): 37-41

McKenzie, M., D. Liolitsa and M. G. Hanna (2004). "Mitochondrial disease: mutations and mechanisms." Neurochem Res **29**(3): 589-600

Mijaljica, D., M. Prescott and R. J. Devenish (2007). "Different fates of mitochondria: alternative ways for degradation?" Autophagy **3**(1): 4-9

Mizushima, N., A. Yamamoto, M. Matsui, T. Yoshimori and Y. Ohsumi (2004). "In vivo analysis of autophagy in response to nutrient starvation using transgenic mice expressing a fluorescent autophagosome marker." Mol Biol Cell **15**(3): 1101-11

Montoya, J., G. L. Gaines and G. Attardi (1983). "The pattern of transcription of the human mitochondrial rRNA genes reveals two overlapping transcription units." Cell **34**(1): 151-9

Montoya, J., D. Ojala and G. Attardi (1981). "Distinctive features of the 5'-terminal sequences of the human mitochondrial mRNAs." Nature **290**(5806): 465-70

Moraes, C. T., S. Shanske, H. J. Tritschler, J. R. Aprille, F. Andreetta, E. Bonilla, E. A. Schon and S. DiMauro (1991). "mtDNA depletion with variable tissue expression: a novel genetic abnormality in mitochondrial diseases." Am J Hum Genet **48**(3): 492-501

Nakamura, Y., M. Ogura, D. Tanaka and N. Inagaki (2008). "Localization of mouse mitochondrial SIRT proteins: shift of SIRT3 to nucleus by co-expression with SIRT5." Biochem Biophys Res Commun **366**(1): 174-9

Nikali, K., A. Suomalainen, J. Saharinen, M. Kuokkanen, J. N. Spelbrink, T. Lonnqvist and L. Peltonen (2005). "Infantile onset spinocerebellar ataxia is caused by recessive mutations in mitochondrial proteins Twinkle and Twinky." Hum Mol Genet **14**(20): 2981-90

Nystrom, T. (2007). "A bacterial kind of aging." PLoS Genet **3**(12): e224

Ojala, D., J. Montoya and G. Attardi (1981). "tRNA punctuation model of RNA processing in human mitochondria." Nature **290**(5806): 470-4

Olichon, A., L. Baricault, N. Gas, E. Guillou, A. Valette, P. Belenguer and G. Lenaers (2003). "Loss of OPA1 perturbates the mitochondrial inner membrane structure and integrity, leading to cytochrome c release and apoptosis." J Biol Chem **278**(10): 7743-6

Olichon, A., L. J. Emorine, E. Descoins, L. Pelloquin, L. Brichese, N. Gas, E. Guillou, C. Delettre, A. Valette, C. P. Hamel, B. Ducommun, G. Lenaers and P. Belenguer (2002). "The human dynamin-related protein OPA1 is anchored to the mitochondrial inner membrane facing the inter-membrane space." FEBS Lett **523**(1-3): 171-6

Olichon, A., T. Landes, L. Arnaune-Pelloquin, L. J. Emorine, V. Mils, A. Guichet, C. Delettre, C. Hamel, P. Amati-Bonneau, D. Bonneau, P. Reynier, G. Lenaers and P. Belenguer (2007). "Effects of OPA1 mutations on mitochondrial morphology and apoptosis: relevance to ADOA pathogenesis." J Cell Physiol **211**(2): 423-30

Onyango, P., I. Celic, J. M. McCaffery, J. D. Boeke and A. P. Feinberg (2002). "SIRT3, a human SIR2 homologue, is an NAD-dependent deacetylase localized to mitochondria." Proc Natl Acad Sci U S A **99**(21): 13653-8

Pelloquin, L., P. Belenguer, Y. Menon, N. Gas and B. Ducommun (1999). "Fission yeast Msp1 is a mitochondrial dynamin-related protein." J Cell Sci **112 (Pt 22)**: 4151-61

Pohjoismaki, J. L., S. Wanrooij, A. K. Hyvarinen, S. Goffart, I. J. Holt, J. N. Spelbrink and H. T. Jacobs (2006). "Alterations to the expression level of mitochondrial transcription factor A, TFAM, modify the mode of mitochondrial DNA replication in cultured human cells." Nucleic Acids Res **34**(20): 5815-28

Pontarin, G., L. Gallinaro, P. Ferraro, P. Reichard and V. Bianchi (2003). "Origins of mitochondrial thymidine triphosphate: dynamic relations to cytosolic pools." Proc Natl Acad Sci U S A **100**(21): 12159-64

Reichard, P. (1988). "Interactions between deoxyribonucleotide and DNA synthesis." Annu Rev Biochem **57**: 349-74

Ropp, P. A. and W. C. Copeland (1996). "Cloning and characterization of the human mitochondrial DNA polymerase, DNA polymerase gamma." Genomics **36**(3): 449-58

Rossignol, R., B. Faustin, C. Rocher, M. Malgat, J. P. Mazat and T. Letellier (2003). "Mitochondrial threshold effects." Biochem J **370**(Pt 3): 751-62

Rotig, A., V. Cormier, S. Blanche, J. P. Bonnefont, F. Ledeist, N. Romero, J. Schmitz, P. Rustin, A. Fischer, J. M. Saudubray and et al. (1990). "Pearson's marrow-pancreas syndrome. A multisystem mitochondrial disorder in infancy." J Clin Invest **86**(5): 1601-8

Sarzi, E., S. Goffart, V. Serre, D. Chretien, A. Slama, A. Munnich, J. N. Spelbrink and A. Rotig (2007). "Twinkle helicase (PEO1) gene mutation causes mitochondrial DNA depletion." Ann Neurol **62**(6): 579-87

Shadel, G. S. and D. A. Clayton (1997). "Mitochondrial DNA maintenance in vertebrates." Annu Rev Biochem **66**: 409-35

Shepard, K. A. and M. P. Yaffe (1999). "The yeast dynamin-like protein, Mgm1p, functions on the mitochondrial outer membrane to mediate mitochondrial inheritance." J Cell Biol **144**(4): 711-20

Shi, T., F. Wang, E. Stieren and Q. Tong (2005). "SIRT3, a mitochondrial sirtuin deacetylase, regulates mitochondrial function and thermogenesis in brown adipocytes." J Biol Chem **280**(14): 13560-7

Scher, M. B., A. Vaquero and D. Reinberg (2007). "SirT3 is a nuclear NAD+-dependent histone deacetylase that translocates to the mitochondria upon cellular stress." Genes Dev **21**(8): 920-8

Schlicker, C., M. Gertz, P. Papatheodorou, B. Kachholz, C. F. Becker and C. Steegborn (2008). "Substrates and regulation mechanisms for the human mitochondrial sirtuins Sirt3 and Sirt5." J Mol Biol **382**(3): 790-801

Schwartz, M. and J. Vissing (2002). "Paternal inheritance of mitochondrial DNA." N Engl J Med **347**(8): 576-80

Schwartz, M. and J. Vissing (2004). "No evidence for paternal inheritance of mtDNA in patients with sporadic mtDNA mutations." J Neurol Sci **218**(1-2): 99-101

Schwer, B., J. Bunkenborg, R. O. Verdin, J. S. Andersen and E. Verdin (2006). "Reversible lysine acetylation controls the activity of the mitochondrial enzyme acetyl-CoA synthetase 2." Proc Natl Acad Sci U S A **103**(27): 10224-9

Schwer, B., B. J. North, R. A. Frye, M. Ott and E. Verdin (2002). "The human silent information regulator (Sir)2 homologue hSIRT3 is a mitochondrial nicotinamide adenine dinucleotide-dependent deacetylase." J Cell Biol **158**(4): 647-57

Song, Z., H. Chen, M. Fiket, C. Alexander and D. C. Chan (2007). "OPA1 processing controls mitochondrial fusion and is regulated by mRNA splicing, membrane potential, and Yme1L." J Cell Biol **178**(5): 749-55

Spees, J. L., S. D. Olson, M. J. Whitney and D. J. Prockop (2006). "Mitochondrial transfer between cells can rescue aerobic respiration." Proc Natl Acad Sci U S A **103**(5): 1283-8

Spelbrink, J. N., F. Y. Li, V. Tiranti, K. Nikali, Q. P. Yuan, M. Tariq, S. Wanrooij, N. Garrido, G. Comi, L. Morandi, L. Santoro, A. Toscano, G. M. Fabrizi, H. Somer, R. Croxen, D. Beeson, J. Poulton, A. Suomalainen, H. T. Jacobs, M. Zeviani and C. Larsson (2001). "Human mitochondrial DNA deletions associated with mutations in the gene encoding Twinkle, a phage T7 gene 4-like protein localized in mitochondria." Nat Genet **28**(3): 223-31

Spinazzola, A. and M. Zeviani (2005). "Disorders of nuclear-mitochondrial intergenomic signaling." Gene **354**: 162-8

Stepien, G., A. Torroni, A. B. Chung, J. A. Hodge and D. C. Wallace (1992). "Differential expression of adenine nucleotide translocator isoforms in mammalian tissues and during muscle cell differentiation." J Biol Chem **267**(21): 14592-7

Suomalainen, A., A. Majander, M. Wallin, K. Setala, K. Kontula, H. Leinonen, T. Salmi, A. Paetau, M. Haltia, L. Valanne, J. Lonnqvist, L. Peltonen and H. Somer (1997). "Autosomal dominant progressive external ophthalmoplegia with multiple deletions of mtDNA: clinical, biochemical, and molecular genetic features of the 10q-linked disease." Neurology **48**(5): 1244-53

Taanman, J. W. (1999). "The mitochondrial genome: structure, transcription, translation and replication." Biochim Biophys Acta **1410**(2): 103-23

Tal, R., G. Winter, N. Ecker, D. J. Klionsky and H. Abeliovich (2007). "Aup1p, a yeast mitochondrial protein phosphatase homolog, is required for efficient stationary phase mitophagy and cell survival." J Biol Chem **282**(8): 5617-24

Tanida, I., T. Ueno and E. Kominami (2004). "LC3 conjugation system in mammalian autophagy." Int J Biochem Cell Biol **36**(12): 2503-18

Taylor, R. W., M. J. Barron, G. M. Borthwick, A. Gospel, P. F. Chinnery, D. C. Samuels, G. A. Taylor, S. M. Plusa, S. J. Needham, L. C. Greaves, T. B. Kirkwood and D. M. Turnbull (2003). "Mitochondrial DNA mutations in human colonic crypt stem cells." J Clin Invest **112**(9): 1351-60

Taylor, R. W. and D. M. Turnbull (2005). "Mitochondrial DNA mutations in human disease." Nat Rev Genet **6**(5): 389-402

Tiranti, V., E. Rossi, A. Ruiz-Carrillo, G. Rossi, M. Rocchi, S. DiDonato, O. Zuffardi and M. Zeviani (1995). "Chromosomal localization of mitochondrial transcription factor A (TCF6), single-stranded DNA-binding protein (SSBP), and endonuclease G (ENDOG), three human housekeeping genes involved in mitochondrial biogenesis." Genomics **25**(2): 559-64

Trifunovic, A., A. Wredenberg, M. Falkenberg, J. N. Spelbrink, A. T. Rovio, C. E. Bruder, Y. M. Bohlooly, S. Gidlof, A. Oldfors, R. Wibom, J. Tornell, H. T. Jacobs and N. G. Larsson (2004). "Premature ageing in mice expressing defective mitochondrial DNA polymerase." Nature **429**(6990): 417-23

Twig, G., A. Elorza, A. J. Molina, H. Mohamed, J. D. Wikstrom, G. Walzer, L. Stiles, S. E. Haigh, S. Katz, G. Las, J. Alroy, M. Wu, B. F. Py, J. Yuan, J. T. Deeney, B. E. Corkey and O. S. Shirihai (2008). "Fission and selective fusion govern mitochondrial segregation and elimination by autophagy." EMBO J **27**(2): 433-46

Tyynismaa, H., K. P. Mjosund, S. Wanrooij, I. Lappalainen, E. Ylikallio, A. Jalanko, J. N. Spelbrink, A. Paetau and A. Suomalainen (2005). "Mutant mitochondrial helicase Twinkle causes multiple mtDNA deletions and a late-onset mitochondrial disease in mice." Proc Natl Acad Sci U S A **102**(49): 17687-92

Tyynismaa, H., H. Sembongi, M. Bokori-Brown, C. Granycome, N. Ashley, J. Poulton, A. Jalanko, J. N. Spelbrink, I. J. Holt and A. Suomalainen (2004). "Twinkle helicase is essential for mtDNA maintenance and regulates mtDNA copy number." Hum Mol Genet **13**(24): 3219-27

van der Vaart, A., M. Mari and F. Reggiori (2008). "A picky eater: exploring the mechanisms of selective autophagy in human pathologies." Traffic **9**(3): 281-9

Van Goethem, G., B. Dermaut, A. Lofgren, J. J. Martin and C. Van Broeckhoven (2001). "Mutation of POLG is associated with progressive external ophthalmoplegia characterized by mtDNA deletions." Nat Genet **28**(3): 211-2

Van Goethem, G., P. Luoma, M. Rantamaki, A. Al Memar, S. Kaakkola, P. Hackman, R. Krahe, A. Lofgren, J. J. Martin, P. De Jonghe, A. Suomalainen, B. Udd and C. Van Broeckhoven (2004). "POLG mutations in neurodegenerative disorders with ataxia but no muscle involvement." Neurology **63**(7): 1251-7

Wallace, D. C. (2005). "The mitochondrial genome in human adaptive radiation and disease: on the road to therapeutics and performance enhancement." Gene **354**: 169-80

Wallace, D. C., G. Singh, M. T. Lott, J. A. Hodge, T. G. Schurr, A. M. Lezza, L. J. Elsas, 2nd and E. K. Nikoskelainen (1988). "Mitochondrial DNA mutation associated with Leber's hereditary optic neuropathy." Science **242**(4884): 1427-30

Wallace, D. C., X. X. Zheng, M. T. Lott, J. M. Shoffner, J. A. Hodge, R. I. Kelley, C. M. Epstein and L. C. Hopkins (1988). "Familial mitochondrial encephalomyopathy (MERRF): genetic, pathophysiological, and biochemical characterization of a mitochondrial DNA disease." Cell **55**(4): 601-10

Wang, Y., Y. L. Lyu and J. C. Wang (2002). "Dual localization of human DNA topoisomerase IIIalpha to mitochondria and nucleus." Proc Natl Acad Sci U S A **99**(19): 12114-9

Yakubovskaya, E., Z. Chen, J. A. Carrodeguas, C. Kisker and D. F. Bogenhagen (2006). "Functional human mitochondrial DNA polymerase gamma forms a heterotrimer." J Biol Chem **281**(1): 374-82

Yang, M. Y., M. Bowmaker, A. Reyes, L. Vergani, P. Angeli, E. Gringeri, H. T. Jacobs and I. J. Holt (2002). "Biased incorporation of ribonucleotides on the mitochondrial L-strand accounts for apparent strand-asymmetric DNA replication." Cell **111**(4): 495-505

Yasukawa, T., A. Reyes, T. J. Cluett, M. Y. Yang, M. Bowmaker, H. T. Jacobs and I. J. Holt (2006). "Replication of vertebrate mitochondrial DNA entails transient ribonucleotide incorporation throughout the lagging strand." EMBO J **25**(22): 5358-71

Yoshimori, T. (2004). "Autophagy: a regulated bulk degradation process inside cells." Biochem Biophys Res Commun **313**(2): 453-8

Zanna, C., A. Ghelli, A. M. Porcelli, M. Karbowski, R. J. Youle, S. Schimpf, B. Wissinger, M. Pinti, A. Cossarizza, S. Vidoni, M. L. Valentino, M. Rugolo and V. Carelli (2008). "OPA1 mutations associated with dominant optic atrophy impair oxidative phosphorylation and mitochondrial fusion." Brain **131**(Pt 2): 352-67

Zeviani, M. and S. Di Donato (2004). "Mitochondrial disorders." Brain **127**(Pt 10): 2153-72

Zeviani, M., C. T. Moraes, S. DiMauro, H. Nakase, E. Bonilla, E. A. Schon and L. P. Rowland (1988). "Deletions of mitochondrial DNA in Kearns-Sayre syndrome." Neurology **38**(9): 1339-46

Zeviani, M., S. Servidei, C. Gellera, E. Bertini, S. DiMauro and S. DiDonato (1989). "An autosomal dominant disorder with multiple deletions of mitochondrial DNA starting at the D-loop region." Nature **339**(6222): 309-11

Zhang, H., J. M. Barcelo, B. Lee, G. Kohlhagen, D. B. Zimonjic, N. C. Popescu and Y. Pommier (2001). "Human mitochondrial topoisomerase I." Proc Natl Acad Sci U S A **98**(19): 10608-13